Development of lipid-based nanoparticles for combination treatment of pancreatic cancer with hyperthermia

by

Cesar Benjamin Aparicio-Lopez

B.S., Kansas State University, 2020
M.S., Kansas State University, 2021

AN ABSTRACT OF A DISSERTATION

submitted in partial fulfillment of the requirements for the degree

DOCTOR OF PHILOSOPHY

Department of Anatomy and Physiology
College of Veterinary Medicine

KANSAS STATE UNIVERSITY
Manhattan, Kansas

2024

Abstract

Pancreatic ductal adenocarcinoma (PDAC) is a highly lethal malignancy, often asymptomatic and typically diagnosed at advanced stages. At the same time, treatment options include surgery, radiotherapy, and chemotherapy, only 20% of patients present with surgically resectable tumors. For most patients, chemotherapy remains the primary therapeutic approach, with gemcitabine, a nucleoside analog, serving as the standard of care. However, the dense fibrotic stroma, irregular blood supply, and heterogeneous tumor cell populations present significant biological and physical barriers, reducing gemcitabine's efficacy and contributing to drug resistance. Drug delivery systems have been developed to address these obstacles by enhancing gemcitabine accumulation at the tumor site, primarily through encapsulation in long-circulating nanoparticles that exploit the enhanced permeation and retention (EPR) effect. Nevertheless, the unique architecture of PDAC tumors often limits the success of this strategy, with poor penetration and low bioactivity of gemcitabine at the tumor site remaining significant challenges. Additionally, gemcitabine's physicochemical properties hinder effective nanoparticle loading, complicating therapeutic outcomes further.

The primary objective of this dissertation is to address two major challenges in drug delivery for PDAC. First, it aims to develop gemcitabine-loaded nanoparticles that prevent drug degradation and enhance stability. Second, it aims to design these nanoparticles to be heat-sensitive, enabling controlled drug release through heat triggering mechanisms.

We first designed and manufactured thermosensitive liposomes using varying ratios of 1,2-dipalmitoyl-sn-glycero-3-phosphocholine (DPPC) and 1,2-distearoyl-sn-glycero-3-phosphocholine (DSPC), optimizing them for minimal drug release at physiological temperature (37°C). A two-stage hot water bath setup was employed to simulate temperature-induced drug

release. In the first stage, the temperature was rapidly increased, followed by a holding stage at hyperthermic levels (42°C). This setup demonstrated that the liposomes exhibited fast drug release at hyperthermia temperatures. Despite successful thermosensitive performance, the liposomes displayed low encapsulation efficiency, which is consistent with existing literature but raises concerns about cost-effectiveness.

To address the limitations of nonspecific hyperthermia, we developed a novel microwave-sensitive microemulsion. Multiple ionic liquids and surfactants were screened to formulate this system. To improve biocompatibility, DPPC, DSPC, 1,2-distearoyl-sn-glycero-3-phosphoethanolamine-N- [amino (polyethylene glycol)-2000] (PEG), and 1-palmitoyl-2-hydroxy-sn-glycero-3-phosphocholine (Lyso-PC) were incorporated. The final formulation included 1-butyl-3-methyl imidazolium bromide ionic liquid as the primary component, Tween 80/20 as surfactants, and ethanol-isopropyl myristate with lipids as co-surfactants. Dielectric measurements confirmed the microemulsion's microwave sensitivity and further hyperthermia treatment demonstrated temperature-dependent cytotoxic effects *in vitro*.

The drug delivery systems developed in this study exhibited negligible drug release at room temperature and physiological conditions (37°C) while showing effective cytotoxicity upon heat stimulation. Incorporating lipids and PEG ensured biocompatibility and stability in suspension, enhancing the potential for clinical application. This proof of concept marks a significant advancement in targeted drug delivery systems. Future improvements in gemcitabine-loaded vehicles, particularly those responsive to hyperthermia, could lead to critical clinical developments in drug delivery and hyperthermia-based treatments for PDAC.

Development of lipid-based nanoparticles for combination treatment of pancreatic cancer with hyperthermia

by

Cesar Benjamin Aparicio-Lopez

B.S., Kansas State University, 2020
M.S., Kansas State University, 2021

A DISSERTATION

submitted in partial fulfillment of the requirements for the degree

DOCTOR OF PHILOSOPHY

Department of Anatomy and Physiology
College of Veterinary Medicine

KANSAS STATE UNIVERSITY
Manhattan, Kansas

2024

Approved by:

Major Professor

Prof. Matthew T. Basel

Copyright

Abstract

Pancreatic ductal adenocarcinoma (PDAC) is a highly lethal malignancy, often asymptomatic and typically diagnosed at advanced stages. At the same time, treatment options include surgery, radiotherapy, and chemotherapy, only 20% of patients present with surgically resectable tumors. For most patients, chemotherapy remains the primary therapeutic approach, with gemcitabine, a nucleoside analog, serving as the standard of care. However, the dense fibrotic stroma, irregular blood supply, and heterogeneous tumor cell populations present significant biological and physical barriers, reducing gemcitabine's efficacy and contributing to drug resistance. Drug delivery systems have been developed to address these obstacles by enhancing gemcitabine accumulation at the tumor site, primarily through encapsulation in long-circulating nanoparticles that exploit the enhanced permeation and retention (EPR) effect. Nevertheless, the unique architecture of PDAC tumors often limits the success of this strategy, with poor penetration and low bioactivity of gemcitabine at the tumor site remaining significant challenges. Additionally, gemcitabine's physicochemical properties hinder effective nanoparticle loading, complicating therapeutic outcomes further.

The primary objective of this dissertation is to address two major challenges in drug delivery for PDAC. First, it aims to develop gemcitabine-loaded nanoparticles that prevent drug degradation and enhance stability. Second, it aims to design these nanoparticles to be heat-sensitive, enabling controlled drug release through heat triggering mechanisms.

We first designed and manufactured thermosensitive liposomes using varying ratios of 1,2-dipalmitoyl-sn-glycero-3-phosphocholine (DPPC) and 1,2-distearoyl-sn-glycero-3-phosphocholine (DSPC), optimizing them for minimal drug release at physiological temperature (37°C). A two-stage hot water bath setup was employed to simulate temperature-induced drug

release. In the first stage, the temperature was rapidly increased, followed by a holding stage at hyperthermic levels (42°C). This setup demonstrated that the liposomes exhibited fast drug release at hyperthermia temperatures. Despite successful thermosensitive performance, the liposomes displayed low encapsulation efficiency, which is consistent with existing literature but raises concerns about cost-effectiveness.

To address the limitations of nonspecific hyperthermia, we developed a novel microwave-sensitive microemulsion. Multiple ionic liquids and surfactants were screened to formulate this system. To improve biocompatibility, DPPC, DSPC, 1,2-distearoyl-sn-glycero-3-phosphoethanolamine-N- [amino (polyethylene glycol)-2000] (PEG), and 1-palmitoyl-2-hydroxy-sn-glycero-3-phosphocholine (Lyso-PC) were incorporated. The final formulation included 1-butyl-3-methyl imidazolium bromide ionic liquid as the primary component, Tween 80/20 as surfactants, and ethanol-isopropyl myristate with lipids as co-surfactants. Dielectric measurements confirmed the microemulsion's microwave sensitivity and further hyperthermia treatment demonstrated temperature-dependent cytotoxic effects *in vitro*.

The drug delivery systems developed in this study exhibited negligible drug release at room temperature and physiological conditions (37°C) while showing effective cytotoxicity upon heat stimulation. Incorporating lipids and PEG ensured biocompatibility and stability in suspension, enhancing the potential for clinical application. This proof of concept marks a significant advancement in targeted drug delivery systems. Future improvements in gemcitabine-loaded vehicles, particularly those responsive to hyperthermia, could lead to critical clinical developments in drug delivery and hyperthermia-based treatments for PDAC.

Table of Contents

List of Figures

List of Tables

Acknowledgments

PhD is not for smart people; it is for stubborn people. During my bachelor's training, an instructor once suggested that I settle for a master's degree if I ever wanted to pursue postgraduate studies. This suggestion came after a semester where my performance was less than optimal. While their advice might have held some truth at the time, fortunately, I'm a stubborn person. After nearly eight years as a student at KSU, I've proven that persistence pays off.

I want to extend my deepest gratitude to my advisor, Dr. Matt Basel, who has been an incredibly knowledgeable professor and a steadfast role model throughout my academic journey. I am truly grateful for his trust and dedication since we first met during my master's program. His research advice and suggested approaches have deeply resonated with the style I aspire to achieve in my work.

I would also like to sincerely thank my committee members, Prof. Stefan Bossmann, Prof. Mark Weiss, Prof. Punit Prakash, and Prof. Tej Sheretha, for their time and commitment to serving on my committee. I am especially grateful to Marla Pyle, MS, for her invaluable assistance with experiments. Your guidance and support throughout my Ph.D. program have been instrumental in shaping my research trajectory. The insightful discussions I've had with each of you have greatly expanded and diversified my thinking.

Special thanks go to my former and current colleagues: Dr. Tuyen Nguyen, Dr. Ramesh Marasini, Dr. Sagar Rayamajhi, Dr. Faraz Chamani, Dr. Anna Bottiglieri, Thitikan Jirakittisonthon, Sandun Gajaweera, Dongoh Lee, and Sarah DeVader. I am incredibly fortunate to have met such supportive individuals who have been there for me in many aspects of my life.

I am grateful to the Anatomy & Physiology Graduate Assistantship Program and the Jhonson Cancer Research Center of Kansas State for their support and funding. Special thanks to

Geraldine Magnin, PhD, for her support with HPLC measurement; Daniel L. Boyle, PhD (KSU Microscopy Facility Division of Biology); and Prem Singh Thapa Chetri, PhD (KU Microscopy and Analytical Imaging Research Resource Core Lab) for their support with the TEM images. Special thanks to Dr. Anna Bottiglieri for her collaboration with the hyperthermia experiment.

Finally, I dedicate this work to my family members who have moved on from this life but left a lasting mark on me. Their memory and inspiration have been instrumental in guiding me to where I am today. You will always be remembered with love.

Dedication

To my Mother and Father

Ma de La Luz Lopez-Varelas and Benjamin Aparicio-Munoz

To my mentor

Dr. Matt Basel

Chapter 1 - Introduction

Cancer is broadly defined as the uncontrolled and abnormal growth of cells, but its impact extends beyond the biological domain. While the physical toll on the body is undeniable, cancer also deeply affects a person's mental and emotional well-being, creating a ripple effect that touches not only the patient but also their loved ones, often leading to the disruption of familial bonds and friendships.[3, 4] Cancer's diversity in origin further compounds the complexities of treatment; cancers arising from different tissues may require distinct therapeutic approaches, with some forms being more easily treatable than others.[5, 6] However, access to such treatments is not uniformly available, as socioeconomic disparities play a significant role in determining the quality and availability of care.[7, 8] In underprivileged populations, a combination of limited healthcare access, financial constraints, and deep-seated misinformation often ingrained in the social fabric exacerbates the problem. The emotional stress caused by the disease, coupled with a general lack of health literacy, frequently leads patients to fall prey to misinformation about so-called "alternative treatments" (Figure 1.1). These alternatives, which are often unproven and ineffective, can drive patients away from medical advice, delaying or derailing potentially life-saving interventions.[9, 10]

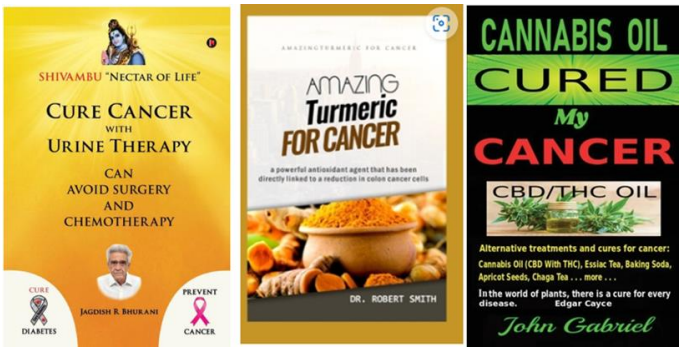

Figure 1.1. Cancer treatment misinformation. Books for sale in the U.S.A.

There have been several warnings from the FDA highlighting the risks associated with unproven cancer therapies.[11] Often, a question arises: what does it take to kill cancer? While it is true that many substances can kill cancer cells in a petri dish, these same substances can also harm healthy tissues within the body, as these two scenarios are different. Effective cancer drugs, though capable of destroying malignant cells, often cause systemic side effects.[12] When analyzing chemotherapy, two key aspects are considered: how the drug affects the tumor and how the body processes it, which refers to the drug's pharmacokinetics and pharmacodynamics.

Figure 1.2. Comic Figure. Source: xkcd: Cells

Conventional chemotherapy drugs often face numerous challenges. They tend to be poorly absorbed and randomly distributed, cause damage to healthy tissues, and are cleared too quickly.[13, 14] Due to enzymatic degradation, pH imbalances, and barriers such as mucosal layers, these drugs may take longer to achieve therapeutic effects.[15, 16] Their immediate bioavailability can also increase toxicity levels in the bloodstream, further complicating treatment.[17] Moreover, many promising therapeutic drugs face challenges in compatibility with the body's environment, whether they are lipophilic or hydrophilic, meaning they are not soluble or cannot diffuse into the target tissue.[18, 19] Drug delivery vehicles have gained popularity to address these issues. These systems offer controlled release, improved distribution, and extended circulation time within the body. These advantages allow higher drug concentrations to be delivered directly to the tumor tissue while reducing interactions with healthy tissues.

Drug delivery systems (DDSs) refer to technological platforms designed to store and administer drugs effectively within the human body.[13, 20] Recently, several novel DDSs have been developed to offer more convenient, controlled, and targeted drug delivery. Each DDS has unique characteristics that influence its release rate and mechanism, largely due to variations in their physical, chemical, and morphological properties.[13, 21, 22] Novel approaches for DDS take advantage of diffusion rate, chemical reaction, solvent interaction, and other stimuli control as major mechanisms driving drug release. These approaches enhance therapeutic efficacy while reducing systemic side effects.[23-26] These new advances featured the stimuli triggered release to the DDS and created the field of nanomedicine.

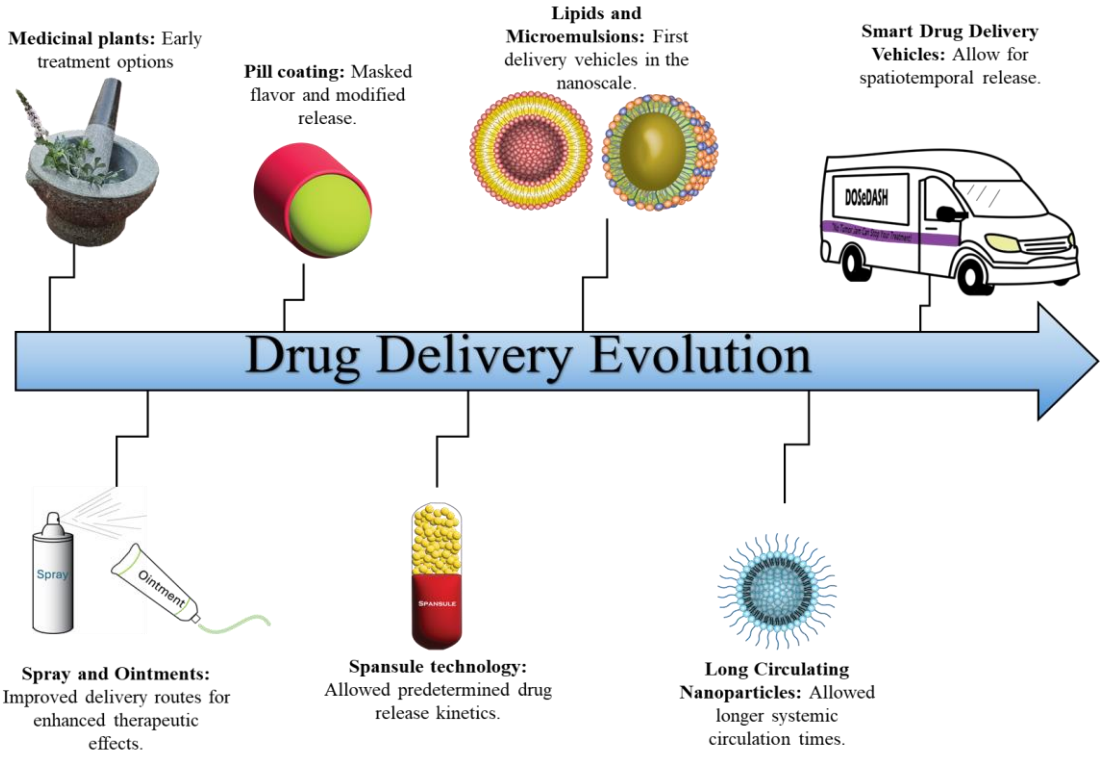

Figure 1.3. Drug Delivery System Evolution. Drug delivery systems aim to improve the therapeutic effects of drugs while reducing side effects.

1.1. Drug Delivery Systems

Humans and their predecessors likely used medicinal plants for treatments in ancient times; old, recorded medical documents can be traced to the Ebers Papyrus, dating back to around 1550 BC, and Mesopotamian tablet clays, 2600 BE.[27] The use of medicinal plants often lacks consistency, homogeneity, and specificity; thus, there has always been an interest in improving medication. With the advancement of chemical purification and synthesis, drugs could be formulated and administrated in controlled dosing, such as infusions, ointments, sprays, and capsules.[28, 29] Efforts continued to improve drug administration and delivery. For example, in the 10th century, Rhazes and Avicenna introduced gold, silver, and pearl-coated tablets to mask drug bitterness.[13] Further efforts to encapsulate the drugs inadvertently provided gradual, controlled release of the drug over time. The advancement of DDS has led to innovations such as polymer conjugates and Spansule technology.[30] This technology takes advantage of coating small granules of the drug being coated with substances that dissolve slowly, facilitating a dissolution-controlled release (Figure 1.3).

Alec Bangham discovered the first DDS vehicle in the early 1960s while researching the structure of biological membranes.[31] Bangham and his colleagues found that when phospholipids were dispersed in an aqueous solution, they spontaneously formed small, spherical vesicles, later known as liposomes. However, it wasn't until the 1970s that Gregory Gregoriadis successfully demonstrated its ability to encapsulate enzymes and deliver them specifically to the lysosomes of tissues within the reticuloendothelial system (RES), which includes organs such as the liver, spleen, and bone marrow.[32] Since then, liposomes have become a versatile option for drug delivery systems. Extensive research in their design and synthesis has led to advancements in their manufacturing and characterization, making the process more efficient and cost-effective.[33,

[34] Composed of natural or synthetic phospholipids, liposomes exhibit high biocompatibility, ensuring their safety in medical applications.[34, 35] The growing knowledge surrounding these delivery vehicles allows researchers to optimize their formulations to improve targeting to specific tissues of interest and enhance drug loading capacity.[36-39]

1.2. Tissue of interest: pancreas and PDAC

The pancreas is the largest accessory organ with endocrine and exocrine functions (Figure 1.4). Located retroperitoneal space with its head nestled in the curve of the duodenum and the tail extending toward the spleen.[40] Anatomically, the pancreas is divided into the head, neck, body, and tail.[40, 41] It consists of both exocrine tissue, which includes acinar cells that

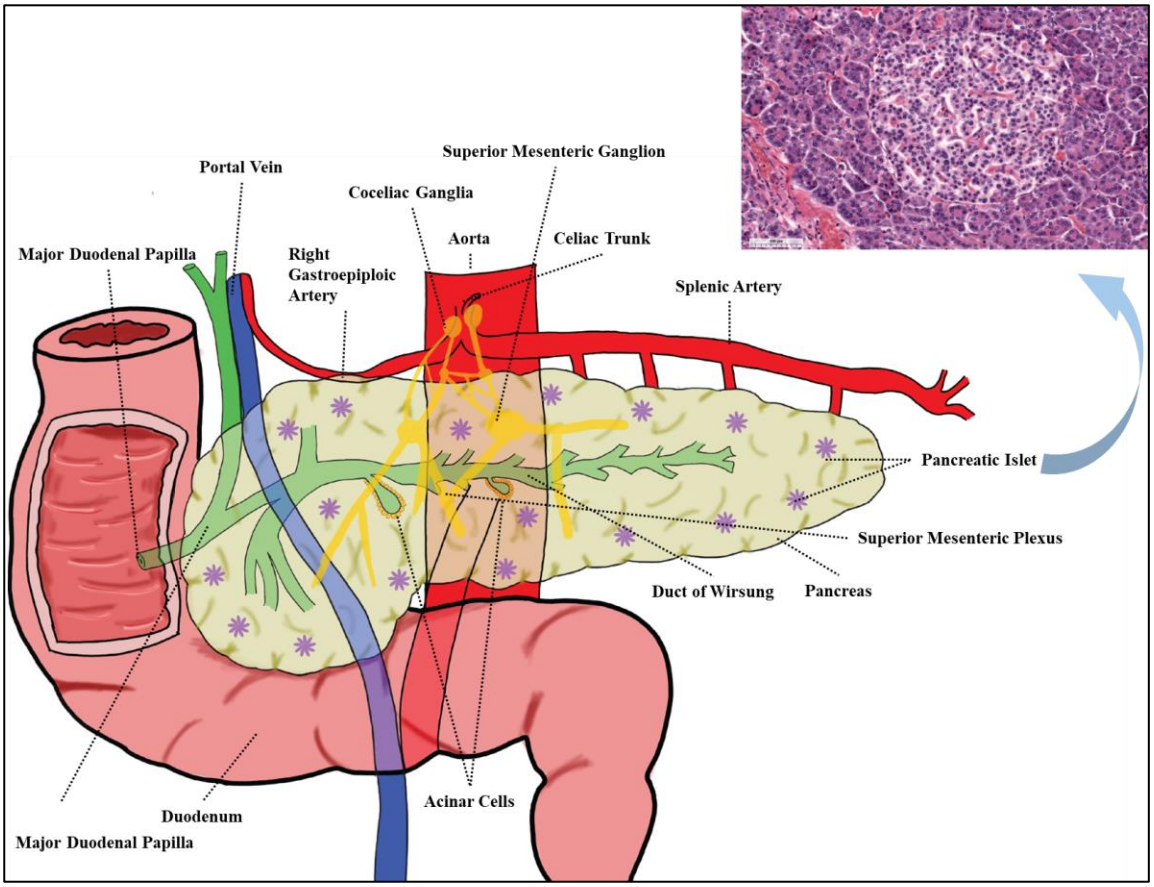

Figure 1.4. Pancreas Anatomy. *Adapted from the pancreas anatomy and histology.*[1, 2] The pancreas lies in a vital region, interacting closely with the nervous, vascular, and endocrine systems to regulate digestion and metabolism.

produce digestive enzymes, and endocrine tissue, organized into islets of Langerhans that contain alpha, beta, delta, PP, and epsilon cells responsible for producing various hormones like glucagon, insulin, somatostatin, pancreatic polypeptide, and ghrelin.[40, 42] The pancreas's duct system comprises the main pancreatic duct (duct of Wirsung), which merges with the common bile duct to empty into the duodenum, and the accessory pancreatic duct (duct of Santorini), which may empty separately.[42, 43] The pancreas receives its blood supply primarily from branches of the celiac trunk and the superior mesenteric artery. A significant contribution comes from the splenic artery, which supplies the body and tail of the pancreas through its numerous small branches. Additionally, the right gastroepiploic artery, a branch of the gastroduodenal artery, supplies the head of the pancreas. Moreover, sympathetic and parasympathetic innervation is primarily through the celiac ganglia and the superior mesenteric ganglion. Sympathetic fibers, originating from the thoracic splanchnic nerves, synapse in the celiac ganglia and the superior mesenteric ganglion, modulating blood flow and enzyme secretion. The dual role in digestion and blood sugar regulation makes the pancreas essential for metabolic homeostasis. Given its crucial functions and location, it is particularly alarming that pancreatic cancer, an extremely aggressive and often asymptomatic disease in its early stages, can severely disrupt these processes and pose significant health risks.[44]

Pancreatic ductal adenocarcinoma (PDAC) is the most prevalent form of pancreatic cancer; it accounts for 90% of pancreatic cancer cases in the U.S. Accompanied by one of the lowest 5-year relative survival rates, hovering at approximately 12%.[45] According to the National Cancer Institute, pancreatic cancer in the U.S. constitutes roughly 3% of all cancer cases and contributes about 7% of all cancer-related deaths, making it the 4th deadliest cancer. In addition, incidence is predicted to double over the next decade due to increased prevalence of risk factors

such as early onset diabetes, obesity, genetics, and smoking. [46-49] Though the diagnosed median age is 70, statistics show an increase among the young population, particularly women.[50] The asymptomatic nature and lack of early detection methods and effective treatments for PDAC further compound the problem. Thus, it is poised to become the second deadliest cancer in the future. [51] Although there is a genetic component to PDAC, there is no evidence that screening high-risk populations offers significant advantages or is cost-effective, as 90% of pancreatic cancers occur sporadically.[52] The tumor cannot be palpable in a physical exam due to the pancreas's location and the tumor's size; thus, pancreas computer tomography (CT) angiography and biopsy are used to diagnose and assess the developmental stage.[53]

The origin and progression of PDAC can be traced back to noninvasive precursor lesions, which include pancreatic intraepithelial neoplasia (PanIN), intraductal papillary mucinous neoplasm (IPMN), intraductal tubular-papillary neoplasm (ITPN), and mucinous cystic neoplasm (MCN).[54, 55] KRAS, CDKN2A, TP53, and SMAD4 drive this process. Their expression varies with the degree of dysplasia and heavily influences the patient's prognosis. KRAS is the most common mutated family in human carcinoma cancers, specifically PDAC; it contributes to initiation, progression, metastases, and therapy resistance. [56, 57]

KRAS mutations influence key aspects of metabolism, including glucose, amino acid, and lipid metabolism. KRAS, or Ki-ras2 Kristen rat sarcoma viral oncogene homolog, encodes a GTPase transducer protein that relays external signals from the cell membrane to the nucleus. Its activation overstimulates downstream effector signaling pathways.[58] KRAS upregulates glucose transporters like GLUT1, enhancing glucose uptake and glycolytic flux by increasing key enzymes.[59] It also drives the hexosamine biosynthesis and pentose phosphate pathways, supporting energy production and redox balance. Likewise, the expression of amino acid

transporters is increased. [59, 60] Finally, the uptake of exogenous fatty acids promotes de novo fatty acid and cholesterol synthesis and induces lipid droplet accumulation while reducing fatty acid oxidation, ultimately aiding tumor growth, metastasis, and adaptation to stress.[60] All these changes result in and support macropinocytosis.[61]

A key characteristic of PDAC is the low cellular density within the primary tumor, which is attributed to extensive fibrosis driven by cancer-associated fibroblasts (CAFs).[62] CAFs play a crucial role in modulating the tumor microenvironment by contributing significantly to the deposition of the extracellular matrix (ECM), composed of laminins, fibronectins, collagens, and hyaluronan.[62, 63] This physical barrier causes desmoplasia-associated hypovascularization related to tumor immunosuppression and low T-cell infiltration.[64] Furthermore, the tumor can recruit macrophages and block $CD4^{+}$T cells, reducing the immune response to the tumor.[65] Without effective immune surveillance to target cancer cells, the tumor persists and progresses, resulting in a critical need for strategies that both enhance drug delivery and restore immune function within the tumor microenvironment

The interplay between these factors significantly impacts the efficacy and prognosis of PDAC treatment. The stage of the disease at diagnosis and the tumor's location in the pancreas, 60-70% are found in the exocrine head, are critical for treatment and late-stage symptoms.[66] Tumors in this region can lead to biliary blockage, complicating treatment.[67] Surgical resection remains the only potentially curative option, typically followed by adjuvant chemotherapy or radiotherapy. However, only 20% of patients are present with resectable tumors; the remaining 80% have locally advanced, non-resectable tumors or distant metastases. Surgical treatment of PDAC is limited by the invasion of nearby tissues, making it difficult to clear surgical margins.[68, 69] For these patients, systemic chemotherapy becomes the primary treatment, particularly with

nucleoside analog drugs, since they can compete with endogenous nucleoside and thus interfere with several functions.

1.3. Gemcitabine

Gemcitabine is a nucleoside analog that acts as an antimetabolite (Figure 1.5). This agent is a weak base (pKa: 3.6) known as 2',2'-difluorodeoxycytidine (dFdC) and is a potent and well-tolerated chemotherapeutic agent with minimal systemic toxicity due to its swift conversion into the less potent difluoro-uridine derivative (dFdU), which is rapidly eliminated through renal clearance. The clearance of gemcitabine is largely influenced by patient age and sex, with geriatric patients showing lower clearance.[70] Notably, females exhibit lower clearance rates and longer half-lives than males in similar age groups.[70] For typical patients receiving short infusions, gemcitabine half-life ranges from 42 to 94 minutes, while longer infusions result in significantly increased half-life ranging from 245 to 638 minutes due to a greatly increased volume of distribution, suggesting that the drug is more widely distributed into tissues throughout the body.[70]

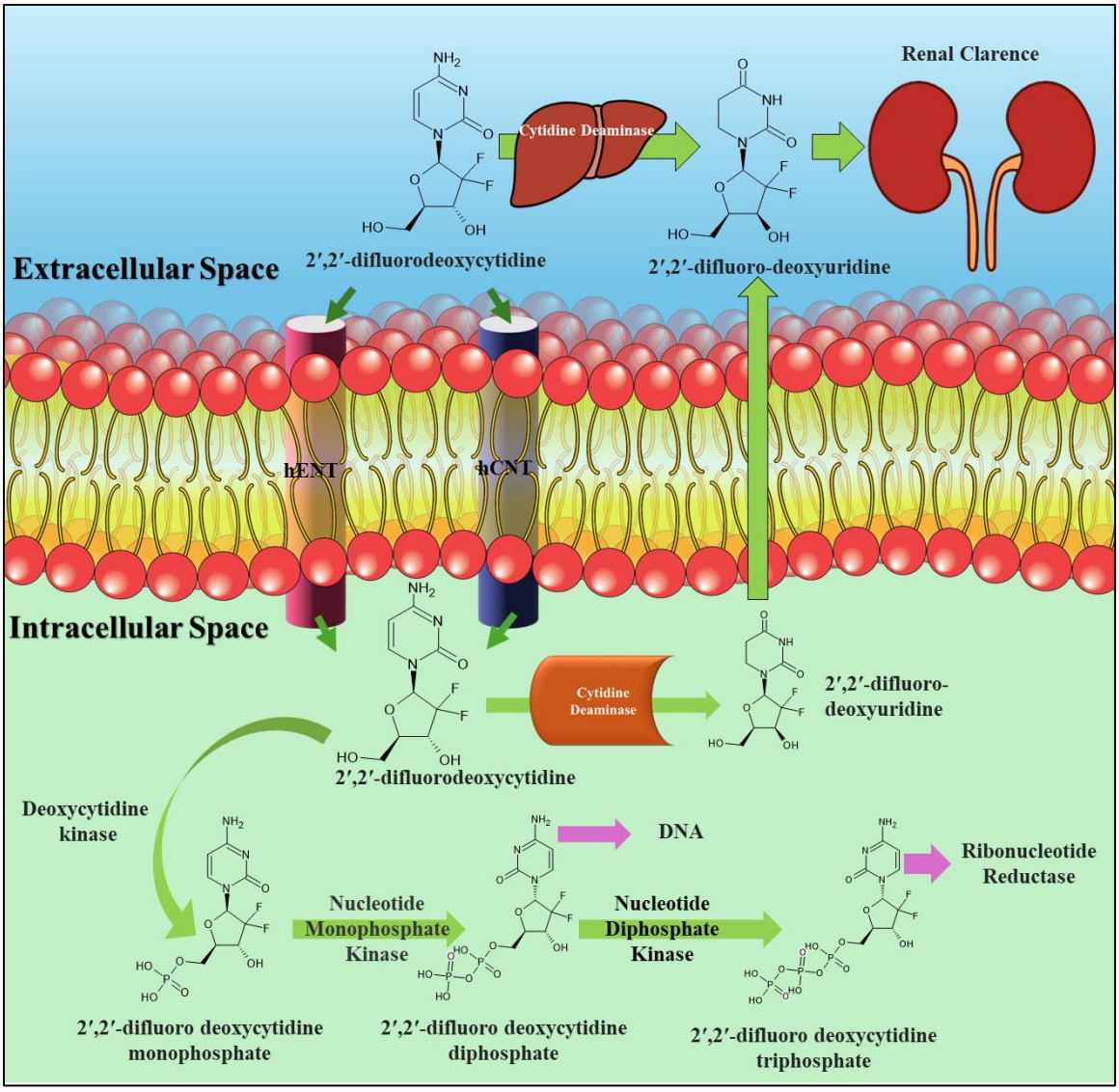

Figure 1.5. Gemcitabine kinetics. Key components include cytidine deaminase, deoxycytidine kinase, nucleotide monophosphate kinase, nucleotide diphosphate kinase, and human nucleoside transporters hENT and hCNT. In cancer cells, genetic variations in membrane transporters, enzymes responsible for gemcitabine activation and deactivation, and pharmacological targets like ribonucleotide reductase significantly influence the drug's therapeutic effectiveness.

Gemcitabine is primarily eliminated through the urine. 92% to 98% of the administered dose is recovered within one week, and gemcitabine and its inactive metabolite dFdU account for 99% of the excreted dose.[70, 71] The active metabolite, gemcitabine triphosphate, can be extracted from peripheral blood mononuclear cells, with a terminal phase half-life ranging from 1.7 to 19.4 hours.[70] The variation in clearance and volume of distribution, influenced by patient-specific

characteristics and infusion duration, results in changes in the drug's half-life and plasma concentrations, necessitating careful consideration of dosing to mitigate adverse effects while ensuring therapeutic efficacy.

Since gemcitabine is a hydrophilic molecule, it requires transporters to enter the cell, particularly human equilibrative nucleoside transporters (hENT) and human concentrative nucleoside transporters (hCNT).[72] Gemcitabine's antitumor mechanism involves arresting the cell cycle at the S-phase by inhibiting ribonucleotide reductase and DNA synthesis through its di-and tri-phosphorylated metabolites (dFdCDP and dFdCTP).[73] Once inside the cancer cell, gemcitabine undergoes initial phosphorylation primarily by deoxycytidine kinase (dCK), with a lesser contribution from extra-mitochondrial thymidine kinase 2, to form gemcitabine diphosphate (dFdCDP) and triphosphate (dFdCTP).[73]

Gemcitabine diphosphate (dFdCDP) inhibits ribonucleotide reductase, an enzyme crucial for generating deoxynucleoside triphosphates necessary for DNA synthesis.[74] This inhibition results in reduced intracellular concentrations of deoxynucleotides, including dCTP.[71, 74] The reduction in dCTP levels enhances the incorporation of gemcitabine triphosphate (dFdCTP) into DNA, a process known as self-potentiation. Gemcitabine triphosphate competes with dCTP for incorporation into the DNA strand, and once incorporated, it allows the addition of only one more nucleotide before halting further DNA synthesis.[71] This premature termination of DNA synthesis eventually triggers apoptotic cell death. Cytidine deaminase (CDA) is highly expressed in plasma and liver tissues, further contributing to the challenges of maintaining effective drug concentrations.[71]

1.4. Resistance to Treatment

A characteristic of PDAC is the development of multidrug resistance, which can be either intrinsic or acquired, though the underlying mechanisms remain poorly understood. Their unique tumor microenvironment is a key factor contributing to multidrug and radiotherapy resistance in solid tumors. Although each cancer architecture type varies, solid tumors are generally characterized by poor vascularization and extensive fibrosis. This reduces blood flow to the tumor's inner regions, leading to nutrient deprivation and low oxygen levels. Additionally, irregular vascularization impairs lymphatic drainage, causing elevated interstitial pressure, low pH, and a chemically reductive environment. These factors and specific cellular characteristics contribute to the limited effectiveness of treatments.

Hypoxia in the tumor microenvironment occurs when oxygen levels fall below 5–10 mm Hg; this occurs due to an imbalance between oxygen supply and consumption caused by the rapid growth of solid tumors and a poor blood supply.[75] Hypoxia comes with multiple gene expressions/adaptations that inactivate apoptosis, such as the increase of anti-apoptotic proteins (Bcl-XL and FLIP) by PI3K/Akt/NF-κB pathways modulation and the hypoxia-inducible factor-1 (HIF-1) which both suppresses apoptosis and induces the expression of multidrug resistance 1 (MDR1) genes causing the efflux of drugs.[76, 77] Furthermore, the suppression of BNIP3 is associated with gemcitabine drug resistance.[78]

Tumor interstitial pressure (TIP) presents a significant physical barrier to PDAC treatment generated by the lack of functional lymphatic vessels causes this inadequacy, the presence of a leaky and immature tumor vasculature, excessive (peripheral) angiogenesis, and interstitial fibrosis.[79] Consequently, TIP hinders convection-driven fluid transport within tumors, resulting in inefficient drug penetration and distribution, compromising the effectiveness of anti-

cancer therapies.[79, 80] The most common cell type in solid fibrotic is cancer-associated fibroblasts and stellate cells. These cells respond and produce chemical signals that help with growth, invasion, and drug resistance by metabolizing gemcitabine, leading to reduced drug concentrations within the tumor microenvironment.[81-85]

The advanced stage of PDAC by the time of diagnosis affects the delivery of gemcitabine to the tumor. In addition, gemcitabine faces obstacles in reaching the active site. To tackle these problems, drug delivery vehicles have been extensively studied, as these vehicles protect gemcitabine from degradation and clearance while minimizing side effects.

1.5. Nanoparticle-based drug delivery for PDAC

Nanoparticle-based drug delivery systems present a promising approach to overcoming the challenges of treating PDAC. The mutations within solid tumors and the characteristics of the tumor microenvironment often led to drug resistance, driven by genetic alterations and the formation of physical barriers. Nanoparticles offer several advantages in this context, including high loading capacities, protection from degradation, and reduced clearance from the body. They also enable targeted delivery and controlled, sustained release of therapeutic agents.
These properties can be further enhanced by manipulating the nanoparticles' size, shape, and surface characteristics.

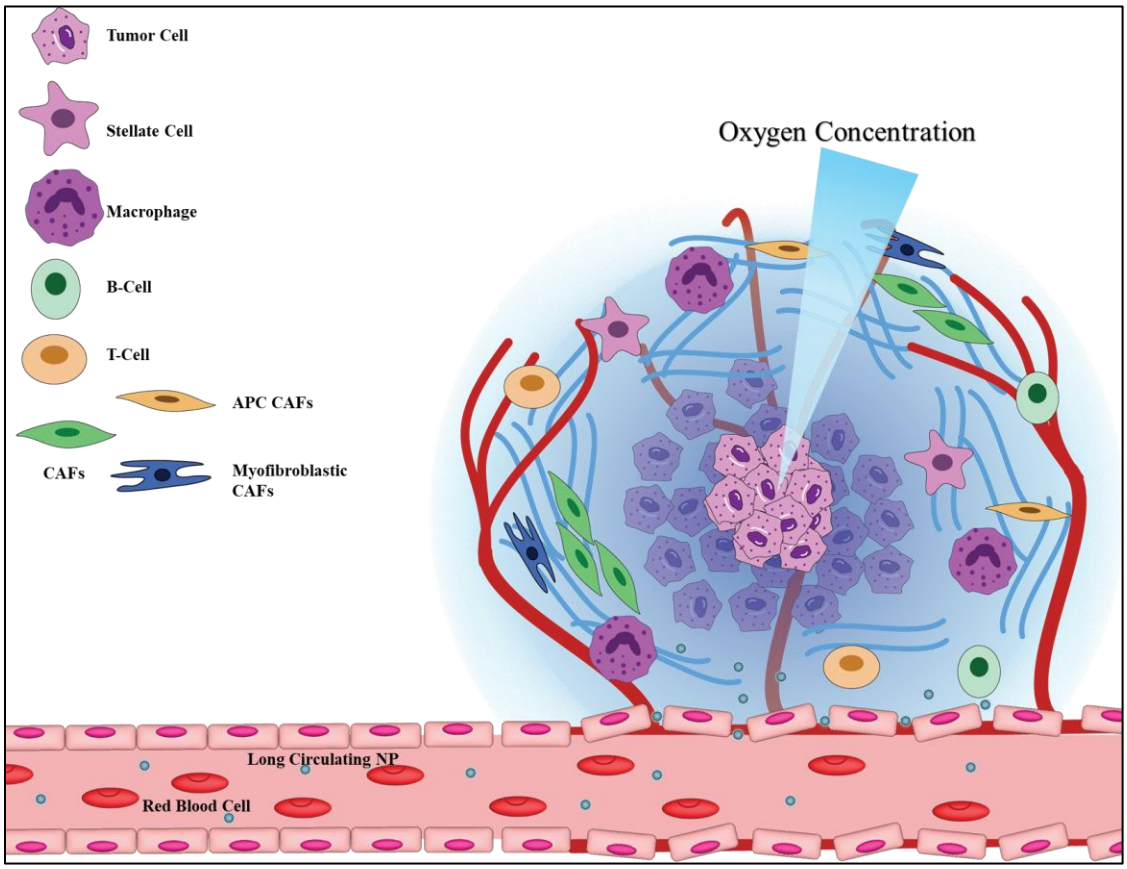

Figure 1.6. Tumor Microenvironment. Various aspects of the PDAC tumor microenvironment contribute to MDR. PDAC presents periphery leaky blood vessels and irregular lymph drainage; this provokes poor circulation and increases interstitial pressure. The cellular components produce chemical messengers that support metastasis, growth, and MDR. Furthermore, the dense fibrosis dimmished the EPR effect.

Although nanoparticles are larger than free drug molecules and can face difficulties in extravasating from healthy capillary beds, their prolonged circulation times, combined with the leaky vasculature typical of solid tumors, facilitate their accumulation in the tumor region (Figure 1.6). This phenomenon, known as the enhanced permeability and retention (EPR) effect, allows for more effective drug concentration at the tumor site, thereby improving therapeutic outcomes while minimizing systemic toxicity.[86] Nevertheless, the EPR effect only favors concentration in the periphery of the tumor and cannot reach the core of the tumor. Furthermore, the poor lymph drainage results in high interstitial fluid pressure, causing passive diffusion out of

the tumor; in addition, the lack of blood flow to the area and desmoplasia further diminish the EPR effect in PDAC cases.[87] Various strategies can be employed to modify the tumor microenvironment to enhance the EPR effect and improve nanoparticle-based drug delivery, increase tumor blood flow to improve nanoparticle access, reduce the stroma to reduce physical barriers, and eliminate cancer cells to diminish their role as a barrier. Hyperthermia has gained significant attention to achieving these modifications. By raising the temperature of the tumor tissue, hyperthermia can increase blood flow, enhance vascular permeability, and disrupt the tumor stroma, thereby improving the delivery and retention of nanoparticle-based therapeutics.

1.6. Hyperthermia

Hyperthermia is an adjuvant anticancer treatment that uses temperatures above the physiological optimal level (37°C) without causing tissue ablation. It can be applied locally, regionally, or to the whole body.[88] The concept of hyperthermia as a therapeutic approach can be traced back to ancient Egypt. The Edwin Smith papyrus describes a treatment called “fire drill,” where a stick was rapidly rotated to generate heat, which was then applied to a breast cancer lesion.[89] This early method reflects the long history of using heat to treat disease. Hippocrates, often called the "Father of Medicine," echoed this sentiment: "Those who cannot be cured by medicine can be cured by surgery. Those who cannot be cured by surgery can be cured by fire [hyperthermia]. Those who cannot be cured by fire are indeed incurable.” [90]

In more modern times, Dr. Wilhelm Busch, a German surgeon in the 19th century, observed in 1866 that cancer patients who developed high fevers after infections, particularly

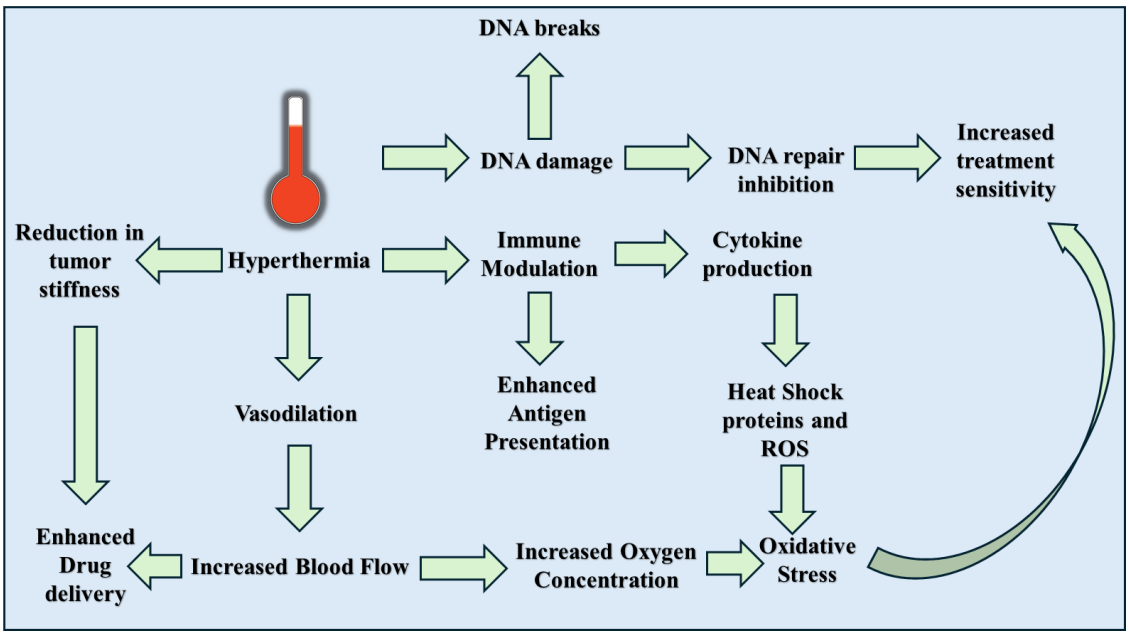

Figure 1.7. Hyperthermia Effects. Hyperthermia has additive effects and synergistic effects.

erysipelas (a bacterial skin infection), experienced tumor regression or remission.[91] Busch's findings laid the groundwork for using hyperthermia and fever-inducing therapies in cancer treatment. This discovery later influenced Dr. William Coley, who developed Coley's toxins in the late 19th century. Coley's approach used bacterial toxins to stimulate the immune system and induce fever, aiming to shrink tumors, marking an early form of immunotherapy.[92] Though clear advantages have been observed with hyperthermia and treatments, the mechanisms by which heat induces its anti-cancer effects remained relatively unknown for many years. Today, we are beginning to understand that the effects of heat on cancer are highly complex. Research shows that hyperthermia can influence tumor homeostasis. Heat can affect cancer cell metabolism, disrupt the tumor microenvironment, and sensitize cancer cells to treatments like chemotherapy and radiation.[88]

Mild hyperthermia is a multifaceted adjuvant cancer treatment that activates biologically relevant mechanisms without directly causing cytotoxicity.[93, 94] Typically applied locally;

hyperthermia is primarily used to enhance the effectiveness of radiotherapy and/or chemotherapy, particularly in patients with recurrent cancers who have undergone extensive prior treatments (Figure 1.7). Hyperthermia is an efficient tool for enhancing the EPR effect by improving tumor blood flow and vascular permeability, lowering interstitial pressure, and disrupting the structure of the ECM.[89] In cancer tissues, angiogenesis is accelerated, leading to higher proliferation and motility rates of endothelial cells in the cancer vasculature than normal endothelial cells.[95] The immediate effect of hyperthermia on blood flow involves vasodilation of blood vessels in the tumor and adjacent normal tissues and a reduction in blood viscosity.[96] The sustained improvement in blood flow is attributed to the persistent decrease in TIP, which relieves pressure on tumor blood vessels and enables better blood flow, thus improving drug delivery.[97] Several studies have established that mild thermal stress can effectively regulate the immune response through dendritic cell (DC) activities, crucial in managing infections and tumor growth. [98] Thermal stress makes the tumor cells visible to immune cells by causing release of damage associated molecular patterns (DAMPs) while enhancing their activity by producing chemical messengers.[99] Furthermore, hyperthermia treatments have been shown to affect DNA by disrupting DNA reparation enzymes and causing oxidative stress, which results from higher oxygen levels.[100]

Nanoparticles can be effectively utilized alongside hyperthermia in two primary ways: as enhancers or as drug carriers. Firstly, nanoparticles can interact synergistically with the hyperthermic medium as enhancers, allowing for targeted heating of specific regions of interest within a tumor (Figure 1.8). This interaction amplifies hyperthermia's thermal effects, improving

heat application precision while minimizing damage to surrounding healthy tissues. By absorbing and converting the applied energy into localized heat, nanoparticles can facilitate the selective destruction of cancer cells, thus enhancing the overall therapeutic efficacy of hyperthermia. Secondly, nanoparticles can serve as sophisticated drug carriers, offering a controlled release of therapeutic agents in conjunction with hyperthermic treatment. Traditional long-circulating nanoparticles typically exhibit an extravascular drug release pattern, wherein drugs are released slowly into the tumor microenvironment over time. This approach prolongs the therapeutic effect and enhances drug accumulation at the tumor site due to the EPR effect, often augmented by hyperthermia. By utilizing nanoparticles to encapsulate chemotherapeutic agents, clinicians can achieve a more effective and targeted delivery system that releases drugs at optimal times and concentrations, particularly when combined with localized hyperthermic treatment.

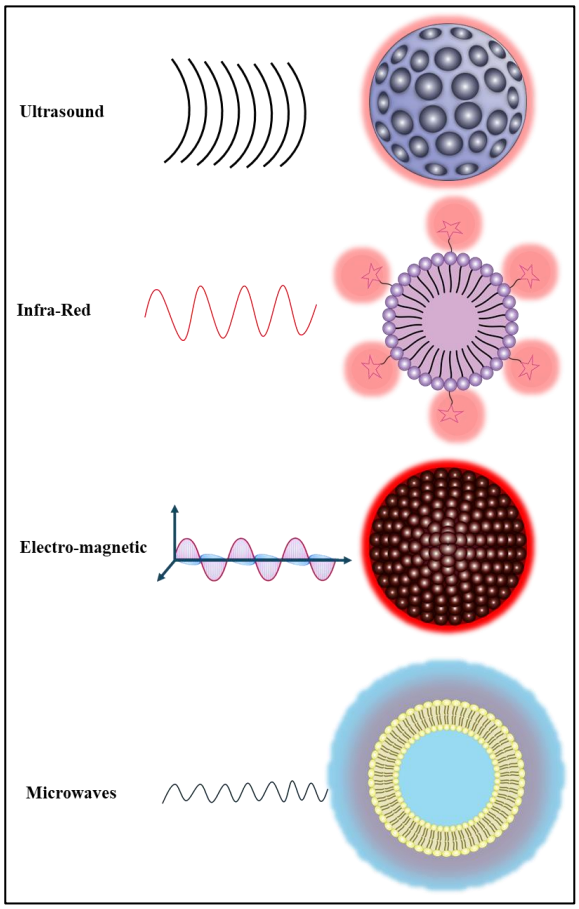

Figure 1.8. Nanoparticles and hyperthermia. Nanoparticles can be designed to interact with the desired radiation to generate heat. Nevertheless, microwaves rely on water interaction to produce heat.

Hyperthermia can be induced by ultrasound, magnetic, infrared (IR), and microwave radiation, each with its benefits and drawbacks. Ultrasound can penetrate deep into tissues, is non-invasive, non-ionizing, cost-effective, and can be combined with imaging. Its targeting can

be enhanced using hollow nanoparticles that collapse and generate heat when stimulated with ultrasound.[101, 102] Magnetic hyperthermia is also non-invasive, reaches deep tissues, and can be combined with MRI imaging. It can be enhanced with magnetic nanoparticles that convert magnetic frequencies into heat. However, these nanoparticles often require contrast agents, which can be toxic and expensive.[103-105] On the other hand, IR hyperthermia cannot reach deep tumors but can be combined with nanoparticles tagged with photoreceptors, improving specificity.[106] Finally, microwaves can penetrate tissues, but invasive approaches may be needed for deeper tumors. The relatively small antennas provide uniform heating, though microwaves are difficult to combine with imaging, and there are no known enhancing nanoparticles for this approach.

Microwave-induced hyperthermia is an innovative cancer treatment technique that uses microwave energy (434-2450 MHz) to heat tumor tissues, raising their temperature to 40-43°C selectively.[107, 108] This heat can directly damage cancer cells and induce apoptosis while also enhancing the efficacy of other treatments like chemotherapy and radiation. The approach is non-invasive or minimally invasive, capable of targeting deep-seated tumors, and offers reduced toxicity to healthy tissues compared to conventional treatments. While clinical trials have demonstrated its potential in cancers such as breast, cervical, and brain tumors, challenges remain in optimizing energy delivery, improving real-time temperature monitoring, and enhancing treatment precision.[109] Current research focuses on refining treatment protocols, exploring the use of nanoparticles to boost heating efficiency, and conducting larger clinical trials to establish its safety and effectiveness.[110]

As previously mentioned, hyperthermia can trigger intravascular drug release, a concept that involves activating nanoparticles to release their therapeutic payload directly within the bloodstream of a heated tumor. This results in a high local concentration of the drug in the tumor's vascular network. From there, the free drug rapidly diffuses into the tumor's interstitial space, driven by concentration gradients, enabling deep penetration into the tumor tissue. This is particularly beneficial for targeting hypoxic regions of the tumor, which are notoriously difficult to treat due to their poor oxygenation and limited drug accessibility.

1.7. Liposomes

Liposomes are spherical nanoparticles mainly consisting of phospholipids, featuring an aqueous inner aqueous core and an outer bilayer membrane.[31] They offer lipophilic and hydrophilic solubility, enzymatic and proteomic degradation of the payload, reduction of nonspecific side effects, readily chemical modification, and biocompatibility.[111] They can be classified by size, lipid composition, and lamellarity. The shape of a liposome is largely determined by the type of lipid used in its formulation, as different lipid combinations lead to various structural conformations. Liposomes can be tailored into different shapes and sizes depending on their intended function, ranging from monolayer to bilayer and even multilayer structures.[34] Additionally, they can be engineered to respond to environmental factors like temperature or pH, allowing for targeted release of their contents at specific sites.[112, 113]

Since their discovery in the 1960s, they have been heavily commercialized and utilized for the delivery of drugs to nucleic acid and other proteins.[114] Conventional liposomes enable drug encapsulation, helping reduce their clearance from the body. However, the reticuloendothelial system (RES) can still recognize liposomes as foreign substances through the action of opsonin, proteins that tag them for destruction, ultimately leading to their

destruction.[115] Thus, polyethylene glycol (PEG) was introduced as a steric stabilizer, preventing the RES from recognizing liposomes. This gave rise to long-circulating liposomes that, with prolonged circulation times, can passively extravasate from the blood vessels into the tumor regions and concentrate (EPR effect).[116] However, PDAC is characterized by extensive fibrosis and hypovasculature, which diminishes the effect of EPR. These factors challenge nanoparticle delivery to the tumor because even if the liposomes are retained in the interstitial space, the PEG prevents interaction with the tumor cell. To overcome this, there have been advancements in the design of liposomes due to their surface functionalization and the lipids used to improve liposome internalization and drug release.[117] These modifications make liposomes sensitive to the TME feature; however, due to the heterogeneous nature of the TME, they provide uncontrollable release. Thus, more work is needed when it comes to designing and manufacturing liposomes.

As mentioned, liposomes can carry hydrophobic drugs within their bilayer membrane or hydrophilic drugs in their aqueous core. The retention of hydrophilic drugs depends on their charged state, as charged molecules are more likely to be retained within the liposomes. In contrast, uncharged molecules can more easily pass through the membrane; there are two major liposome manufacturing methods: passive and active loading.[31] Passive loading involves incorporating a drug during the liposome formation process by mixing it with the lipids as they are hydrated to form liposomes. This method is most suitable for water-soluble drugs dissolved in the aqueous phase during liposome formation. However, trapping efficiencies are usually low, ranging between 10-50%[113, 118, 119]. Although passive loading is a simple and straightforward technique, it typically results in lower drug encapsulation than active loading. Active loading involves incorporating a drug into preformed liposomes, utilizing a transmembrane pH gradient

or ion gradient to drive drug uptake. This highly efficient method results in high intraliposomal drug concentrations and is most effective for weakly basic, ionizable drugs.

Common techniques include pH gradient loading, ammonium sulfate, and ion gradient loading (Figure 1.9).[120, 121] Active loading allows for higher drug-to-lipid ratios compared to passive loading, and the drug can be loaded immediately before use, enhancing stability during storage.[120] It is generally preferred for ionizable drugs due to its much higher encapsulation efficiency. However, passive loading may be necessary for non-ionizable or highly hydrophobic drugs that cannot be actively loaded. Ultimately, the choice of method depends on the physicochemical properties of the specific drug being encapsulated.

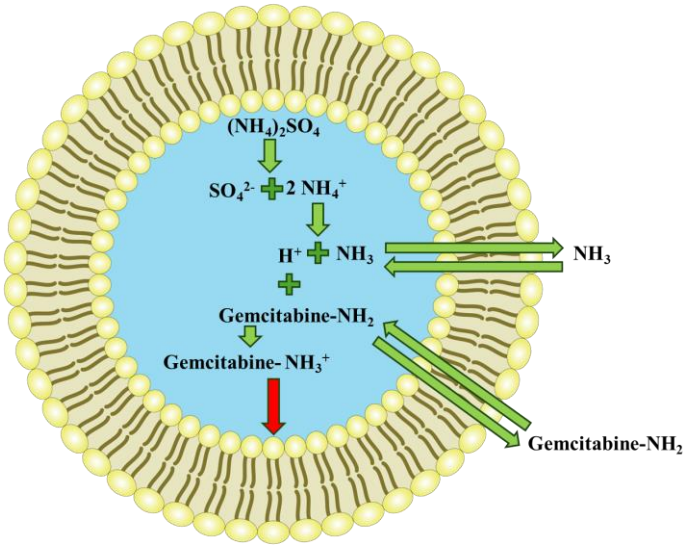

Figure 1.9. pH gradient loading.

Figure 1.10 depicts general manufacturing protocol starts with the dissolution of lipids in organic solvents, typically chloroform and methanol, allowing for uniform mixing of the lipid components. The organic solvents are then removed, usually by rotary evaporation, to create a thin lipid film on the walls of a round-bottom flask. This lipid film is hydrated with an aqueous buffer solution, forming multilamellar vesicles (MLVs). MLVs undergo size and lamellarity reduction through sonication, heat extrusion through polycarbonate membranes, or high-pressure homogenization. Drug Loading occurs during two different stages depending on the technique. In passive loading, the drug is incorporated during the hydration step, mixed with the aqueous buffer used to hydrate the lipid film. On the other hand, active

loading is performed after the liposomes are formed, using methods like the pH gradient, ammonium sulfate gradient, or ion gradient techniques.

Purification and Characterization are essential to remove unencapsulated drugs and any residual organic solvents. Purification methods such as dialysis, column chromatography, or tangential flow filtration are commonly used. The final liposome formulation is then characterized by particle size, distribution, and zeta potential to ensure proper formulation.

Gemcitabine (pKa of 3.6) requires a significantly lower pH than other drugs to be efficiently retained within the liposomes under normal physiological conditions. Thus, both

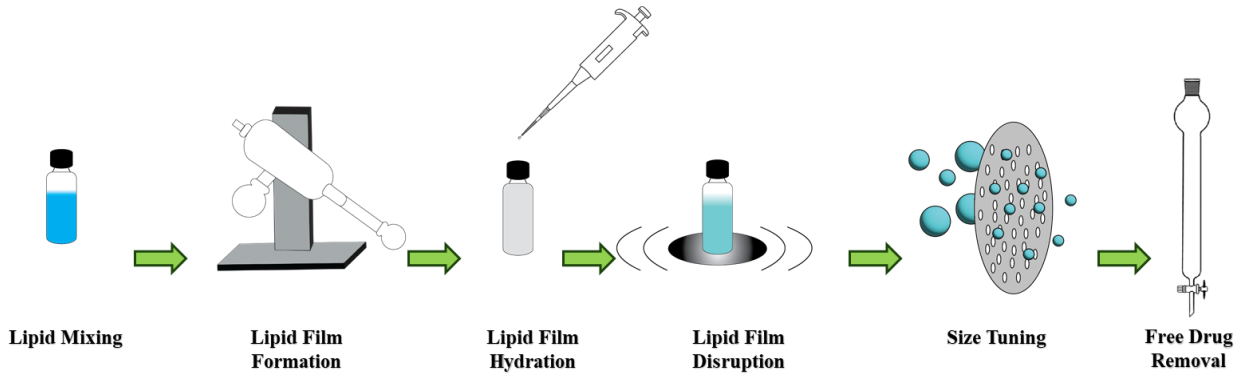

Figure 1.10. Liposome manufacturing. Passive loading is a widely used technique for encapsulating drugs in liposomes. This method first forms a lipid film by evaporating organic solvents from a lipid mixture. The dry film is then hydrated with an aqueous solution, causing the lipids to self-assemble into liposomes. The size and lamellarity of the liposomes are fine-tuned through extrusion, where the suspension is passed through membranes of defined pore sizes. Finally, the liposomes are purified by column chromatography to remove unencapsulated compounds, ensuring a homogenous and stable formulation.

passive and active methods can load gemcitabine into the liposomes. Nevertheless, the low pKa of gemcitabine limits the ionization in the relatively acidic aqueous compartment of liposomes (Figure 1.9). Gemcitabine liposomal formulations showcase a low encapsulation rate compared to other drugs. Efforts have been made to enhance the retention of gemcitabine in liposomes by incorporating derivatives, prodrugs, chelation, or modifying solvents. However, these modifications can alter the release profile of gemcitabine, and the prolonged circulation of

nanoparticles may lead to their accumulation in non-target tissues, potentially reducing the drug's efficacy and increasing off-target effects.

To further increase the targeting capacity of the liposomes, novel systems were developed by using heat to trigger the release of the payload in a specific area. This mechanism depends on the thermotropic phase transition of phospholipids, where, upon heat stimulation, they go from an ordered gel state to a disordered crystal state. The mismatches of the acyl chain create release pockets from which gemcitabine can be released. This approach tackles the slow release of gemcitabine from accumulated nanoparticles. However, gemcitabine remains with poor loading efficiency due to the pH-dependent lipophilicity of gemcitabine. Thus, new nanoparticles can be formulated to modify retention, release, and even trigger sensitivity.

1.9. Microemulsions

Microemulsions (MEs) have emerged as promising drug delivery systems. MEs are thermodynamically stable, optically isotropic liquid solutions composed of oil, water, surfactants, and co-surfactants.[122] With droplet sizes ranging from 10 to 300 nm, these systems exhibit unique properties that make them potential carriers for drug delivery; as small nanoparticles can undergo renal clearance, and larger nanoparticles tend to be up taken by phagocytes [15, 123] The small droplet size and low surface tension contribute to their high absorption and permeation, ensuring efficient encapsulation and transport of the drug.

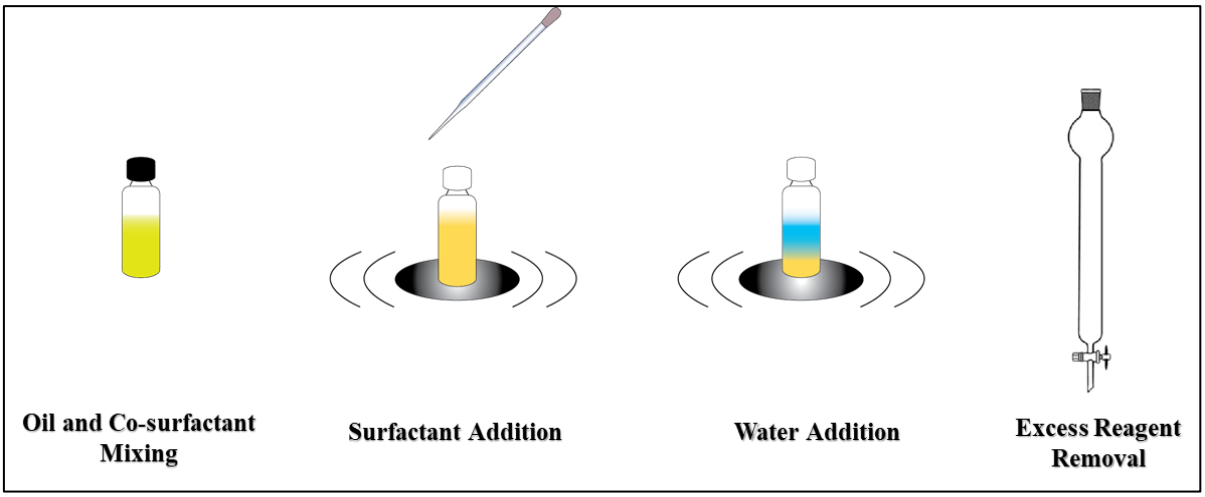

Figure 1.11. Microemulsion manufacturing. Spontaneous microemulsion is a simple manufacturing process. It relies on combining hydrophilic and hydrophobic phases and mixing them; then, the surfactant is added to create microemulsions. Column chromatography is used to remove excess surfactants.

Hoard and Schulman first observed the formation of MEs in 1943 by titrating a milky emulsion with hexanol.[122] MEs comprise three components: surfactant, co-surfactant, and solvents (hydrophilic, hydrophobic, or both).[124, 125] Since their discovery, microemulsions have developed mainly for transdermal or oral drug delivery. The two most common microemulsion systems are oil-in-water (O/W) MEs and water-in-oil (W/O) MEs, which allow versatile drug incorporation.[126] Nevertheless, they can incorporate substances other than oil and water due to their versatility. Unlike liposomes, MEs are composed of a single-layer membrane with an aqueous or oil core, which allows various drugs to be loaded.

Using a low-shear reverse micellar method, Sarma and collaborators designed insulin-encapsulated microemulsions to maintain the insulin structure.[127] The formulation included triacetin as the oil phase, insulin solution as the aqueous phase, didodecyldimethylammonium bromide as the surfactant, and propylene glycol as the co-surfactant. The study found that these MEs enhanced the oral bioavailability of insulin and slightly lowered blood glucose levels in diabetic rats. Oral administration has been found to benefit greatly from the use of

microemulsions. Water-in-oil (W/O) microemulsions improve oral bioavailability by offering protection against enzymatic degradation and modifying the fluidity of the mucosal membrane. For example, an in vitro study showed that a peptide incorporated into a W/O microemulsion was safeguarded from enzymatic degradation. Additionally, when the HIV transactivator protein TAT was delivered orally using a W/O microemulsion, it demonstrated a longer half-life than the free form of the drug.[128]

Due to the wide range of available ingredients, the selection and compatibility of components in a microemulsion system are critical. These choices depend on factors such as the drug's physicochemical properties, the stability of the system, and the intended route of administration. Common methods for manufacturing microemulsions include the Phase Inversion Temperature method, spontaneous emulsification, and ultrasound-assisted emulsification (Figure 1.11).[129] Typically, the process involves blending the oil, surfactant, and co-surfactant, then gradually adding the aqueous phase with heating, cooling, or ultrasound adjustments to optimize the formulation. The characterization is like those of liposomes mentioned above.

An advantage of MEs over liposomes for cancer treatment is that they allow for a wider administration route, as MEs tend to be more resistant to non-aqueous environments. However, unlike liposomes, the components of MEs tend not to be biocompatible, and certain solvents of interest are found difficult to include in the formulation.

Chapter 2 - Thermosensitive Liposomes for Gemcitabine Delivery to Pancreatic Ductal Adenocarcinoma

Published: Aparicio-Lopez CB, Timmerman S, Lorino G, Rogers T, Pyle M, Shrestha TB, Basel MT. Thermosensitive Liposomes for Gemcitabine Delivery to Pancreatic Ductal Adenocarcinoma. Cancers (Basel). 2024 Sep 1;16(17):3048. doi: 10.3390/cancers16173048. PMID: 39272906; PMCID: PMC11394165.

2.1 Abstract

Treatment of pancreatic ductal adenocarcinoma with gemcitabine is limited by an increased desmoplasia, poor vascularization, and short plasma half-life. Heat-sensitive liposomes modified by polyethylene glycol (PEG; PEGylated liposomes) can increase plasma stability, reduce clearance, and decrease side effects. Nevertheless, translation of heat-sensitive liposomes to the clinic has been hindered by the low loading efficiency of gemcitabine and by the difficulty of inducing hyperthermia in vivo. This study was designed to investigate the effect of phospholipid content on the stability of liposomes at 37 °C and their release under hyperthermia conditions; this was accomplished by employing a two-stage heating approach. First the liposomes were heated at a fast rate, then they were transferred to a holding bath. Thermosensitive liposomes formulated with DPPC: DSPC: PEG2k (80:15:5, mole%) exhibited minimal release of carboxyfluorescein at 37°C over 30 min, indicating stability under physiological conditions. However, upon exposure to hyperthermic conditions (43 °C and 45 °C), these liposomes demonstrated a rapid and significant release of their encapsulated content. The encapsulation efficiency for gemcitabine was calculated at 16.9%. Additionally, fluorescent analysis during the removal of unencapsulated gemcitabine revealed an increase in pH. In vitro tests with BxPC3

and KPC cell models showed that these thermosensitive liposomes induced a heat-dependent cytotoxic effect comparable to free gemcitabine at temperatures above 41 °C. This study highlights the effectiveness of the heating mechanism and cell models in understanding the current challenges in developing gemcitabine-loaded heat-sensitive liposomes.
Keywords: liposomes, thermosensitive, controlled release, gemcitabine, pancreatic cancer

2.2. Introduction

Pancreatic ductal adenocarcinoma (PDAC) is the most prevalent form of pancreatic cancer in the U.S. Its incidence continues to rise nationwide, accompanied by one of the lowest 5-year relative survival rates, hovering at approximately 10% [66, 130-132] According to the National Cancer Institute, pancreatic cancer in the U.S. constitutes roughly 3% of all cancer cases and contributes about 7% of all cancer-related deaths, making it the 4th deadliest cancer. Due to shifting demographics of aging, diabetes, and obesity, the incidence of PDAC is projected to double over the next decade.[66] The problem is further compounded by the lack of early detection methods and effective treatments for PDAC. Thus, it is poised to become the second deadliest cancer in the future.[66, 133, 134]

The efficacy and prognosis of PDAC treatment are largely dependent upon the disease's stage at the time of diagnosis and location in the pancreas, with 65% being located in the head of the pancreas.[133, 135] The only potentially curative therapy available is surgical resection, followed by adjuvant chemotherapy or radiotherapy.[136] However, only 20% of PDAC patients present with resectable tumors, whereas 80% exhibit locally advanced, non-resectable tumors or distant metastases.[137] In cases where resection is not feasible or borderline resectability presents, systemic chemotherapy emerges as the primary treatment approach. This includes the

administration of gemcitabine and capecitabine (nucleoside analogs) or 5-fluorouracil (pyrimidine analog).[138, 139]

Gemcitabine is a chemotherapy drug that acts as an antimetabolite. Free gemcitabine is a weak base (pKa: 3.6) also known as 2′,2′-difluorodeoxycytidine (dFdC) and serves as a potent and well-tolerated chemotherapeutic agent.[140] Its minimal systemic toxicity stems from its swift conversion into the less potent difluoro-uridine derivative (dFdU), which is rapidly eliminated through renal processes, giving gemcitabine a plasma half-life of approximately 15 min.[113, 141, 142] The antitumor mechanism of action relies on the arrest of the cell cycle at the S-phase by inhibiting ribonucleotide reductase and DNA synthesis through the di- and tri-phosphorylated metabolites (dFdCDP and dFdCTP), respectively.[140] Nevertheless, due to fast clearance and degradation, high and frequent doses are required to achieve therapeutic effects, leading to an increase in adverse side effects [143]

Liposomes are spherical nanoparticles mainly consisting of phospholipids, featuring an aqueous inner core and an outer bilayer membrane.[144-146] Their exceptional biocompatibility and versatility in fabrication render them highly effective delivery vehicles for drugs.[147] Gemcitabine loading depends on the acidity of the liposome inner core, which protonates and positively charges gemcitabine, preventing it from crossing out of the lipid bilayer.[36] With a pKa of 3.6, gemcitabine requires a significantly lower pH compared to other drugs to be efficiently retained within the liposomes under normal physiological conditions. Thus, the increase of intraliposomal pH during processing could result in loss of gemcitabine and poor encapsulation efficiency.

Coating liposomes with polyethylene glycol (PEG) prevents plasma clearance by the reticuloendothelial system.[145, 148, 149] PEGylated liposomes show an increase in passive targeting due to longer circulation times; liposomes can infiltrate the interstitial space around the tumor

due to leaky blood vessels and faulty lymph drainage (enhanced permeation and retention effect).[116, 150, 151] Nonetheless, in highly desmoplastic tumors such as those found in pancreatic cancer, this effect is diminished due to physical barriers, such as fibrosis and positive interstitial pressure, which limit the number of molecules that can reach the tumor cells.[116, 152] Therefore, exogenous stimuli such as heat (hyperthermia) have been used to increase permeability of the tumor fibrosis and induce angiogenesis; these effects favor the infiltration of particles and molecules to the tumor cells.[153-155]

Mild hyperthermia (defined as tissue temperatures of 41–44 °C) increases blood perfusion and tumor permeability. The increased permeability can lead to the extravasation and retention of liposomes within the tumor region.[156] Similarly, hyperthermia induces the production of heat shock proteins due to heat stress. These proteins activate antigen-presenting cells, initiating an immune response to the tumor. [96, 157, 158] Despite the improved accumulation of liposomes accomplished by hyperthermia, gemcitabine is not biologically available because its slow release from the carrier keeps the concentrations below the effective dosage.[159] Thermosensitive liposomes (TSLs) possess the capability to release encapsulated drugs in response to increases in temperature; this release is made possible by the reversible thermotropic transition properties of phospholipids.[160, 161] The increase in temperature induces transition of the phospholipid phase from an ordered state to a disordered state, allowing the release of the payload.[161] Furthermore, the use of phospholipids with different transition temperatures allows researchers to shift the release temperature of liposomes, depending on the fractional percentages and transition temperatures of the phospholipids used.[162] The trigger release of TSLs occurs exclusively in tumor blood vessels where heat is applied, with minimal drug uptake by the tumor at normal temperatures.[163] The combination of TSLs and hyperthermia offers control of

gemcitabine's spatiotemporal release such that higher drug concentrations are released from the TSLs in the hyperthermic region.

Here, we propose to enhance gemcitabine's targeting capabilities by encapsulating it in thermosensitive liposomes for more focused spatial–temporal release. In this study, we developed and characterized gemcitabine-loaded TSLs. We explored their behavior in pancreatic cancer cell models, particularly assessing how their cytotoxic effects vary with changes in temperature. This research aims to give insight into the potential of these liposomes for targeted use in pancreatic cancer treatment.

2.3. Materials and Methods

2.3.1. Materials

1,2-dipalmitoyl-sn-glycero-3-phosphocholine (DPPC; 850355); 1,2-distearoyl-sn-glycero-3-phosphocholine (DSPC; 850365); and 1,2-dipalmitoyl-sn-glycero-3-phosphoethanolamine-N-[methoxy(polyethylene glycol)-2000] (ammonium salt; PEG2k; 880160) were purchased from Avanti Polar Lipids, Alabaster, AL. Oregon Green ™ 514 Carboxylic Acid, Succinimidyl Ester (O6139), and 5(6)-carboxyfluorescein (404105000) were purchased from Thermo Fisher Scientific, Waltham, MA, USA . Gemcitabine hydrochloride (G0367) was purchased from TCI America, Portland, OR, USA. Dulbecco′s Phosphate Buffered Saline (PBS) (D8537) and RPMI-1640 medium (R8758) were purchased from Sigma Aldrich, St. Louis, MO, USA. Dulbecco′s Modified Eagle′s Medium–high glucose (D6429) and dimethyl sulfoxide (D128) were purchased from Fisher Scientific, Hampton, NH, USA. T-thermocouple (30AC8642) was purchased from Omega Engineering, Norwalk, CT, USA. MTT reagent (M922050) was purchased from RPI Corp., Mount Prospect, IL, USA.

2.3.2. Carboxyfluorescein Thermosensitive Liposome Manufacturing and Release

Temperature-sensitive liposomes (TSLs) were prepared by thin-film hydration followed by freeze-thaw cycling and heat extrusion at 50 °C. Phosphatidyl liposomes were composed of DPPC: DSPC: PEG2k with DSPC-PEG set at 5 mol% and DPPC = 100-X -5(PEG), DSPC = X; X: 30, 25, 20, 15, 10, or 5 mol%. Formulations are referred to by the percentage of DPPC in the formulation.

A hydrating solution of 50 mM carboxyfluorescein (CF) was prepared using a 250 mM sodium chloride base solution, followed with pH adjustment to physiological pH (7.4) using 0.1 M NaOH. Lipids at the selected ratios were mixed in chloroform to create a homogenous mixture and chloroform was slowly evaporated by air flush and heat cycles to create a thin lipid film in a 20 mL crystal vial. Next, the hydrating solution and the lipid film were heated up to 45 °C and the mix was vortexed to induce lipid film disruption and liposomal formation until no lipid residuals were seen on the vial. Subsequently, the lipid mix was subjected to 10 freeze-thaw cycles using liquid nitrogen and a 45 °C hot water bath; this was followed by 10 cycles of heat extrusion at 50 °C through a polycarbonate membrane with a 100 nm pore diameter. Unencapsulated CF was removed by using a 20 cm × 1 cm chromatography column filled with Sephadex G-50 resin equilibrated with 1x PBS. Fractions containing CF-loaded liposomes were collected for later analysis.

CF-loaded liposomes were prepared as described above and each of the solutions was standardized to set the fluorescence within the linear range (5–12 mM CF) by diluting with PBS. A total of 100 µL of the liposome solution was then added to a well in a 96-well plate. To measure the temperature in real time, a 96-well plate was equipped with four T-type thermocouples and attached to a TC08 data logger. Two hot water baths were set up, one at 55

°C for temperature ramp-up and another for temperature holding (37, 42, and 45 °C). The liposomes were placed in the ramp-up bath until the desired temperature was reached, as measured by the thermocouple plate, and then transferred to the holding water bath. The plates were kept in the holding water bath for a set amount of time and then transferred to an ice-cold bath to prevent further CF release.

Plates were exposed to the holding temperature for 2, 5, 10, 15, 20, 25, or 30 min; the baseline is the fluorescence of the liposomes at room temperature. Fluorescence was read using Spectramax i3x.

2.3.3. Gemcitabine-Loaded Thermosensitive Liposome Manufacturing and Release

The liposome DPPC fraction that showed no significant release for 30 min at 37 °C was used for succeeding studies. A 2.5 mg/mL gemcitabine hydrochloride solution was prepared with 250 mM sodium chloride solution, and pH was adjusted to 2.8 with 0.1 M NaOH. The lipid film formation was created as described above. Lipid films were hydrated with the gemcitabine solution at 45 °C with vigorous mixing for 5 min to form gemcitabine liposomes. Freeze–thaw and heat extrusion cycles were performed as described above.

To evaluate gemcitabine loading in liposomes and the efficiency of drug release at various times and temperatures, several 100 μL aliquots were taken and diluted 10 times in 1X PBS: (I) a sample of liposomes after the freeze–thaw and heat extrusion cycles was kept to determine encapsulation efficiency; (II) a sample of Gemcitabine-loaded liposomes was kept at 37 °C for 30 min to measure base release of gemcitabine; (III) 0.1% Triton™ X-100 was added to liposomes at 60 °C for 30 min to quantify the total amount of gemcitabine in the final solution (TX-100); and (IV) samples heated at various temps with gentle mixing for 30 min to assess the release of gemcitabine from liposomes. A sample of liposomes was also added to 10%

FBS/DMEM media to assess its stability in serum. Treated solutions were passed through Amicon® Ultra spin filters (7kD MWCO) at 10,000 rpm at 4 °C for 15 min to extract free gemcitabine. A standard curve was created by dissolving gemcitabine in PBS. The absorbance at 270 nm of the resulting filtrate was measured in triplicate using a NanoDrop Spectrophotometer, and gemcitabine concentration in each liposome formulation was determined by interpolation to standard curves created for gemcitabine. Sample III was used to adjust the concentration of encapsulated gemcitabine to 250 μM, which was used for cell treatments.

2.3.4. Intraliposomal pH Measurements

The changes in intraliposomal pH are hypothesized to directly affect the gemcitabine retention. Oregon Green 514 was used to measure pH changes in the liposomes during preparation. This experiment was adapted from the work of DiCiccio [41]. A calibration curve was constructed by creating Oregon Green in DI water solutions at various pHs with a concentration of 34 μM Oregon Green; 150 μL of the Oregon Green solutions was added to a lipid film. The fluorescence of the solutions was measured with a SpectraMax i3X with an excitation wavelength of 488 nm; emission spectra were recorded from 513 nm to 700 nm. Spectra were normalized by dividing the respective wavelength fluorescence values by the fluorescence at peak emission (523 nm) to determine a pH-dependent emission peak. The emission intensity ratio of 523 nm/558 nm was then plotted against pH to produce a standard curve.

To measure pH changes in liposomes during processing, liposomes were prepared as described above using a hydration solution of 2.5 mg/mL gemcitabine (pH 3.2) with 34 μM Oregon Green 514. Free gemcitabine/Oregon Green was removed using the Sephadex G-50 resin column chromatography method described above. The liposomal mixture emission spectrum was

read before and after column chromatography purification. Then, the results were compared to the calibration curve described above to determine the pH inside the liposomes.

2.3.5. Cell Culture

KPC cells were cultured in T25 flasks in Dulbecco's Modified Eagle medium (DMEM) supplemented with 10% fetal bovine serum (FBS) and 1% penicillin-streptomycin. BXPC3 cells were cultured in T75 flasks in RPMI-1640 supplemented with 10% FBS and 1% penicillin-streptomycin. All cells were kept at 37 °C in a humidified 5% CO_2 incubator. Both cell lines were allowed to reach 90% confluency before being seeded into 96-well plates for experimental procedures. KPC cells were seeded at a density of 25,000 cells/cm2 and BXPC3 cells were seeded at 50,000 cells/cm2.

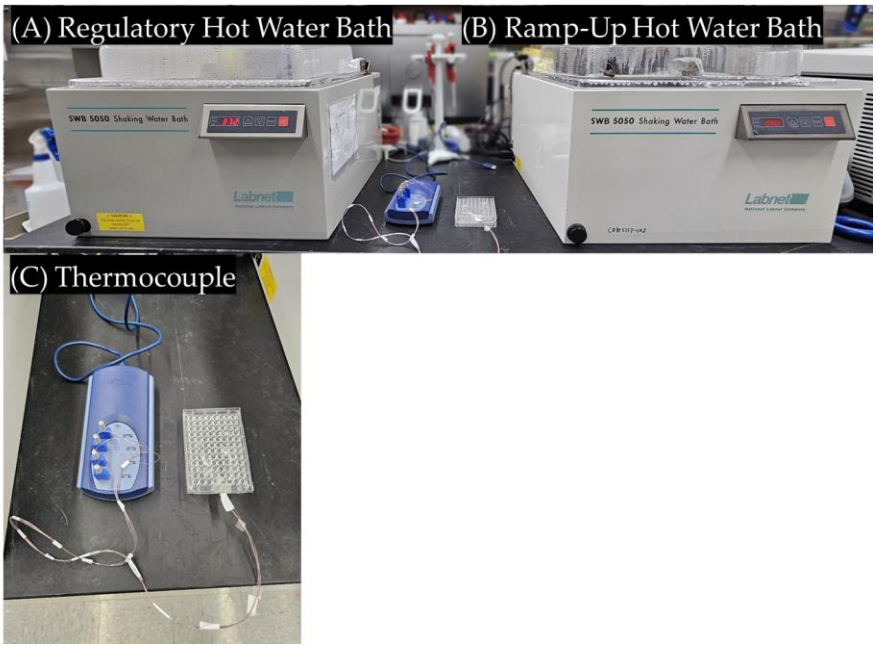

Figure 2.1. *Hyperthermia induction setup to improve the heating protocol and reduce the undesired release, a ramp-up water bath is used to increase the temperature at a rapid rate (B). The temperature of the cell is correlated to a homologous plate equipped with four thermocouples (C). Once the desired temperature is reached, the plates are transferred to the regulatory bath (A).

*Developed by Dr. Anna Bottiglieri and Dr. Faraz Chamani

2.3.6. Cell Hyperthermia Treatment

The 96-well plates seeded with KPC or BxPC3 cells were prepared as described above. A two-water bath setup was used; the temperature changes were measured with a 96-well plate

equipped with several T-thermocouples (Figure 2.1).[164] First, a 55 °C water bath was used to rapidly increase the temperature to the desired set point. Once the desired temperature was reached, the 96-well plates were transferred to a second water bath set to the temperature desired for holding (37, 39, 41, 43, or 45 °C. The plate was divided into negative control (no treatment), positive control (unencapsulated gemcitabine), and experimental (encapsulated gemcitabine) groups (9 wells per group). Free gemcitabine or gemcitabine-TSLs (250 μM of gemcitabine) were added to DMEM or RPMI with no FBS or antibiotics for cell treatment. The probe plate and the cell-containing plate were placed in the 55 °C bath until the target temperature was reached, and then both plates were transferred to the temperature-holding bath. Plates were held in the holding bath for 20 min and then were removed from the water baths. Immediately, the media on the plates was removed and replaced with fresh 10% FBS-containing media. The plates were then returned to the incubator at standard environments (37 °C, 5% CO2, 95 % humidity). After 24 h, the plates were treated with 100 μL of 0.5 mg/mL MTT reagent for 3 hrs. Then, 125 μL of DMSO was added to dissolve the MTT crystals formed, and the plates were incubated for another 2 h. The absorbance of the wells was then read at 570 nm with a reference at 650 nm using a BioTek Synergy™ H1 hybrid multi-mode microplate reader.

2.3.7. Statistical Analysis

Statistical analysis was conducted in GraphPad Prism 10. Two-way ANOVA with a Tukey's multiple comparison test was used with $\alpha < 0.05$. The Tukey p values are adjusted based on the number of replicates (see each analysis).

2.5. Results

2.5.1. Liposome Characterization

Particle size and zeta potential in CF-loaded liposomes showed no clear differences in hydrodynamic size (HS), ranging from 114 nm to 126 nm (Table 2.1). The TEM images show a narrow size distribution (Figure 2.2). Likewise, gemcitabine-loaded thermosensitive liposomes had an HS of 120 ± 8 nm. Zeta potentials for CF-loaded and gemcitabine-loaded liposomes were approximately -2.1 ± 0.21 mV (Table 2.1).

Table 2.1. Size distribution and zeta potential for CF-loaded liposomes.

DPPC Content	Size (nm)	PDI	Z-Potential (mV)
65%	125.7 ± 2.5	0.058 ± 0.010	-1.89
70%	123.3 ± 3.1	0.092 ± 0.022	-2.31
75%	119.1 ± 3.6	0.040 ± 0.009	-2.17
80%	114.7 ± 3.5	0.083 ± 0.013	-1.82
85%	124.8 ± 3.4	0.049 ± 0.027	-2.24
90%	124.8 ± 3.2	0.052 ± 0.024	-1.97

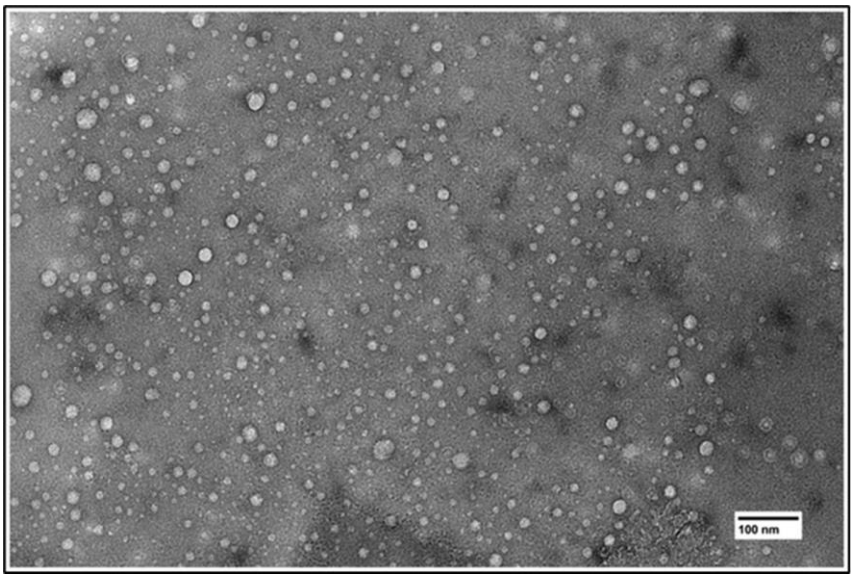

Figure 2.2. TEM image of synthesized liposomes.

2.5.2. Liposome Stability

The stability of the liposomes was measured by finding the rate of release of CF from liposomes with different DPPC ratios over time; the fluorescence reading of each TSL prep at room temperature was used as the baseline fluorescence. The maximum release was determined by lysing the TSLs with 10% Triton-X. The baseline was subtracted from all fluorescence

measurements. Then, the percentage release was calculated as the ratio of Triton-X to each temperature-dependent fluorescence measurement. Analysis showed the 80% DPPC liposomes to be the most stable with non-significant change in release percentage during 30 min at 37 °C (Figure 2.3A). The 80% DPPC liposomes were selected for later experiments. To determine whether the liposomes showed heat-dependent release, liposomes were exposed to constant-temperature baths and CF release was measured. The 80% DPPC liposomes loaded with CF demonstrated a trend toward maximal release at 43 °C with a maximum percent release of 53% (Figure 2.3B). There is a decrease in fluorescence at 45 °C; this change can be attributed to evaporation from the well and condensation into the plate lid; this causes the concentration of CF to increase due to the reduction of volume. At higher concentrations, CF self-quenches, effectively reducing fluorescence.

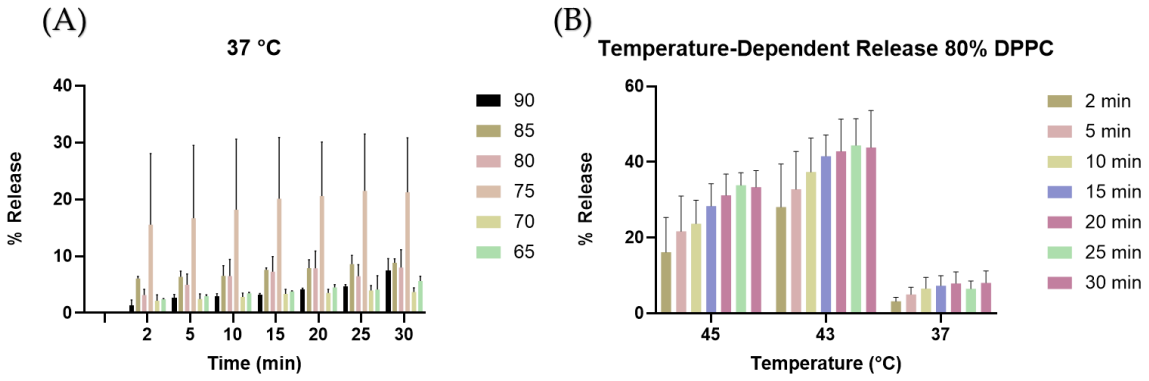

Figure 2.3. Release of CF as a function of time and temperature. (A) Release of CF at 37 °C versus time. (B) Temperature-dependent CF release from 80% DPPC fraction liposomes.

2.5.3. Encapsulation Efficiency

Gemcitabine encapsulation efficiency for gemcitabine-loaded liposomes was determined. The Equation (1) for calculating encapsulation efficiency, EE, is:

$$EE = \frac{S - F}{S} \times 100$$

Equation 1

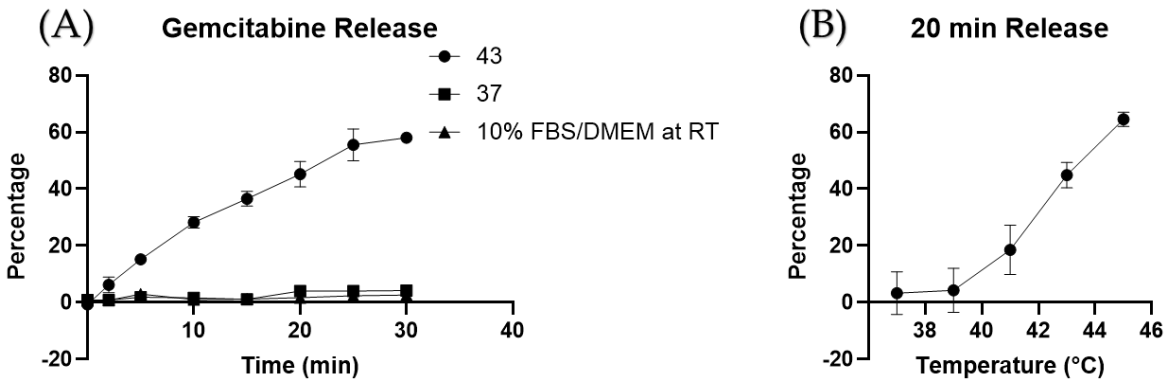

Figure 2.4. Gemcitabine release. Gemcitabine release is temperature-dependent (A). Gemcitabine-loaded TSLs under normal vs. hyperthermia conditions for 20 min (B).

where S is the initial gemcitabine concentration in the loading buffer and F is the final concentration in the loading buffer after loading. The loading efficiency measured for the gemcitabine-loaded liposomes was 16.9% ± 2%. Gemcitabine-loaded liposomes were also stable at 37 °C for 30 min and in 10% FBS/DMEM media, as determined by percentage release versus time (Figure 2.4A). The maximum release temperature was determined to be between 41 °C and 42 °C (Figure 2.4B).

To assess the encapsulation efficiency of gemcitabine relative to pH, changes in intraliposomal pH were determined by measuring the fluorescence shifts of Oregon Green. First, normalization against fluorescence at 523 nm of pH-dependent fluorescence showed a pH-dependent peak at 558 nm (green arrow, Figure 2.5A). A ratio between the pH-independent peak (red arrow) and the pH-dependent peak (green arrow) is plotted against pH, yielding a sigmoidal curve (Figure 2.5B). This yielded a fluorescence linear range between a pH of 3.2 and 4.3 (Figure 16C). Finally, the expected protonation percentage was calculated and plotted against pH values (Figure 2.5D). Using the fluorometric ratio calculation previously set, intraliposomal

Table 2.2. Liposome pH

	Pre-Column	Post-Column
523/558	1.5	2.3
Calculated pH	3.2	4.2

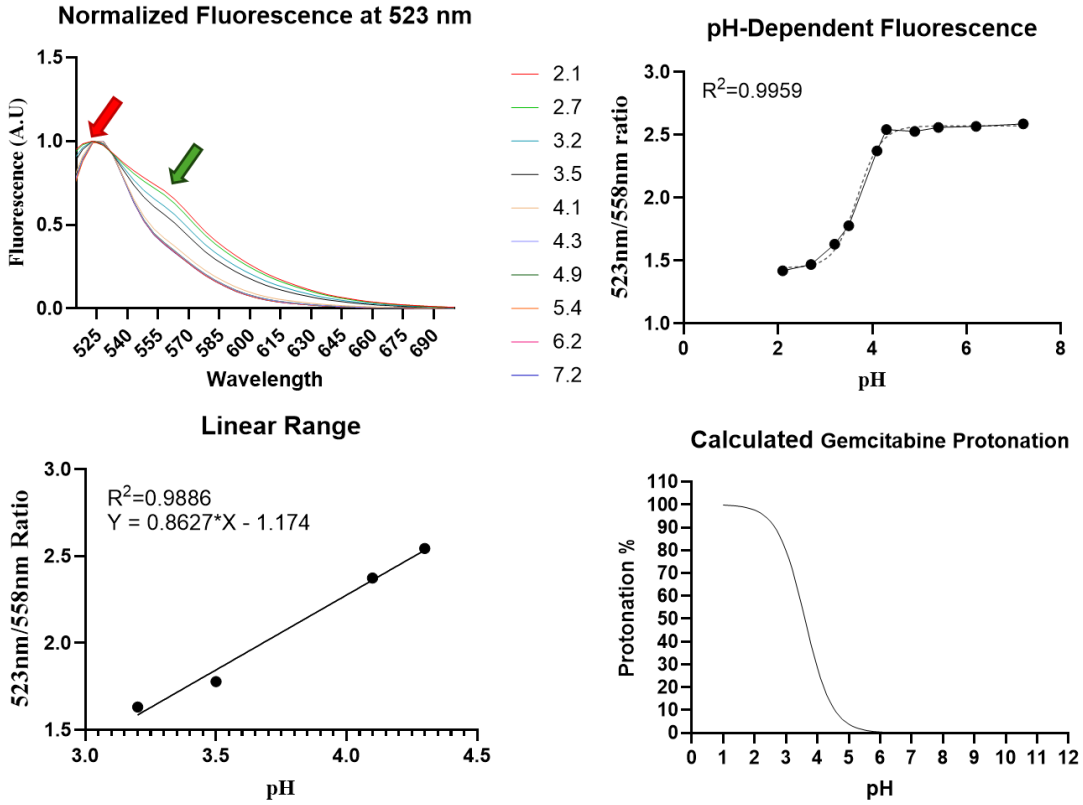

Figure 2.5. Oregon Green pH determination. (A) Normalization of signal to remove concentration variation. (B) pH vs. ratio plot. (C) pH–fluorescence linear range. (D) Calculated protonation percentages of gem.

pH was calculated (Table 2.2). The 80% DPPC liposomal formulation shows a change of pH values after liposomes were processed with the Sephadex 50G resin chromatography column.

2.5.4. In Vitro Viability Studies

In vitro cytotoxicity assays were conducted with two cell line models (BxPC3 and KPC) using liposomal gemcitabine or a free gemcitabine concentration of 250 µM, simultaneous hyperthermia treatment (39, 41, 43, and 45 °C), and a treatment time of 20 min. In the KPC cell

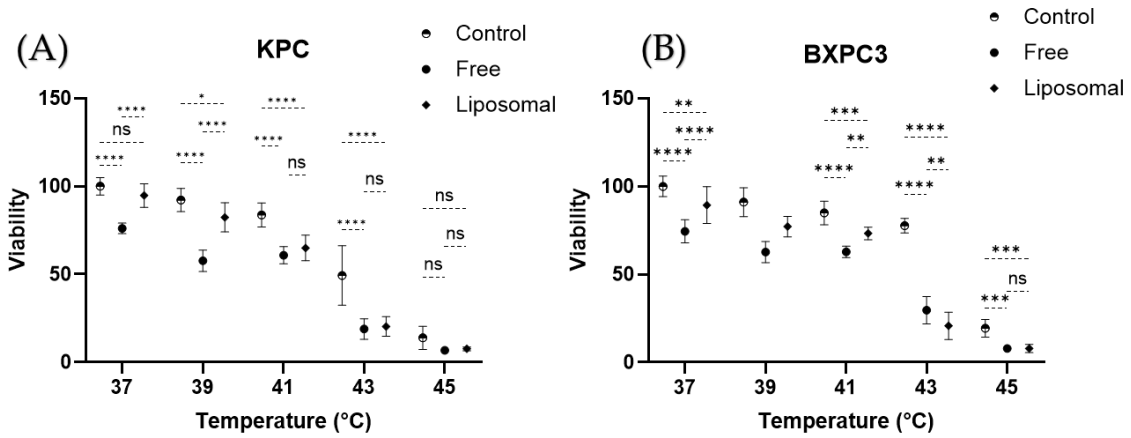

Figure 2.6. ns: P > 0.05; *: P ≤ 0.05; ** :P ≤ 0.01; ***: P ≤ 0.001; ****: P ≤ 0.0001. MTT cytotoxicity studies. (A) KPC cell line. (B) BXPC3 cell line**.**

model (Figure 2.6A), a 37 °C control shows no significant difference when compared to the liposomal gemcitabine (p > 0.05), while there is a decline in cell viability of free gemcitabine against the untreated control (p < 0.05). When the temperature is increased to 41 °C, liposomal gemcitabine and free gemcitabine present no significant difference (p > 0.05), while the control group differs from the liposomal gemcitabine group (p > 0.05). On the other hand, the BxPC3 model (Figure 2.6B) shows significant differences amongst the three groups at any temperature; nevertheless, a similar temperature-dependent trend can be observed (Figure 2.6B).

2.6. Discussion

This study shows that gemcitabine-loaded thermosensitive liposomes that have transition temperatures in the mild hyperthermia range can be synthesized; this can be achieved by varying the fraction of phospholipids with different transition temperatures. The liposomes can be used to reduce off-target side effects and to narrow the treatment area to any hyperthermic region. These two characteristics allow the treatment of pancreatic cancer while sparing healthy tissue.

The lipid fractions used in this study yield liposomes of similar sizes and dispersity indexes (Figure 2.2 and Table 2.1). Thus, size was not a factor when choosing the DPPC fraction to be used in later studies. Similarly, the Z-potential of the liposomes was similar due to the same proportion of PEG (5% mol) being used in all formulations (Table 2.1). It is widely known that the temperature-dependent release of drugs from thermosensitive liposomes depends on the transition temperature of the lipids being used. The transition temperature of DPPC is 41 °C, while that of DSPC is 55 °C.[162] Nevertheless, due to the geometrical interactions of the phospholipids, liposomes can burst release at temperatures below the lowest transition temperature. This is demonstrated with the 75% DPPC fraction in Figure 2.3A, which shows a large release variability at 37 °C. In addition, since the term “transition temperature” refers to the temperature where the membrane is most permeable [165], some release can be expected from all formulations at temperatures below the membrane transition temperature. Thus, despite most of the DPPC fractions demonstrating some release at 37 °C, the 80% fraction was chosen after statistical analysis showed no significant release changes over time (Figure 2.3B).

Typically, liposomal cargo loading is done using hydrating solutions at physiological pH because the molecules of interest have a pKa larger than 7.4. However, because gemcitabine must be charged to be entrapped within the liposomes, the pH needs to be lowered to increase the

protonation of gemcitabine, and the resultant percentage of molecules entrapped. First, we added the gemcitabine to the hydrating solution while keeping the pH low in order to trap the gemcitabine molecules after liposome formulation. Encapsulation efficiency was used to assess the amount of gemcitabine entrapped by measuring the starting concentration of gemcitabine and the concentration after heat extrusion (Equation (1)). Usually, the release profile graph of a TSL shows a decrease in release after the phase transition temperature is reached.[162] However, due to the low concentration of gemcitabine used in our experiments, the low gemcitabine gradient across the liposomal gradient prevents the burst release of gemcitabine, causing a continued increase in release, as seen in Figure 2.4A, B. As mentioned, poor loading efficiency has characterized liposomal formulations of gemcitabine. Though the loading methods can improve loading efficiency, we hypothesize that the proton concentration is high at the hydration step and later increases during chromatography (Table 2.2). The reduction in concentration of both protons and payload (gemcitabine/Oregon Green) during the chromatography step can cause changes in absorbance and fluorescence. The use of a ratiometric graph allows us to overcome the loss of Oregon Green molecules (Figure 2.5A). Then, by using the lowest pH value within the linear range of a pH against fluorescence graph 3.2 (Figure 2.5B, C), we assess the pH after liposomal purification (Table 2.2). Figure 2.5D predicts the protonation percentage of gemcitabine at a given pH. The protonation percentage can then be inferred to be the maximal amount of gemcitabine that can be kept inside a liposome. When comparing the protonation percentage at the calculated pH from Table 2.2, the expected protonation and the loading efficiency are close values. In short, we learned that there is a difference between pH pre- and post-column chromatography for unencapsulated gemcitabine.

Two cell lines, BXPC3 and KPC, were used to evaluate the killing capacities of gemcitabine in a temperature-dependent manner. An ideal gemcitabine-loaded TSL would have no effect on cell viability at temperatures below hyperthermia regardless of exposure time, thus maintaining viability like the negative control group. However, upon heat stimulation, the release of gemcitabine from liposomes would be expected to have effects like those of the free gemcitabine treatment. We compared the cytotoxic effect of gemcitabine-loaded TSLs against that of free gemcitabine. Hence, we limited the exposure of the cells to gem formulations to 20 min. Several studies use exposures of over 12 h, which does not emulate the conditions of the drug in the body, since gemcitabine has such a short plasma half-life.[138, 140] Only the KPC cell line demonstrated a response to liposomal treatment similar to that expected of an ideal TSL. In addition, there are marked growth differences between the two cell lines. KPC cells are characterized by their high growth rate, while BXPC3 cells tend to reach confluency at a slower rate.[166, 167] These metabolic states could strongly affect the response to chemotherapeutic agents, precluding correct release–cytotoxicity correlation comparisons. It is worth noting that pancreatic cancer is protected by physical barriers (fibrosis and hypovasculature), so that drug delivery depends mostly on the peripheral circulation of the tumor.[167, 168]

2.7. Conclusions

Gemcitabine-containing liposomes were successfully synthesized and were stable at temperatures below 41 °C but quickly released their contents above 43 °C. These liposomes may be able to be used in combination hyperthermia–gemcitabine treatments to increase delivery to the tumor while reducing systemic exposure to gemcitabine.

Chapter 3 - Microwave-triggered lipid-surfactant Stabilized Ionic Liquid Microemulsion for Gemcitabine Delivery.

Submitted to ACS nano journal; Cesar B. Aparicio-Lopez[1], Tej B. Shrestha[3], Marla Pyle[1], Punit Prakash[2], Matthew T Basel[1]*

1 Department of Anatomy and Physiology, College of Veterinary Medicine, Kansas State University, Manhattan, KS 66506, USA

2 Department of Electrical and Computer Engineering, Kansas State University, Manhattan, KS 66506, USA

3 Nanotechnology Core of Anatomy & Physiology, Kansas State University, Manhattan, KS 66506, USA

* Correspondence: mbasel@vet.k-state.edu

3.1. ABSTRACT:

The treatment of pancreatic ductal adenocarcinoma (PDAC) faces significant challenges due to the tumor's dense stroma, limited vascularization, and heterogeneous cell population, which impede drug delivery and contribute to resistance against therapies like gemcitabine. This study investigates the development of a microwave-sensitive,

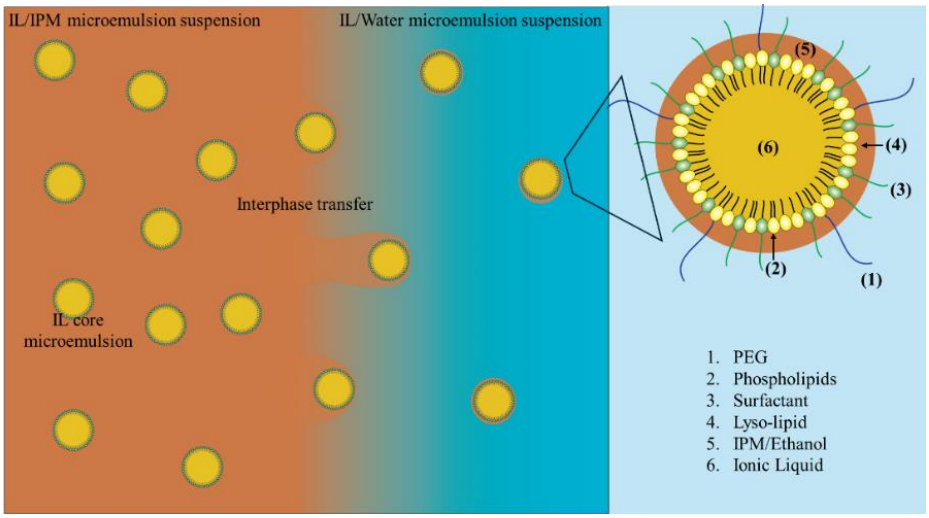

Figure 3.1. **Graphical abstract**.

lipid-stabilized ionic liquid microemulsion system to improve gemcitabine delivery to PDAC. First, gemcitabine solubility was determined in different imidazolium-based ionic liquids and water. 1,2-dipalmitoyl-sn-glycero-3-phosphocholine (DPPC); 1,2-distearoyl-sn-glycero-3-phosphocholine (DSPC); and 1,2-dipalmitoyl-sn-glycero-3-phosphoethanolamine-N- [methoxy (polyethylene glycol)-2000] (PEG), 16:0 Lyso-PC were added to the microemulsion formulation, yielding nanoparticles with a consistent size (~120 nm). Dielectric properties studies suggested microwave sensitivity of ionic liquid and microemulsions. *In vitro*, cytotoxicity assays using the KPC cell line showed hyperthermia-dependent toxicity of micro-emulsified gemcitabine, with significantly higher cytotoxicity at hyperthermic temperatures (42°C) compared to standard conditions (37°C). These results highlight the potential of this microemulsion system, which combines the solubilizing capability of ionic liquids (IL) and the advantages of localized hyperthermia, as a promising approach to address the challenges of PDAC treatment and enhance therapeutic outcomes.

3.2. Introduction:

Effective treatment of PDAC faces significant obstacles, aside from late diagnosis.[66, 169] The dense stromal environment, poor vascularization, and heterogeneous cell populations create significant barriers for therapy, contributing to intrinsic and acquired resistance to treatments like gemcitabine, a first-line therapy for non-resectable PDAC.[170-172] Despite its widespread use, gemcitabine's efficacy is considered to be limited by to its poor accumulation at the tumor site, which is caused by PDAC-asscociated desmoplasia and reduced vascular supply.[173] This, combined with gemcitabine’s administration via intravenous (IV) infusion, leads to off-target toxicity and frequent dosing, which can result in severe side effects.[174, 175] Therefore, innovative

drug delivery systems that overcome these obstacles and enhance therapeutic outcomes are crucial.

Gemcitabine, a nucleoside analog antimetabolite, arrests DNA synthesis, leading to apoptosis.[140] However, its short plasma half-life, which can range from 1.7 to 19 hours depending on patient factors, necessitates frequent administration, increasing the likelihood of systemic toxicity.[70] Nanoparticle-based drug delivery systems offer a promising solution to the challenges faced in treating PDAC by leveraging the enhanced permeability and retention (EPR) effect, which allows for better accumulation of chemotherapeutic agents at the tumor site while minimizing off-target effects.[15, 176, 177] Additionally, nanoparticles can be engineered with surface modifications that ease targeted delivery to cancer cells, improving the treatment's efficacy.[178] The ability to encapsulate drugs within nanoparticles also protects them from premature degradation.[179, 180]

Microemulsions, which are thermodynamically stable colloids composed of oil, water, surfactant, and cosurfactant, have emerged as a versatile platform for drug delivery due to their solubility, scalability, and ease of production.[122, 181] Recent advances have seen the use of ionic liquids, a class of poorly coordinated salts with low melting points, in drug delivery.[181-184] Ionic liquids offer several advantages, including dissolving a wide range of drugs.[185] Ionic-liquid-based microemulsions are particularly interesting for transdermal delivery, and they have shown promise in improving drug solubility and stability.[181, 186]

An exciting application of these systems is in conjunction with microwave-induced mild hyperthermia (MHT). Ionic liquids possess strong dielectric properties that enable them to respond to microwave stimuli generating heat.[187] MHT can increase tumor permeability by enhancing blood flow and vascular permeability, promoting nanoparticle extravasation into the

tumor microenvironment.[188] Due to their nonionizing nature and ability to penetrate deep tissues, microwaves offer a practical and efficient method for inducing localized hyperthermia in cancer treatment.[107]

This study explores the development of microwave-sensitive, lipid-saturated-stabilized ionic liquid microemulsion for gemcitabine delivery. We began by evaluating the gemcitabine solubility in various imidazolium-based ionic liquids. Next, surfactants and co-surfactants were screened, incorporating lipids to stabilize the microemulsion. Microemulsion morphology and stability, as well as the dielectric properties, were characterized to confirm microwave sensitivity. In vitro cytotoxicity studies with KPC cells assessed drug delivery efficiency, comparing encapsulated and unencapsulated gemcitabine under standard and hyperthermic conditions. Together, these findings establish a novel drug delivery platform that addresses the limitations of current drug delivery systems by combining the solubilizing capacity of ionic liquids, their microwave sensitivity, the stabilizing effects of lipid-surfactant systems, and hyperthermia as trigger release.

3.3. Results and Discussion

The alkylation reaction successfully synthesized 1-butyl-3-methylimidazolium bromide. Unreacted reagents were successfully removed by ethyl acetate precipitation of the product. ^{1}H and ^{13}C NMR confirmed a highly pure product, with spectra analyzed using MestreNova 15.0.1. The observed peaks corresponded to the predicted frequencies based on the compound's structure (Supplementary Information, S1).

Bromobutane ^{1}H NMR (400 MHz, CHLOROFORM-*d*) δ ppm 0.92 (t, *J*=7.46 Hz, 3 H) 1.45 (dq, *J*=14.92, 7.46 Hz, 2 H) 1.78 - 1.87 (m, 2 H) 3.39 (t, *J*=6.78 Hz, 2 H); ^{13}C NMR (101 MHz, CHLOROFORM-*d*) δ ppm 13.13 (s, 1 C) 21.31 (s, 1 C) 33.45 (s, 1 C) 34.80 (s, 1 C).

Methyl-Imidazole ^{1}H NMR (400 MHz, DEUTERIUM OXIDE) δ ppm 3.42 (s, 7 H) 6.77 (s, 2 H) 6.82 (s, 2 H) 7.32 (s, 2 H); ^{13}C NMR (101 MHz, DEUTERIUM OXIDE) δ ppm 32.78 (s, 1 C) 121.11 (s, 1 C) 127.45 (s, 1 C) 138.24 (s, 1 C)

1-Butyl-3-methylimidazolium Bromide ^{1}H NMR (400 MHz, DEUTERIUM OXIDE) δ ppm 0.90 (t, *J*=7.46 Hz, 1 H) 1.31 (dq, *J*=14.92, 7.46 Hz, 2 H) 1.80 - 1.90 (m, 2 H) 3.91 (s, 3 H) 4. 21 (t, *J*=7.29 Hz, 2 H) 7.46 (d, *J*=2.03 Hz, 1 H) 7.52 (d, *J*=2.03 Hz, 1 H) 8.77 (s, 1 H); ^{13}C NMR (101 MHz, DEUTERIUM OXIDE) δ ppm 12.93 (s, 1 C) 18.92 (s, 1 C) 31.42 (s, 1 C) 36.00 (s, 1 C) 49.41 (s, 1 C) 122.98 (dd, *J*=124.98, 4.36 Hz, 2 C) 135.93 (s, 1 C).

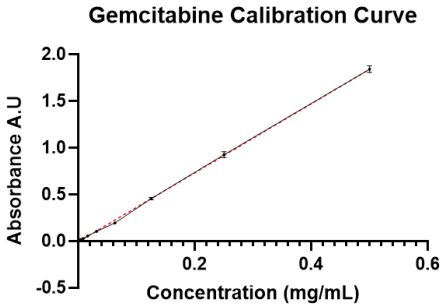

Goodness of Fit	
R squared	0.9990
Sy.x	0.01916
Equation	Y = 3.693*X - 0.007792

Figure 3.2. Gemcitabine calibration curve for ionic liquid mixtures.

To assess gemcitabine's solubility in ionic liquids, we tested two candidates: 1-butyl-3-methylimidazolium bromide (Br-IL) and 1-butyl-3-methylimidazolium hexafluorophosphate (F_6P-IL). The ionic liquids were saturated with gemcitabine to determine the maximum solubility. A methanol/water solution allowed the separation of the gemcitabine, yielding a usable calibration curve (Figure 3.2). Br-IL was selected due to its established biocompatibility and widespread use in biomedical applications, while F_6P-IL was chosen for its commercial availability.[181, 184] Br-IL significantly outperformed F_6P-IL, achieving a gemcitabine solubility of 92.42 mg/mL compared to only 1.1 mg/mL for F_6P-IL. Gemcitabine's solubility in deionized water was 70.91 mg/mL (Table 3.1). Br-IL was selected for subsequent experiments based on its superior solubility and favorable biocompatibility.

Table 3.1. The concentration of gemcitabine in saturated solutions.

	Saturated Water	Saturated F_6P-IL	Saturated Br-IL
Concentration (mg/mL)	70.91±1.48	1.10±0.32	92.42±1.55

To determine the optimal surfactant mixture to make ionic liquid-core microemulsion soluble in water, multiple nonionic surfactants with varying hydrophilic-lipophilic balance (HLB) values were evaluated. Tween (80 and 20) and Span (80 and 20) were combined in 2:1 (80:20) ratios (referred to as SurMix), with ethanol selected as a co-surfactant due to its lipid-dissolving properties and emulsification potential with isopropyl myristate (IPM). A 1:1 IPM/Br-IL mixture was emulsified using these nonionic surfactants. As shown in Figure 3.3A, all combinations successfully produced IL/IPM microemulsion identified as a transparent single-phase mixture. However, water solubility is crucial for IV delivery. Figure 3.3B illustrates the addition of water to the IL/IPM microemulsions, forming a double-phase solution. The IL/IPM microemulsion acts as a gel in water, but it can become water-suspended over time. Tween surfactants pose a high HLB, meaning that they favor W/O microemulsion. Thus, Figure 3.3C shows that Tween 80-based microemulsions can transition to water as a single-phase solution. This contrasts with Span surfactant, which possesses a low HLB and forms a two-phase solution in water.[189] In addition,

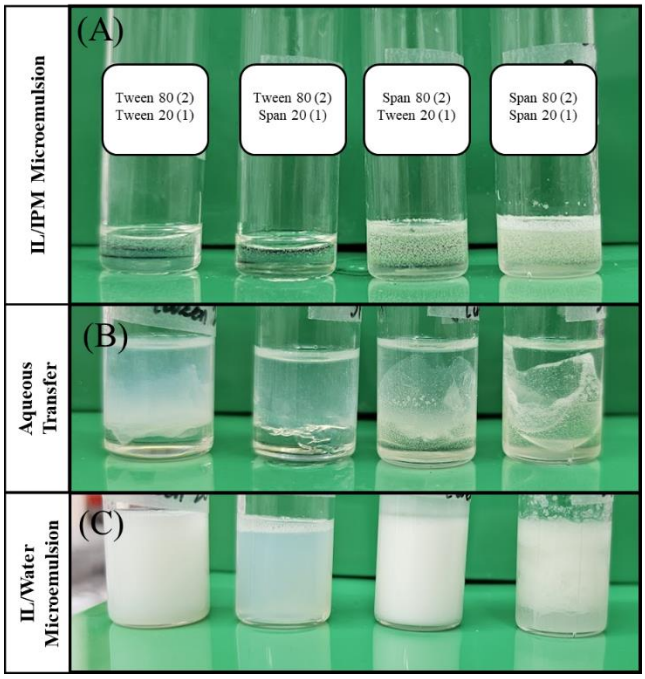

Figure 3.3. Surfactant screening for water transfer of microemulsions. (A) shows that all surfactant mixtures can form Il/IPM microemulsions. (B) Water was added for microemulsion transfer. (C) Tween 80-based surfactant mixtures show single-phase microemulsion suspension.

the surfactant mixture must be incorporated into the IPM-IL mixture dropwise to enable the formation of an IL/O microemulsion that can successfully transition into water; if they are added out of order, water transition is not viable and insoluble gels are formed. Thus, the Tween 80/Tween 20 (2:1) surfactant mix was used for subsequent experiments.

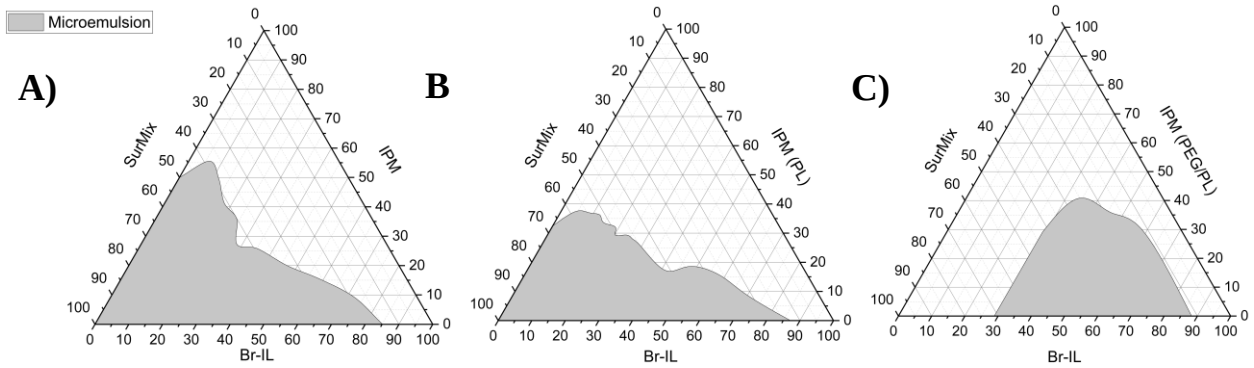

Figure 3.4 Pseudo ternary phase diagrams. (A) shows IPM with no phospholipid added. (B) DPPC, DPSC, and Lyso-lipid were added to increase biocompatibility. (C) It shows that PEG reduced the need for a surfactant mix.

To understand the microemulsion formation and size tuning process, all SurMix were used to emulsify Br-IL and IPM (alone) at concentrations from 0% to 100% at 10% increments. Using DLS measurements, no apparent trend was observed within the individual SurMix. Nevertheless, Table 3.2 shows that Tween80/Tween20 produced microemulsions with sizes within the range for ideal drug delivery.

Table 3.2. Size distributions of microemulsions in water suspension.

SurMix	Mean	Size Range
Tween80/Tween20	187.7033	128.7-271.6
Tween80/Span20	55.16533	29.74-84.73
Span80/Tween20	108.2356	67.18-153.5
Span80/Span20	824.0733	274.6-2198

To analyze the effects of adding lipids and PEG to the formulation, pseudo-ternary phase diagrams were constructed. Using Br-IL, Tween80/Tween20, and multiple IPM formulations. This also permits the mapping of concentrations where microemulsion is permitted. Figure 3.4A depicts the microemulsion region for IPM without phospholipids (PL), whereas Figure 3.4B includes the PL mixture. The microemulsion formation area changed when PEG was added to the IPM

mixture (Figure 3.4C); only concentrations of IL-Br over 30% show the formation of microemulsions. Despite this, all phase diagrams exhibit broad microemulsion regions, underscoring the strong potential for formulation. Nevertheless, the smooth transition and consistent formation of nanoparticles in water are more optimal and reproducible when the surfactant mixture is closer to the interphase line. Excess surfactant can be challenging to remove from the microemulsion solution. Thus, 85% Br-IL was chosen to maximize the ionic liquid in the formulation.

To show the microwave sensitivity of Br-IL compared to water and how this is incorporated into microemulsion, the complex permittivity was measured. Br-IL to deionized (DI) water, 0.9% saline solution, and DMEM to mimic the range of solvents encountered in practical applications. The dielectric loss tangent (δ) is defined as the ratio of the imaginary part (ε") to the real part (ε') of the complex permittivity, reflecting the material's ability to generate heat when an electric field is applied. A higher δ indicates a greater capacity to convert microwave energy into heat. For instance, water's

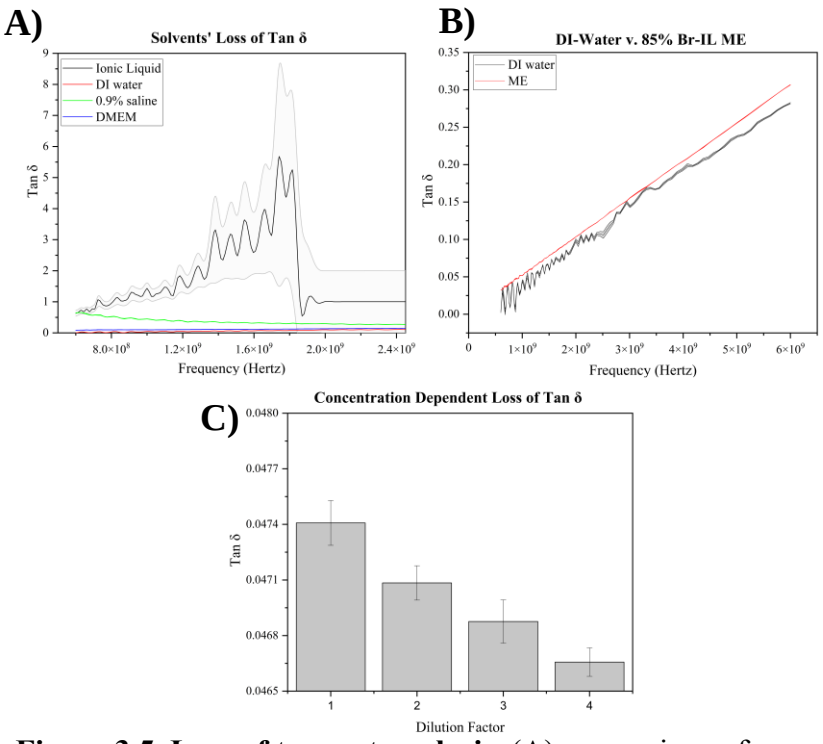

Figure 3.5. Loss of tangent analysis. (A) comparison of dielectric properties of solvents. (B) Microemulsion has more sensitivity than water. (C) Microemulsions show a concentration-dependent microwave sensitivity.

dipole moment allows it to absorb microwaves efficiently, a property commonly exploited in household microwave cooking.

Figure 3.5A presents DI water as the baseline (red line), with the addition of 0.9% sodium chloride (green line) leading to an increased δ value, attributed to the strong dielectric properties of sodium and chloride ions. In contrast, DMEM lowers the δ values, likely due to macromolecules exhibiting poor dielectric properties. Pure Br-IL significantly increases δ values, with saturation occurring at frequencies above 1,990 MHz. A comparison between a concentrated 85% Br-IL microemulsion (ME) and DI water (Figure 3.5B) reveals that ME more efficiently converts microwave energy into heat than DI water. While the tan δ value of the ME

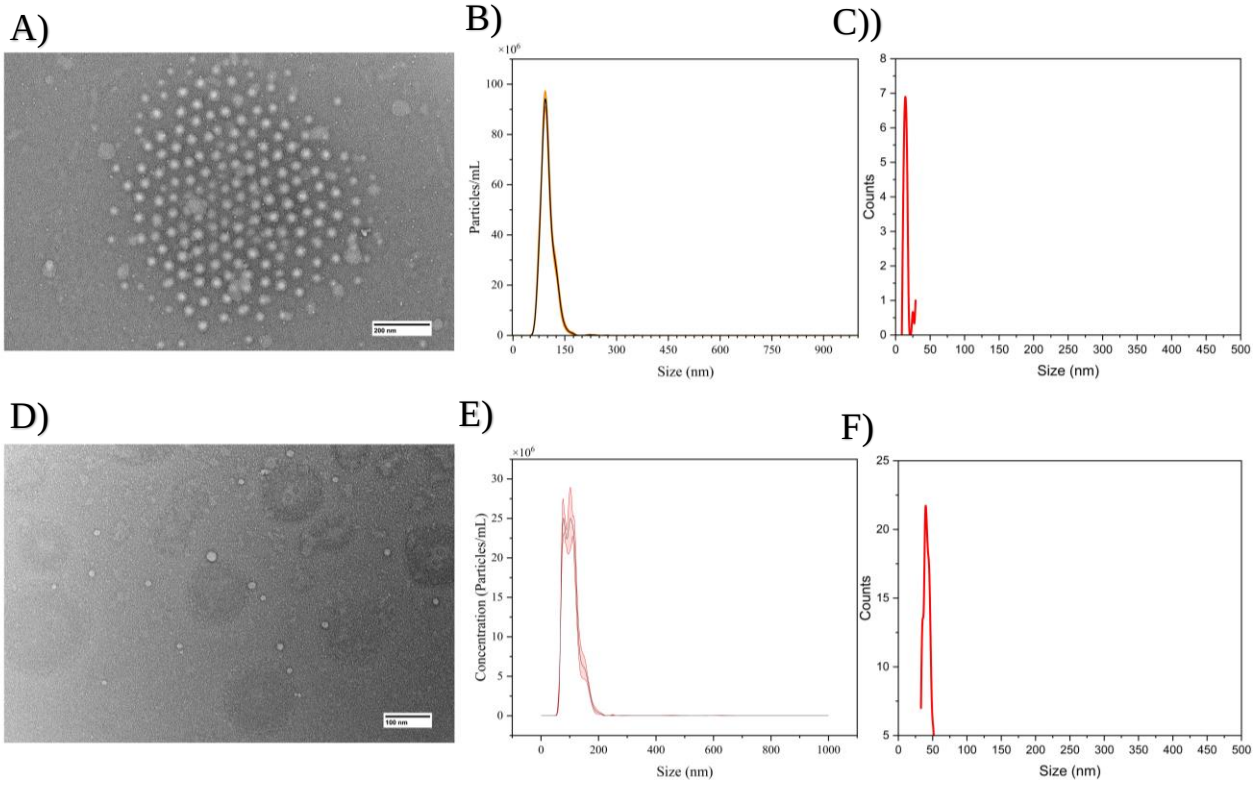

Figure 3.6. TEM and NTA analysis. A) TEM of IMP/PL microemulsion shows a circular morphology and narrow size distribution; B) shows the size distribution with NTA; C) shows the size distribution of the TEM micrographs*. D) shows that PEG-containing microemulsions have a narrow size distribution and circular morphology; E) demonstrates the NTA size distribution; F) shows the size distribution from the TEM micrographs*.

*imageJ was used to measure particle size.

is lower overall than that of 0.9% saline, this is likely due to the compartmentalization of Br-IL within the microemulsion and the solvation effect of NaCl in water, which enhances dipole interactions. Figure

3.5C highlights the concentration-dependent changes in tan δ values at 912 MHz, a frequency range frequently employed for microwave heating in laboratory experiments.[190]

We used nanoparticle tracking analysis (NTA) and transmission electron microscopy (TEM) to determine the microemulsions' size and morphology. The interaction between 2% uranyl acetate and the phospholipids in the membrane produced a dark contrast, allowing for detailed visualization. The TEM could not visualize microemulsions with only IPM. Figure 3.6A shows IPM(PL) microemulsions, revealing a uniform size distribution (Figures 3.6B-C) and confirming the presence of lipids in the outer membrane. Figure 3.6B shows a hydration radius of 120 nm. PEG was added to the PL formulation to enhance shelf-life stability, as temperatures below 4°C tend to destabilize microemulsion. The lipid-stabilized microemulsion zeta potential average is -7.15 +/- 0.08 mV, while the microemulsion with no lipids is -6.92 +/- 0.79 mV. Considering the broader size distribution of IPM-only microemulsion and zeta potential similarities, we hypothesized that the Tween 80 molecules entrapped IPM/ethanol from the IPM mixtures. Thus, yielding more stable lipid-containing microemulsions while keeping a similar surface charge explains the smooth transition of the microemulsion to water. Furthermore, as Tween 80 molecules are larger than PEG molecules, surface charge contributions come from Tween 80.

Since microemulsions are formed in the IPM phase, the stability of the microemulsion during the water transition step needs to be determined (e.g., to determine if the core flips out, causing the release of the payload). To further investigate the transfer of microemulsions from the IL/IPM phase to the aqueous phase, 5(6)-carboxyfluorescein (CF) was dissolved in Br-IL (10% w/w), and MEs were prepared. At high concentrations (e.g., when loaded in microemulsion), CF undergoes self-quenching, showing an orange-based color. In contrast, at lower concentrations (e.g., when released from the microemulsion and diluted in the medium), it exhibits a bright neon green color. Figure 3.7A shows the microemulsions in the aqueous phase with an orange hue. In contrast, Figure 3.7B displays a similar sample of CF-containing Br-IL lysed with an ethanol solution, characterized by CF's fluorescent green color. This observation confirms that the core of the microemulsion contains Br-IL and effectively limits the exposure of the dissolved molecules to the aqueous environment. In addition, this suggests that microemulsions do not undergo any catastrophic morphological changes that cause release of payload when water transfer occurs.

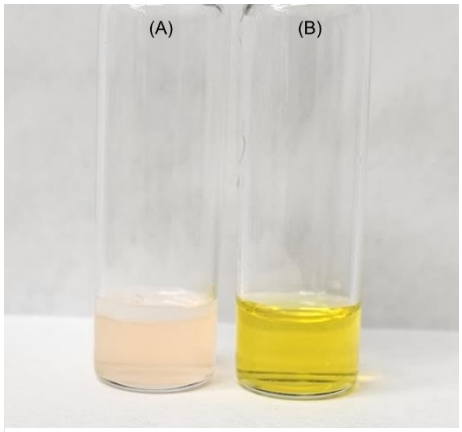

Figure 3.7. Water transfer of CF microemulsions. (A) Microemulsion suspension in water. (B) Lysed microemulsion with ethanol.

Next, microemulsions were made with gemcitabine-saturated Br-IL for cytotoxicity studies. Unlike CF, high concentrations of gemcitabine were detected in the water supernatant after removing unencapsulated gemcitabine and excess surfactants. This indicates that gemcitabine can transfer from the ionic liquid to water during processing. This effect is attributed to

gemcitabine's low lipophilicity; therefore, to improve entrapment, gemcitabine derivatives with higher lipophilicity could be used to improve loading efficiency.[140]

Microemulsions are widely recognized for their ability to deliver drugs topically into deep tissue layers. However, PDAC cannot be targeted via transdermal delivery, highlighting the need for microemulsion to form a stable water solution for intravenous administration. Since hyperthermia has been shown to enhance drug delivery to PDAC, this study explored the combined effects of microemulsions and hyperthermia on PDAC cells. *In vitro* cytotoxicity assays were performed using the KPC murine PDAC cell line to assess the efficacy of micro-emulsified gemcitabine and free gemcitabine (100 µM) under standard (37°C) and hyperthermic (42°C) conditions, with each treatment lasting 20 minutes.

As shown in Figure 3.8, the negative control groups at both 37°C and 42°C exhibited similar levels of cell viability, indicating that hyperthermia alone did not cause significant cell death in the absence of gemcitabine. This suggests that the mild elevation in temperature was insufficient to impact cell viability. When treated with free gemcitabine, the cytotoxicity levels at both 37°C and 42°C were comparable, indicating that the hyperthermic condition did not significantly alter the effectiveness of free gemcitabine. In contrast, a marked difference was observed when KPC cells were treated with micro-emulsified gemcitabine. At 37°C, micro-emulsified gemcitabine induced moderate cell death, distinct from free gemcitabine. However, at 42°C, micro-emulsified gemcitabine caused a significant reduction in cell viability, similar to that observed with free

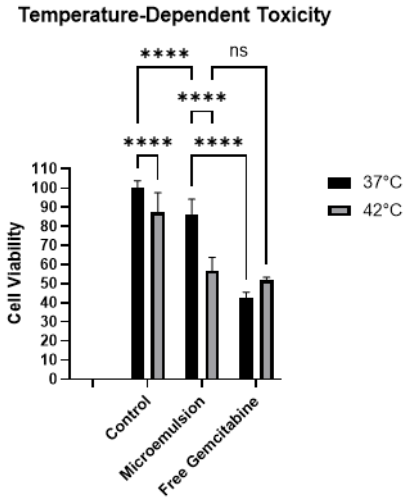

Figure 3.8. Cytotoxicity of gemcitabine formulations. P vales; ns, P>0.05; *, P<0.05; **, P<0.01; ***, P<0.001; ****, P<0.0001

gemcitabine at the same temperature. This pronounced decrease in cell viability at 42°C suggests a temperature-dependent enhancement of the cytotoxic effects of micro-emulsified gemcitabine. This study demonstrates the potential to treat PDAC with gemcitabine using an innovative delivery system consisting of a microwave-sensitive, lipid-surfactant stabilized ionic liquid microemulsion. 1-Butyl-3-methylimidazolium as the ionic liquid significantly enhanced gemcitabine solubility, outperforming conventional solvents such as water. Additionally, the dielectric properties of microemulsion show promising efficient microwave-induced hyperthermia.

Overall, DPPC, DSPC, and Lyso- PC, with PEG incorporation, improved shelf-life and preserved functionality during storage and treatment. Notably, hyperthermia significantly amplified the cytotoxic effect of encapsulated gemcitabine in PDAC cells, particularly at elevated temperatures, indicating a synergistic effect between localized heating and drug efficacy.

3.4. Materials and Methods

1,2-dipalmitoyl-sn-glycero-3-phosphocholine (DPPC); 1,2-distearoyl-sn-glycero-3-phosphocholine (DSPC); and 1,2-dipalmitoyl-sn-glycero-3-phosphoethanolamine-N- [methoxy (polyethylene glycol)-2000] (ammonium salt; PEG2k), and 16:0 Lyso-PC were purchased from Avanti Polar Lipids, Alabaster, AL. Gemcitabine hydrochloride was purchased from TCI America, Portland, OR. Dulbecco′s Phosphate Buffered Saline (PBS) was purchased from Sigma Aldrich, St. Louis, MO. Chloroform-d and deuterium oxide were purchased from Thermoscientific, Fair Lawn, NJ. Polyoxymethylene sorbitan ester surfactants Tween® 20, Tween® 80, and sorbitan ester Span® 80 and Span® 20 were bought from Sigma-Aldrich, St. Louis, MO. Methyl-butyl imidazolium hexafluorophosphate. 1-Butyl-3-methylimidazolium

hexafluorophosphate,1-Methyl imidazole, and Bromobutane were purchased from Sigma Aldrich, St. Louis, MO. The KPC cell model was a gift from the Troyer lab.
Software used: Origin2024b, MastreNova 15.0.1, GraphPad Prism 10, ImageJ

3.4.1. 1-Butyl-3-methylimidazolium bromide synthesis

The synthesis of the Br-IL was conducted by adding 70 mL acetonitrile to a three-neck round bottom flask heated to 70 °C for five minutes, then 5.16 mL bromobutane (6.55 g, 47.8 mmol, Aldrich) and *N*-methyl imidazole (3.18 mL, 39.9 mmol, Aldrich) were added to the flask. The mixture was refluxed at 80 °C for five hours. After the reaction, the mixture was cooled to room temperature and thin-layer chromatography was used to check the reaction progress. Excess acetonitrile was removed by rotavapor, and the product was washed three times with ethyl acetate. Pale-yellow oil was produced with a yield of 75%. ^{13}C and ^{1}H NMR were carried out with 400 MHz Avance Neo Bruker NMR. Methyl imidazolium and the ionic liquid product were dissolved in D_2O, and Bromobutane was dissolved in $CDCl_3$.

3.4.2. Gemcitabine Solubility Studies

Saturated 1-Butyl-3-methylimidazolium bromide, 1-Butyl-3-methylimidazolium hexafluorophosphate, and deionized water were prepared by adding excess gemcitabine hydrochloride; the mixtures were stirred at 39 °C for 48 hours. Afterward, the undissolved gemcitabine was separated by decantation. A calibration curve was prepared by dissolving gemcitabine in a 2:1 water-methanol solution, and UV absorption was measured using a NanoDrop 8000 spectrophotomter (ThermoFisher, Waltham, MA) at a wavelength of 272 nm. A reference solution was prepared by dissolving each ionic liquid at the same concentration as its

saturated counterpart. Both solutions were diluted until no ionic liquid contribution was detected at 272 nm.

3.4.2. Dielectric Measurements

A probe connected to an Agilent network analyzer (Agilent Technologies, Inc., Santa Clara, CA) measures the imaginary part of the complex permittivity (ε") and the real part of the complex permittivity (ε'). The instrument was calibrated with air and DI water. The frequencies 0.6 GHz to 6 GHz were used to obtain the ε" and ε' values. DI water, 0.9% saline, and DMEM were controls, and pure ionic liquid and microemulsions were set as analytes of interest. The loss of tangent was calculated by finding the ratio of ε" over ε'. The results were graphed using Origin2024 software.

3.4.3. Surfactant and Co-surfactant Screening

Mixtures of Tween 80, Tween 20, Span 80, and Span 20 were screened for their ability to emulsify 1-Butyl-3-methylimidazolium bromide. Likewise, propylene glycol and ethanol were screened for their ability to emulsify IPM, DPPC, DSPC, and Lyso PC. Various surfactant mixtures (SurMix) were then prepared in a 2:1 ratio: Tween 80/Tween 20, Tween 80/Span 20, Span 80/Tween 20, and Span 80/Span 20. Br-IL was mixed with IPM in a 1:1 ratio, and the SurMix was added dropwise to the BrIL-IPM mixture while vortexing. The microemulsion formation was confirmed when the mixture became a single-phase clear solution.

These Surmix and IPM alone were used to make Br-IL microemulsions. In short, Br-IL was added to IPM at concentrations from 0% to 100% w/w. The SurMix were added until microemulsion formation was observed (clear mixture), and then they were transferred to water, size distribution was measured by ZetaSizer Nano ZSP (Malvern Panalytical, Westborough, MA).

A phospholipid-containing solution was prepared. In short, 2.4 mL DPPC in chloroform (20 mg/mL), 2.4 mL DSPC in chloroform (20 mg/mL), and 200 µL Lyso-lipid in chloroform (20 mg/mL) were mixed. The chloroform was evaporated using a rotavapor, followed by filtered air flushing cycles. 0.833 mL ethanol was added to the dried lipid film, followed by 4.167 mL IPM. This mixture was referred to as IPM(PL) and was characterized by gelatinous consistency at RT. PEG was added to the phospholipid mixture to improve microemulsion stability, 0.905 mL DPPC in chloroform (20 mg/mL), 0.905 mL DSPC in chloroform (20 mg/mL), 0.094 mL Lyso-lipid in chloroform (20 mg/mL), and .094 mL PEG chloroform (20 mg/mL) were mixed. The chloroform was evaporated using a rotavapor followed by filtered air flushing cycles. To this dried lipid film, 0.333 mL ethanol was added, followed by 1.667 mL IPM, to make the mixture designated IPM (PEG/PL) in this report.

IPM, IPM(PL), and IPM(PEG/PL) were used as co-surfactants. The ionic liquid was added to the IPM mixture in 10% increments, ranging from 0 to 100%. Subsequently, Tween 80/Tween 20, mixture was added dropwise until a single-phase clear solution was achieved, indicating the formation of a microemulsion. The mass of the surfactant mixture required to reach this point was recorded, after which an excess amount of the surfactant mixture was added.

3.4.4. Morphology Analysis

Using nano-tracking analysis, microemulsion size was measured on a NanoSight LM10 with a 405 nm laser module (Malvern Panalytical, Westborough, MA). Microemulsion zeta potential was calculated using the ZetaSizer Nano ZSP (Malvern Panalytical, Westborough, MA) for dynamic light scattering. The University of Kansas MAI conducted TEM in a Hitachi Transmission Electron Microscope (Model H-8100). In short, a 10 µL sample was added to a

grid and stained with a 2% uranyl acetate solution. ImageJ software analyzed the ME size distribution data from the TEM images.

To obtain a deeper insight into the morphology of microemulsions, 5(6) carboxyfluorescein was dissolved in Br-IL in a 10% w/w ratio. Then, a microemulsion was created to see if the CF was retained during water transfer.

3.4.5. Cytotoxicity Studies

KPC cells were cultured in T25 flasks in Dulbecco's Modified Eagle medium (DMEM) supplemented with 10% Fetal bovine serum (FBS); they were incubated under standard conditions (humidified 5% CO_2 incubator at 37°C). The cell culture was allowed to reach 90% confluency before being seeded into 96-well plates for experimental procedures. KPC cells were seeded at a density of 20,000 cells per cm^2. The experiment included three groups: negative control (no treatment), positive control (unencapsulated gemcitabine), and experimental (encapsulated gemcitabine). The free gemcitabine and micro emulsified-gemcitabine (both at 100 µM gemcitabine) were added to 10% FBS-DMEM media for treatment. For MHT treatment, a two-water-bath system was employed, and temperature changes were monitored using T-thermocouples placed in a 96-well plate, as previously described. [118] The plated cells were first placed in a 55°C water bath to rapidly raise the temperature to the target set point. Once the desired temperature was reached, the plates were moved to a second water bath set to either 37°C or 41°C for temperature maintenance for 20 minutes. After treatment, the media in each well was aspirated and replaced with 100 uL per well of fresh DMEM containing 10% FBS, and the plates were returned to the incubator. After 24 hours, an MTT assay was done to assess cytotoxicity. For the MTT assay, the medium was aspirated and replaced with 100 uL of MTT reagent (0.5 mg/mL), incubated for 7 hours. 125 µL of an SDS-based solubilization agent was added to

dissolve the resultant formazan crystals, followed by five additional hours of incubation in the incubator. Absorbance was measured at 570 nm, with a reference at 650 nm, using a BioTek SynergyTM H1 hybrid multi-mode microplate reader (Agilent Technologies, Inc., Santa Clara, CA).

Results are presented as mean ± SD, with multiple replicates being run in parallel. Statistical comparisons were performed using one-way and two-way ANOVA in GraphPad Prism 10. The P-value style chosen was GP.

Chapter 4 - Summary and Future Outlook

Lipid-based nanoparticles present exciting opportunities due to their colloidal stability, biocompatibility, scalability, ability to encapsulate hydrophobic and hydrophilic drugs, and potential for chemical modifications to enhance targeting. This dissertation focuses on two heat-responsive drug delivery systems, liposomes and microemulsions, designed to overcome the physical and biological barriers in PDAC treatment and improve drug delivery. The primary goal was to address two key challenges: (1) preventing premature gemcitabine release at storage and physiological temperatures and (2) triggering release through heat. Thermosensitive liposomes (TSLs) were engineered with optimized phospholipid compositions, achieving stability at 37°C and rapid release at 42°C (Chapter 2). Although these TSLs showed promising in vitro results, gemcitabine loading and microwave sensitivity challenges persisted. An ionic liquid-based microemulsion was developed (Chapter 3), combining transdermal delivery principles with phospholipid stabilization to enhance biocompatibility and heat responsiveness. Both systems demonstrated colloidal stability at 37°C and triggered release at 42°C.

Through these projects, we identified the phospholipid mixtures that provided the most stable liposome formulations at room temperature, improving formulation reliability. Monitoring liposome pH changes allowed us to uncover mechanisms contributing to gemcitabine degradation, offering valuable insights into drug stability and release dynamics. A two-step hyperthermia induction process, using a ramp-up followed by a maintenance water bath, improved thermal precision and better simulating clinical treatment conditions. Additionally, the scalability of the manufacturing process opens new possibilities for broader applications in drug delivery and commercial production. In the microemulsion project, we demonstrated the ionic liquid's ability to dissolve gemcitabine and characterized its dielectric properties, confirming its

ability to generate heat under microwave exposure. Phospholipids were successfully incorporated into the microemulsion membrane, while the ionic liquid remained localized at the core, validating the system's heat sensitivity and potential for temperature-responsive drug release.

Both projects also faced limitations. In the liposome system, low gemcitabine encapsulation efficiency due to pH sensitivity impacted cost-effectiveness, and passive cellular uptake made it difficult to distinguish heat-triggered release from diffusion. Furthermore, the system's reliance on water heating, with limited NaCl content due to isotonic constraints, reduced its heat transmission capacity. Future efforts will explore using glycosylated lipids for membrane stabilization and gemcitabine derivatives with higher pKa values to improve encapsulation. In the microemulsion project, gemcitabine leakage during water transfer and excess surfactant destabilized colloidal suspensions, while centrifugation and chromatography limited production scalability. Future work will involve testing phospholipids of varying chain lengths to protect the ionic liquid core better, using gemcitabine derivatives to enhance retention, and studying the direct effects of microwaves on microemulsions. Optimizing solvent systems to separate surfactants from ionic liquids will also improve formulation efficiency.

Both systems would benefit from in vivo studies using animal models to compare the concentration of gemcitabine delivered to tumor sites. Studies include three animal groups with BXPC3 tumor xenograft: a negative control group (no treatment), a positive control group (treated with free gemcitabine), and an experimental group, treated with (liposomal or microemulsion gemcitabine formulation. For TSL all three groups would receive hyperthermia treatment using a dermic thermocouple in the tumor area. Then the liver function, tumor size, and gemcitabine metabolites are compared. These tests will allow us to demonstrate the targeting

capabilities of TLS by showing tumor size reduction while liver function is maintained. For the microemulsions, a microwave antenna will be used for hyperthermia induction, here, four groups are treated, the positive and negative control, the treatment groups are a TSL and microemulsion gemcitabine. This set up allows us to compare the sensitivity of microemulsion to microwaves and compare it to TSL. Additionally, future research could explore combinations of gemcitabine with other chemotherapy agents or derivatives with slight modifications in lipophilicity to enhance retention, making these approaches more cost-effective. While scalable manufacturing has been demonstrated, addressing gemcitabine loss during formulation will be critical for clinical translation. This work offers important insights into the design and performance of lipid-based drug delivery systems, highlighting their potential to synergize with hyperthermia while paving the way for future innovations in drug delivery technology.

Bibliography

(1) University, O. S. *The Pancreas*. Open Oregon Educational Resources, https://open.oregonstate.education/aandp/chapter/17-9-the-pancreas/#fig-ch18_09_01 (accessed September 26, 2024.

(2) Michigan, U. o. *Liver and Pancreas Histology Slide, 40X Magnification*. September 26, 2024. https://histologyslides.med.umich.edu/Histology/Digestive%20System/Liver%20and%20Pancreas/190B_HISTO_40X.htm (accessed.

(3) Caruso, R.; Breitbart, W. Mental health care in oncology. Contemporary perspective on the psychosocial burden of cancer and evidence-based interventions. *Epidemiology and Psychiatric Sciences* **2020**, *29*. DOI: 10.1017/S2045796019000866.

(4) Roij, J. v.; Brom, L.; Soud, M. Y.-E.; Poll-Franse, L. v. d.; Raijmakers, N. J. H. Social consequences of advanced cancer in patients and their informal caregivers: a qualitative study. *Supportive Care in Cancer* **2019**, *27* (4). DOI: 10.1007/s00520-018-4437-1.

(5) Debela, D. T.; Muzazu, S. G.; Heraro, K. D.; Ndalama, M. T.; Mesele, B. W.; Haile, D. C.; Kitui, S. K.; Manyazewal, T. New approaches and procedures for cancer treatment: Current perspectives. *SAGE Open Medicine* **2021**, *9*. DOI: 10.1177/20503121211034366.

(6) Institute, N. C. *Cancer Classification*. https://training.seer.cancer.gov/disease/categories/classification.html (accessed 2024 Sep 20).

(7) Gupta, A.; Omeogu, C.; Islam, J. Y.; Joshi, A.; Zhang, D.; Braithwaite, D.; Karanth, S. D.; Tailor, T. D.; Clarke, J. M.; Akinyemiju, T.; et al. Socioeconomic disparities in immunotherapy use among advanced-stage non-small cell lung cancer patients: analysis of the National Cancer Database. *Scientific Reports 2023 13:1* **2023-05-20**, *13* (1). DOI: 10.1038/s41598-023-35216-2.

(8) dos-Santos-Silva, I.; Gupta, S.; Orem, J.; Shulman, L. N.; dos-Santos-Silva, I.; Gupta, S.; Orem, J.; Shulman, L. N. Global disparities in access to cancer care. *Communications Medicine 2022 2:1* **2022-04-07**, *2* (1). DOI: 10.1038/s43856-022-00097-5.

(9) Holden, C. E.; Wheelwright, S.; Harle, A.; Wagland, R. The role of health literacy in cancer care: A mixed studies systematic review. *PLoS ONE* **2021**, *16* (11). DOI: 10.1371/journal.pone.0259815.

(10) Teplinsky, E.; Ponce, S. B.; Drake, E. K.; Garcia, A. M.; Loeb, S.; Londen, G. J. v.; Teoh, D.; Thompson, M.; Schapira, L.; (COSMO), f. t. C. f. O. u. S. M. i. O. Online Medical Misinformation in Cancer: Distinguishing Fact From Fiction. *JCO Oncology Practice* **2022-August**, *18* (8). DOI: 10.1200/OP.21.00764.

(11) *Products Claiming to "Cure" Cancer Are a Cruel Deception*. U.S. Food and Drug Administration, 2020. https://www.fda.gov/consumers/consumer-updates/products-claiming-cure-cancer-are-cruel-deception (accessed 2024 October 15).

(12) Lustberg, M. B.; Kuderer, N. M.; Desai, A.; Bergerot, C.; Lyman, G. H.; Lustberg, M. B.; Kuderer, N. M.; Desai, A.; Bergerot, C.; Lyman, G. H. Mitigating long-term and delayed adverse events associated with cancer treatment: implications for survivorship. *Nature Reviews Clinical Oncology 2023 20:8* **2023-05-25**, *20* (8). DOI: 10.1038/s41571-023-00776-9.

(13) Ezike, T. C.; Okpala, U. S.; Onoja, U. L.; Nwike, C. P.; Ezeako, E. C.; Okpara, O. J.; Okoroafor, C. C.; Eze, S. C.; Kalu, O. L.; Odoh, E. C.; et al. Advances in drug delivery systems, challenges and future directions. *Heliyon* **2023/06**, *9* (6). DOI: 10.1016/j.heliyon.2023.e17488.

(14) Navya, P. N.; Kaphle, A.; Srinivas, S. P.; Bhargava, S. K.; Rotello, V. M.; Daima, H. K.; Navya, P. N.; Kaphle, A.; Srinivas, S. P.; Bhargava, S. K.; et al. Current trends and challenges in

cancer management and therapy using designer nanomaterials. *Nano Convergence 2019 6:1* **2019-07-15**, *6* (1). DOI: 10.1186/s40580-019-0193-2.
(15) Yao, Y.; Zhou, Y.; Liu, L.; Xu, Y.; Chen, Q.; Wang, Y.; Wu, S.; Deng, Y.; Zhang, J.; Shao, A. Nanoparticle-Based Drug Delivery in Cancer Therapy and Its Role in Overcoming Drug Resistance. *Frontiers in Molecular Biosciences* **2020**, *7*. DOI: 10.3389/fmolb.2020.00193.
(16) Zargar, A.; Chang, S.; Kothari, A.; Snijders, A. M.; Mao, J.-H.; Wang, J.; Hernández, A. C.; Keasling, J. D.; Bivona, T. G. Overcoming the challenges of cancer drug resistance through bacterial-mediated therapy. *Chronic Diseases and Translational Medicine* **2019/12**, *5* (4). DOI: 10.1016/j.cdtm.2019.11.001.
(17) Senapati, S.; Mahanta, A. K.; Kumar, S.; Maiti, P.; Senapati, S.; Mahanta, A. K.; Kumar, S.; Maiti, P. Controlled drug delivery vehicles for cancer treatment and their performance. *Signal Transduction and Targeted Therapy 2018 3:1* **2018-03-16**, *3* (1). DOI: 10.1038/s41392-017-0004-3.
(18) Preeti; Sambhakar, S.; Saharan, R.; Narwal, S.; Malik, R.; Gahlot, V.; Khalid, A.; Najmi, A.; Zoghebi, K.; Halawi, M. A.; et al. Exploring LIPIDs for their potential to improves bioavailability of lipophilic drugs candidates: A review. *Saudi Pharmaceutical Journal : SPJ* **2023/12**, *31* (12). DOI: 10.1016/j.jsps.2023.101870.
(19) Mohite, P.; Singh, S.; Pawar, A.; Sangale, A.; Prajapati, B. G. Frontiers | Lipid-based oral formulation in capsules to improve the delivery of poorly water-soluble drugs. *Frontiers in Drug Delivery* **2023/08/24**, *3*. DOI: 10.3389/fddev.2023.1232012.
(20) Vargason, A. M.; Anselmo, A. C.; Mitragotri, S.; Vargason, A. M.; Anselmo, A. C.; Mitragotri, S. The evolution of commercial drug delivery technologies. *Nature Biomedical Engineering 2021 5:9* **2021-04-01**, *5* (9). DOI: 10.1038/s41551-021-00698-w.
(21) Mitchell, M. J.; Billingsley, M. M.; Haley, R. M.; Wechsler, M. E.; Peppas, N. A.; Langer, R.; Mitchell, M. J.; Billingsley, M. M.; Haley, R. M.; Wechsler, M. E.; et al. Engineering precision nanoparticles for drug delivery. *Nature Reviews Drug Discovery 2020 20:2* **2020-12-04**, *20* (2). DOI: 10.1038/s41573-020-0090-8.
(22) Ridolfo, R.; Tavakoli, S.; Junnuthula, V.; Williams, D. S.; Urtti, A.; Hest, J. C. M. v. Exploring the Impact of Morphology on the Properties of Biodegradable Nanoparticles and Their Diffusion in Complex Biological Medium. *Biomacromolecules* **June 8, 2020**, *22* (1). DOI: 10.1021/acs.biomac.0c00726.
(23) Lee, J. H.; Yeo, Y. Controlled drug release from pharmaceutical nanocarriers. *Chemical Engineering Science* **2015/03/24**, *125*. DOI: 10.1016/j.ces.2014.08.046.
(24) Gao, W.; Chan, J.; Farokhzad, O. C. pH-responsive Nanoparticles for Drug Delivery. *Molecular Pharmaceutics* **2010/12/12**, *7* (6). DOI: 10.1021/mp100253.
(25) Saito, G.; Swanson, J. A.; Lee, K.-D. Drug delivery strategy utilizing conjugation via reversible disulfide linkages: role and site of cellular reducing activities. *Advanced Drug Delivery Reviews* **2003/02/10**, *55* (2). DOI: 10.1016/S0169-409X(02)00179-5.
(26) Nultsch, K.; Germershaus, O. Matrix metalloprotease triggered bioresponsive drug delivery systems – Design, synthesis and application. *European Journal of Pharmaceutics and Biopharmaceutics* **2018/10/01**, *131*. DOI: 10.1016/j.ejpb.2018.08.010.
(27) Elendu, C. The evolution of ancient healing practices: From shamanism to Hippocratic medicine: A review. *Medicine* **July 12, 2024**, *103* (28). DOI: 10.1097/MD.0000000000039005.
(28) Murthy, S. N.; Murthy, S. N. Approaches for Delivery of Drugs Topically. *AAPS PharmSciTech 2019 21:1* **2019-12-19**, *21* (1). DOI: 10.1208/s12249-019-1582-x.

(29) Gourdon, B.; Chemin, C.; Moreau, A.; Arnauld, T.; Baumy, P.; Cisternino, S.; Péan, J.-M.; Declèves, X. Functionalized PLA-PEG nanoparticles targeting intestinal transporter PepT1 for oral delivery of acyclovir. *International Journal of Pharmaceutics* **2017/08/30**, *529* (1-2). DOI: 10.1016/j.ijpharm.2017.07.024.
(30) Yun, Y. H.; Lee, B. K.; Park, K. Controlled Drug Delivery: Historical perspective for the next generation. *Journal of controlled release : official journal of the Controlled Release Society* **2015/12/12**, *219*. DOI: 10.1016/j.jconrel.2015.10.005.
(31) Liu, P.; Chen, G.; Zhang, J. A Review of Liposomes as a Drug Delivery System: Current Status of Approved Products, Regulatory Environments, and Future Perspectives. *Molecules* **2022 Feb 17**, *27* (4). DOI: 10.3390/molecules27041372.
(32) Gregoriadis, G. Liposomes as Carriers of Drugs Observations on Vesicle Fate after Injection and Its Control. *Subcellular Biochemistry* **1989**, *14*.
(33) Shah, S.; Dhawan, V.; Holm, R.; Nagarsenker, M. S.; Perrie, Y. Liposomes: Advancements and innovation in the manufacturing process. *Advanced Drug Delivery Reviews* **2020/01/01**, *154-155*. DOI: 10.1016/j.addr.2020.07.002.
(34) Nsairat, H.; Khater, D.; Sayed, U.; Odeh, F.; Bawab, A. A.; Alshaer, W. Liposomes: structure, composition, types, and clinical applications. *Heliyon* **2022/05**, *8* (5). DOI: 10.1016/j.heliyon.2022.e09394.
(35) Dymek, M.; Sikora, E. Liposomes as biocompatible and smart delivery systems – the current state. *Advances in Colloid and Interface Science* **2022/11/01**, *309*. DOI: 10.1016/j.cis.2022.102757.
(36) Hassan, T.; Jinho, P.; H., G. H.; Masters, A. R.; Abdel-Aleem, J. A.; Abdelrahman, S. I.; Abdelrahman, A. A.; Lyle, L. T.; Yeo, Y. Development of liposomal gemcitabine with high drug loading capacity. *Molecular pharmaceutics* **2019/07/07**, *16* (7). DOI: 10.1021/acs.molpharmaceut.8b01284.
(37) Ibrahim, M.; Abuwatfa, W. H.; Awad, N. S.; Sabouni, R.; Husseini, G. A. Encapsulation, Release, and Cytotoxicity of Doxorubicin Loaded in Liposomes, Micelles, and Metal-Organic Frameworks: A Review. *Pharmaceutics* **2022/02**, *14* (2). DOI: 10.3390/pharmaceutics14020254.
(38) Nogueira, E.; Gomes, A. C.; Preto, A.; Cavaco-Paulo, A. Design of liposomal formulations for cell targeting. *Colloids and Surfaces B: Biointerfaces* **2015/12/01**, *136*. DOI: 10.1016/j.colsurfb.2015.09.034.
(39) and, A. L. B.; Cullis, P. R. Membrane Fusion with Cationic Liposomes: Effects of Target Membrane Lipid Composition†. **February 18, 1997**. DOI: 10.1021/bi961173.
(40) Karpińska, M.; Czauderna, M. Frontiers | Pancreas—Its Functions, Disorders, and Physiological Impact on the Mammals' Organism. *Frontiers in Physiology* **2022/03/30**, *13*. DOI: 10.3389/fphys.2022.807632.
(41) A-Kader, H. H.; Ghishan, F. K. The Pancreas. *Textbook of Clinical Pediatrics* **2012**. DOI: 10.1007/978-3-642-02202-9_198.
(42) Bendayan, M.; Bendayan, M. Contacts between endocrine and exocrine cells in the pancreas. *Cell and Tissue Research 1982 222:1* **1982/01**, *222* (1). DOI: 10.1007/BF00218303.
(43) Dimitriou, I.; Katsourakis, A.; Nikolaidou, E.; Noussios, G. The Main Anatomical Variations of the Pancreatic Duct System: Review of the Literature and Its Importance in Surgical Practice. *Journal of Clinical Medicine Research* **2018/03/16**, *10* (5). DOI: 10.14740/jocmr3344w.
(44) Haugk, B.; Raman, S. Pancreatic pathology: an update. *Surgery (Oxford)* **2016/06/01**, *34* (6). DOI: 10.1016/j.mpsur.2016.03.012.

(45) Society, A. C. *Cancer Facts & Figures 2023*; American Cancer Society:, Atlanta, GA, USA, 2023. https://www.cancer.org/research/cancer-facts-statistics/all-cancer-facts-figures/2023-cancer-facts-figures.html.
(46) Eibl, G.; Cruz-Monserrate, Z.; Korc, M.; Petrov, M. S.; Goodarzi, M. O.; Fisher, W. E.; Habtezion, A.; Lugea, A.; Pandol, S. J.; Hart, P. A.; et al. Diabetes Mellitus and Obesity as Risk Factors for Pancreatic Cancer. *Journal of the Academy of Nutrition and Dietetics* **2018/04**, *118* (4). DOI: 10.1016/j.jand.2017.07.005.
(47) Becker, A. E.; Hernandez, Y. G.; Frucht, H.; Lucas, A. L. Pancreatic ductal adenocarcinoma: Risk factors, screening, and early detection. *World Journal of Gastroenterology : WJG* **2014 Aug 28**, *20* (32). DOI: 10.3748/wjg.v20.i32.11182.
(48) Society, A. C. *Pancreatic Cancer Risk Factors*. 2024. https://www.cancer.org/cancer/types/pancreatic-cancer/causes-risks-prevention/risk-factors.html (accessed.
(49) Wolfgang, C. L.; Herman, J. M.; Laheru, D. A.; Klein, A. P.; Erdek, M. A.; Fishman, E. K.; Hruban, R. H. Recent progress in pancreatic cancer. *CA: A Cancer Journal for Clinicians* **2013/09/01**, *63* (5). DOI: 10.3322/caac.21190.
(50) Abboud, Y.; Samaan, J. S.; Oh, J.; Jiang, Y.; Randhawa, N.; Lew, D.; Ghaith, J.; Pala, P.; Leyson, C.; Watson, R.; et al. Increasing Pancreatic Cancer Incidence in Young Women in the United States: A Population-Based Time-Trend Analysis, 2001–2018. *Gastroenterology* **2023/05/01**, *164* (6). DOI: 10.1053/j.gastro.2023.01.022.
(51) Halbrook, C. J.; Lyssiotis, C. A.; Magliano, M. P. d.; Maitra, A. Pancreatic cancer: Advances and challenges. *Cell* **2023/04/13**, *186* (8). DOI: 10.1016/j.cell.2023.02.014.
(52) Caban, M.; Małecka-Wojciesko, E. Gaps and Opportunities in the Diagnosis and Treatment of Pancreatic Cancer. *Cancers* **2023/12**, *15* (23). DOI: 10.3390/cancers15235577.
(53) Elbanna, K. Y.; Jang, H.-J.; Kim, T. K.; Elbanna, K. Y.; Jang, H.-J.; Kim, T. K. Imaging diagnosis and staging of pancreatic ductal adenocarcinoma: a comprehensive review. *Insights into Imaging 2020 11:1* **2020-04-25**, *11* (1). DOI: 10.1186/s13244-020-00861-y.
(54) Opitz, F. V.; Haeberle, L.; Daum, A.; Esposito, I.; Opitz, F. V.; Haeberle, L.; Daum, A.; Esposito, I. Tumor Microenvironment in Pancreatic Intraepithelial Neoplasia. *Cancers 2021, Vol. 13, Page 6188* **2021-12-08**, *13* (24). DOI: 10.3390/cancers13246188.
(55) Ren, B.; Liu, X.; Suriawinata, A. A. Pancreatic Ductal Adenocarcinoma and Its Precursor Lesions: Histopathology, Cytopathology, and Molecular Pathology. *The American Journal of Pathology* **2019/01/01**, *189* (1). DOI: 10.1016/j.ajpath.2018.10.004.
(56) Luo, J. KRAS mutation in pancreatic cancer. *Seminars in Oncology* **2021/02/01**, *48* (1). DOI: 10.1053/j.seminoncol.2021.02.003.
(57) Morris, J. P.; Wang, S. C.; Hebrok, M. KRAS, Hedgehog, Wnt and the twisted developmental biology of pancreatic ductal adenocarcinoma. *Nature Reviews Cancer* **2010**, *10* (10), 683-695. DOI: 10.1038/nrc2899 (acccessed 2022-10-13 19:38:14).www-nature-com.er.lib.k-state.edu.
(58) Waters, A. M.; Der, C. J. KRAS: The Critical Driver and Therapeutic Target for Pancreatic Cancer. *Cold Spring Harbor Perspectives in Medicine* **2018 Sep**, *8* (9). DOI: 10.1101/cshperspect.a031435.
(59) Mukhopadhyay, S.; Heiden, M. G. V.; McCormick, F. The Metabolic Landscape of RAS-Driven Cancers from biology to therapy. *Nature cancer* **2021/03**, *2* (3). DOI: 10.1038/s43018-021-00184-x.

(60) Tuerhong, A.; Xu, J.; Shi, S.; Tan, Z.; Meng, Q.; Hua, J.; Liu, J.; Zhang, B.; Wang, W.; Yu, X.; et al. Overcoming chemoresistance by targeting reprogrammed metabolism: the Achilles' heel of pancreatic ductal adenocarcinoma. *Cellular and Molecular Life Sciences: CMLS* **2021 Jun 15**, *78* (14). DOI: 10.1007/s00018-021-03866-y.
(61) Recouvreux, M. V.; Commisso, C. Macropinocytosis: A Metabolic Adaptation to Nutrient Stress in Cancer. *Frontiers in Endocrinology* **2017**, *8*. (acccessed 2022-10-19 15:13:47).Frontiers.
(62) Liot, S.; Balas, J.; Aubert, A.; Prigent, L.; Mercier-Gouy, P.; Verrier, B.; Bertolino, P.; Hennino, A.; Valcourt, U.; Lambert, E. Stroma Involvement in Pancreatic Ductal Adenocarcinoma: An Overview Focusing on Extracellular Matrix Proteins. *Frontiers in Immunology* **2021**, *12*. DOI: 10.3389/fimmu.2021.612271.
(63) Walker, C.; Mojares, E.; Hernández, A. D. R.; Walker, C.; Mojares, E.; Del Río Hernández, A. Role of Extracellular Matrix in Development and Cancer Progression. *International Journal of Molecular Sciences 2018, Vol. 19, Page 3028* **2018-10-04**, *19* (10). DOI: 10.3390/ijms19103028.
(64) Vonderheide, R. H.; Bayne, L. J. Inflammatory networks and immune surveillance of pancreatic carcinoma. *Current Opinion in Immunology* **2013/04/01**, *25* (2). DOI: 10.1016/j.coi.2013.01.006.
(65) Yang, S.; Liu, Q.; Liao, Q. Frontiers | Tumor-Associated Macrophages in Pancreatic Ductal Adenocarcinoma: Origin, Polarization, Function, and Reprogramming. *Frontiers in Cell and Developmental Biology* **2021/01/11**, *8*. DOI: 10.3389/fcell.2020.607209.
(66) Orth, M.; Metzger, P.; Gerum, S.; Mayerle, J.; Schneider, G.; Belka, C.; Schnurr, M.; Lauber, K.; Orth, M.; Metzger, P.; et al. Pancreatic ductal adenocarcinoma: biological hallmarks, current status, and future perspectives of combined modality treatment approaches. *Radiation Oncology 2019 14:1* **2019-08-08**, *14* (1). DOI: 10.1186/s13014-019-1345-6.
(67) Mazur, R.; Trna, J. Principles of Palliative and Supportive Care in Pancreatic Cancer: A Review. *Biomedicines* **2023/10**, *11* (10). DOI: 10.3390/biomedicines11102690.
(68) Torgeson, A.; Garrido-Laguna, I.; Tao, R.; Cannon, G. M.; Scaife, C. L.; Lloyd, S. Value of surgical resection and timing of therapy in patients with pancreatic cancer at high risk for positive margins. *ESMO Open* **2018/01/01**, *3* (1). DOI: 10.1136/esmoopen-2017-000282.
(69) Selvaggi, F.; Melchiorre, E.; Casari, I.; Cinalli, S.; Cinalli, M.; Aceto, G. M.; Cotellese, R.; Garajova, I.; Falasca, M. Perineural Invasion in Pancreatic Ductal Adenocarcinoma: From Molecules towards Drugs of Clinical Relevance. *Cancers* **2022/12**, *14* (23). DOI: 10.3390/cancers14235793.
(70) Inc., P. *gemcitabine injection solution Highlights*. 2024. https://www.pfizermedicalinformation.com/gemcitabine/highlights#S6.1 (accessed 2024 October 8).
(71) Derissen, E. J. B.; Huitema, A. D. R.; Rosing, H.; Schellens, J. H. M.; Beijnen, J. H. Intracellular pharmacokinetics of gemcitabine, its deaminated metabolite 2′,2′-difluorodeoxyuridine and their nucleotides. *British Journal of Clinical Pharmacology* **2018/06**, *84* (6). DOI: 10.1111/bcp.13557.
(72) Hagmann, W.; Jesnowski, R.; Löhr, J. M. Interdependence of Gemcitabine Treatment, Transporter Expression, and Resistance in Human Pancreatic Carcinoma Cells. *Neoplasia (New York, N.Y.)* **2010/09**, *12* (9). DOI: 10.1593/neo.10576.
(73) Montano, R.; Khan, N.; Hou, H.; Seigne, J.; Ernstoff, M. S.; Lewis, L. D.; Eastman, A. Cell cycle perturbation induced by gemcitabine in human tumor cells in cell culture, xenografts and

bladder cancer patients: implications for clinical trial designs combining gemcitabine with a Chk1 inhibitor. *Oncotarget* **2017/09/09**, *8* (40). DOI: 10.18632/oncotarget.18834.
(74) Bergman, A. M.; Eijk, P. P.; Ruiz van Haperen, V. W. T.; Smid, K.; Veerman, G.; Hubeek, I.; van den IJssel, P.; Ylstra, B.; Peters, G. J. In vivo Induction of Resistance to Gemcitabine Results in Increased Expression of Ribonucleotide Reductase Subunit M1 as the Major Determinant. *Cancer Research* **2005/10/15**, *65* (20). DOI: 10.1158/0008-5472.CAN-05-0989.
(75) Chen, Z.; Han, F.; Du, Y.; Shi, H.; Zhou, W. Hypoxic microenvironment in cancer: molecular mechanisms and therapeutic interventions. *Signal Transduction and Targeted Therapy* **2023**, *8* (1). DOI: 10.1038/s41392-023-01332-8.
(76) Liu, R.; Chen, Y.; Liu, G.; Li, C.; Song, Y.; Cao, Z.; Li, W.; Hu, J.; Lu, C.; Liu, Y.; et al. PI3K/AKT pathway as a key link modulates the multidrug resistance of cancers. *Cell Death & Disease 2020 11:9* **2020-09-24**, *11* (9). DOI: 10.1038/s41419-020-02998-6.
(77) Petrova, V.; Annicchiarico-Petruzzelli, M.; Melino, G.; Amelio, I.; Petrova, V.; Annicchiarico-Petruzzelli, M.; Melino, G.; Amelio, I. The hypoxic tumour microenvironment. *Oncogenesis 2018 7:1* **2018-01-24**, *7* (1). DOI: 10.1038/s41389-017-0011-9.
(78) Abe, T.; Toyota, M.; Suzuki, H.; Murai, M.; Akino, K.; Ueno, M.; Nojima, M.; Yawata, A.; Miyakawa, H.; Suga, T.; et al. Upregulation of BNIP3 by 5-aza-2′-deoxycytidine sensitizes pancreatic cancer cells to hypoxia-mediated cell death. *Journal of Gastroenterology 2005 40:5* **2005/05**, *40* (5). DOI: 10.1007/s00535-005-1576-1.
(79) Ariffin, A. B.; Forde, P. F.; Jahangeer, S.; Soden, D. M.; Hinchion, J. Releasing Pressure in Tumors: What Do We Know So Far and Where Do We Go from Here? A Review. *Cancer Research* **2014/05/15**, *74* (10). DOI: 10.1158/0008-5472.CAN-13-3696.
(80) Böckelmann, L. C.; Schumacher, U. Targeting tumor interstitial fluid pressure: will it yield novel successful therapies for solid tumors? *Expert Opinion on Therapeutic Targets* **2019-12-2**, *23* (12). DOI: 10.1080/14728222.2019.1702974.
(81) Guo, Z.; Zhang, H.; Fu, Y.; Kuang, J.; Zhao, B.; Zhang, L.; Lin, J.; Lin, S.; Wu, D.; Xie, G.; et al. Cancer-associated fibroblasts induce growth and radioresistance of breast cancer cells through paracrine IL-6. *Cell Death Discovery 2023 9:1* **2023-01-13**, *9* (1). DOI: 10.1038/s41420-023-01306-3.
(82) Zhong, B.; Cheng, B.; Huang, X.; Xiao, Q.; Niu, Z.; Chen, Y.-f.; Yu, Q.; Wang, W.; Wu, X.-J.; Zhong, B.; et al. Colorectal cancer-associated fibroblasts promote metastasis by up-regulating LRG1 through stromal IL-6/STAT3 signaling. *Cell Death & Disease 2021 13:1* **2021-12-20**, *13* (1). DOI: 10.1038/s41419-021-04461-6.
(83) Bedeschi, M.; Marino, N.; Cavassi, E.; Piccinini, F.; Tesei, A. Cancer-Associated Fibroblast: Role in Prostate Cancer Progression to Metastatic Disease and Therapeutic Resistance. *Cells* **2023/03**, *12* (5). DOI: 10.3390/cells12050802.
(84) Zhang, T.; Ren, Y.; Yang, P.; Wang, J.; Zhou, H.; Zhang, T.; Ren, Y.; Yang, P.; Wang, J.; Zhou, H. Cancer-associated fibroblasts in pancreatic ductal adenocarcinoma. *Cell Death & Disease 2022 13:10* **2022-10-25**, *13* (10). DOI: 10.1038/s41419-022-05351-1.
(85) Dalin, S.; Sullivan, M. R.; Lau, A. N.; Grauman-Boss, B.; Mueller, H. S.; Kreidl, E.; Fenoglio, S.; Luengo, A.; Lees, J. A.; Heiden, M. G. V.; et al. Deoxycytidine Release from Pancreatic Stellate Cells Promotes Gemcitabine Resistance. *Cancer research* **2019 Sep 4**, *79* (22). DOI: 10.1158/0008-5472.CAN-19-0960.
(86) Nakamura, Y.; Mochida, A.; Choyke, P. L.; Kobayashi, H. Nanodrug Delivery: Is the Enhanced Permeability and Retention Effect Sufficient for Curing Cancer? *Bioconjugate Chemistry* **September 2, 2016**, *27* (10). DOI: 10.1021/acs.bioconjchem.6b00437.

(87) Tanaka, H. Y.; Kano, M. R. Stromal barriers to nanomedicine penetration in the pancreatic tumor microenvironment. *Cancer Science* **2018/07/01**, *109* (7). DOI: 10.1111/cas.13630.
(88) Cheng, Y.; Weng, S.; Yu, L.; Zhu, N.; Yang, M.; Yuan, Y. The Role of Hyperthermia in the Multidisciplinary Treatment of Malignant Tumors. *Integrative Cancer Therapies* **2019**, *18*, 1534735419876345. DOI: 10.1177/1534735419876345 (acccessed 2023-10-03 15:47:43).PubMed Central.
(89) Hannon, G.; Tansi, F. L.; Hilger, I.; Prina-Mello, A. The Effects of Localized Heat on the Hallmarks of Cancer. *Advanced Therapeutics* **2021/07/01**, *4* (7). DOI: 10.1002/adtp.202000267.
(90) Molls, M.; Scherer, E. The Combination of Hyperthermia and Radiation: Clinical Investigations. *Hyperthermia and the Therapy of Malignant Tumors* **1987**. DOI: 10.1007/978-3-642-82955-0_4.
(91) Kleef R, D. H. E. Fever, Pyrogens and Cancer. In *Madame Curie Bioscience Database*, Landes Bioscience, 2000-2013.
(92) Carlson, R. D.; John C. Flickinger, J.; Snook, A. E. Talkin' Toxins: From Coley's to Modern Cancer Immunotherapy. *Toxins* **2020/04**, *12* (4). DOI: 10.3390/toxins12040241.
(93) Kirui, D. K.; Koay, E. J.; Guo, X.; Cristini, V.; Shen, H.; Ferrari, M. Tumor vascular permeabilization using localized mild hyperthermia to improve macromolecule transport. *Nanomedicine : nanotechnology, biology, and medicine* **2014/10**, *10* (7). DOI: 10.1016/j.nano.2013.11.001.
(94) Dou, Y. N.; Chaudary, N.; Chang, M. C.; Dunne, M.; Huang, H.; Jaffray, D. A.; Milosevic, M.; Allen, C. Tumor microenvironment determines response to a heat-activated thermosensitive liposome formulation of cisplatin in cervical carcinoma. *Journal of Controlled Release* **2017**, *262*, 182-191. DOI: 10.1016/j.jconrel.2017.07.039 (acccessed 2023-10-05 22:09:02).ScienceDirect.
(95) Azzi, S.; Hebda, J. K.; GAVARD, J. Frontiers | Vascular Permeability and Drug Delivery in Cancers. *Frontiers in Oncology* **2013/08/15**, *3*. DOI: 10.3389/fonc.2013.00211.
(96) Vaupel, P.; Piazena, H.; Notter, M.; Thomsen, A. R.; Grosu, A.-L.; Scholkmann, F.; Pockley, A. G.; Multhoff, G. From Localized Mild Hyperthermia to Improved Tumor Oxygenation: Physiological Mechanisms Critically Involved in Oncologic Thermo-Radio-Immunotherapy. *Cancers* **2023**, *15* (5), 1394. DOI: 10.3390/cancers15051394 (acccessed 2023-10-05 21:09:16).PubMed Central.
(97) Stylianopoulos, T.; Munn, L. L.; Jain, R. K. Reengineering the Tumor Vasculature: Improving Drug Delivery and Efficacy. *Trends in cancer* **2018/04**, *4* (4). DOI: 10.1016/j.trecan.2018.02.010.
(98) Ostberg, J. R.; Repasky, E. A. Emerging evidence indicates that physiologically relevant thermal stress regulates dendritic cell function. *Cancer Immunology, Immunotherapy : CII* **2006/03**, *55* (3). DOI: 10.1007/s00262-005-0689-y.
(99) Toraya-Brown, S.; Fiering, S. Local tumour hyperthermia as immunotherapy for metastatic cancer. *International Journal of Hyperthermia* **2014-12-1**, *30* (8). DOI: 10.3109/02656736.2014.968640.
(100) Mantso, T.; Goussetis, G.; Franco, R.; Botaitis, S.; Pappa, A.; Panayiotidis, M. Effects of hyperthermia as a mitigation strategy in DNA damage-based cancer therapies. *Seminars in Cancer Biology* **2016/06/01**, *37-38*. DOI: 10.1016/j.semcancer.2016.03.004.
(101) Chatterjee, S.; Singh, S.; Barry, S.; Guha, C. Abstract 709: Enhancing prostate cancer treatment: Synergistic effects of mechano-thermal focused ultrasound and radiation therapy. *Cancer Research* **2024/03/15**, *84* (6_Supplement). DOI: 10.1158/1538-7445.AM2024-709.

(102) Chowdhury, S. M.; Abou-Elkacem, L.; Lee, T.; Dahl, J.; Lutz, A. M. Ultrasound and microbubble mediated therapeutic delivery: Underlying mechanisms and future outlook. *Journal of Controlled Release* **2020/10/10**, *326*. DOI: 10.1016/j.jconrel.2020.06.008.
(103) Béalle, G.; Di Corato, R.; Kolosnjaj-Tabi, J.; Dupuis, V.; Clément, O.; Gazeau, F.; Wilhelm, C.; Ménager, C. Ultra Magnetic Liposomes for MR Imaging, Targeting, and Hyperthermia. *Langmuir* **2012**, *28* (32), 11834-11842. DOI: 10.1021/la3024716 (acccessed 2022-08-11 19:03:02).ACS Publications.
(104) Healy, S.; Bakuzis, A. F.; Goodwill, P. W.; Attaluri, A.; Bulte, J. W. M.; Ivkov, R. Clinical magnetic hyperthermia requires integrated magnetic particle imaging. *Wiley Interdisciplinary Reviews. Nanomedicine and Nanobiotechnology* **2022 Mar 3**, *14* (3). DOI: 10.1002/wnan.1779.
(105) Rivera, D.; Schupper, A. J.; Bouras, A.; Anastasiadou, M.; Kleinberg, L.; Kraitchman, D. L.; Attaluri, A.; Ivkov, R.; Hadjipanayis, C. G. Neurosurgical Applications of Magnetic Hyperthermia Therapy. *Neurosurgery clinics of North America* **2023 Jan 30**, *34* (2). DOI: 10.1016/j.nec.2022.11.004.
(106) Ashkbar, A.; Rezaei, F.; Attari, F.; Ashkevarian, S.; Ashkbar, A.; Rezaei, F.; Attari, F.; Ashkevarian, S. Treatment of breast cancer in vivo by dual photodynamic and photothermal approaches with the aid of curcumin photosensitizer and magnetic nanoparticles. *Scientific Reports 2020 10:1* **2020-12-03**, *10* (1). DOI: 10.1038/s41598-020-78241-1.
(107) Altintas, G.; Akduman, I.; Janjic, A.; Yilmaz, T. A Novel Approach on Microwave Hyperthermia. *Diagnostics* **2021/03**, *11* (3). DOI: 10.3390/diagnostics11030493.
(108) Rodrigues, D. B.; Dobsicek-Trefna, H.; Curto, S.; Winter, L.; Molitoris, J. K.; Vrba, J.; Vrba, D.; Sumser, K.; Paulides, M. M. Radiofrequency and microwave hyperthermia in cancer treatment. *Principles and Technologies for Electromagnetic Energy Based Therapies* **2022/01/01**. DOI: 10.1016/B978-0-12-820594-5.00007-1.
(109) Bevacqua, M. T.; Gaffoglio, R.; Bellizzi, G. G.; Righero, M.; Giordanengo, G.; Crocco, L.; Vecchi, G.; Isernia, T. Field and Temperature Shaping for Microwave Hyperthermia: Recent Treatment Planning Tools to Enhance SAR-Based Procedures. *Cancers* **2023 Mar 2**, *15* (5). DOI: 10.3390/cancers15051560.
(110) Paulides, M. M.; Dobsicek Trefna, H.; Curto, S.; Rodrigues, D. B. Recent technological advancements in radiofrequency- andmicrowave-mediated hyperthermia for enhancing drug delivery. *Advanced Drug Delivery Reviews* **2020**, *163-164*, 3-18. DOI: 10.1016/j.addr.2020.03.004 (acccessed 2022-08-13 04:15:26).ScienceDirect.
(111) Allen, T. M.; Hansen, C. B.; de Menezes, D. E. L. Pharmacokinetics of long-circulating liposomes. *Advanced Drug Delivery Reviews* **1995**, *16* (2), 267-284. DOI: 10.1016/0169-409X(95)00029-7 (acccessed 2023-09-27 17:18:29).ScienceDirect.
(112) Nahire, R.; Hossain, R.; Patel, R.; Paul, S.; Meghnani, V.; Ambre, A. H.; Gange, K. N.; Katti, K. S.; Leclerc, E.; Srivastava, D. K.; et al. pH-Triggered Echogenicity and Contents Release from Liposomes. **October 16, 2014**. DOI: 10.1021/mp500186.
(113) Tucci, S. T.; Kheirolomoom, A.; Ingham, E. S.; Mahakian, L. M.; Tam, S. M.; Foiret, J.; Hubbard, N. E.; Borowsky, A. D.; Baikoghli, M.; Cheng, R. H.; et al. Tumor-specific delivery of gemcitabine with activatable liposomes. *Journal of controlled release : official journal of the Controlled Release Society* **2019**, *309*, 277-288. DOI: 10.1016/j.jconrel.2019.07.014 (acccessed 2022-07-22 17:22:03).PubMed Central.
(114) Jensen, G. M.; Hodgson, D. F. Opportunities and challenges in commercial pharmaceutical liposome applications. *Advanced Drug Delivery Reviews* **2020/01/01**, *154-155*. DOI: 10.1016/j.addr.2020.07.016.

(115) Gregoriadis, G. Liposomes in Drug Delivery: How It All Happened. *Pharmaceutics* **2016 May 24**, *8* (2). DOI: 10.3390/pharmaceutics8020019.
(116) Torchilin, V. Tumor delivery of macromolecular drugs based on the EPR effect. *Advanced Drug Delivery Reviews* **2011**, *63* (3), 131-135. DOI: 10.1016/j.addr.2010.03.011 (acccessed 2024-04-29 11:44:48).ScienceDirect.
(117) Weber, C.; Voigt, M.; Simon, J.; Danner, A.-K.; Frey, H.; Mailänder, V.; Helm, M.; Morsbach, S.; Landfester, K. Functionalization of Liposomes with Hydrophilic Polymers Results in Macrophage Uptake Independent of the Protein Corona. *Biomacromolecules* **2019**, *20* (8), 2989-2999. DOI: 10.1021/acs.biomac.9b00539 (acccessed 2023-01-11 21:52:05).ACS Publications.
(118) Aparicio-Lopez, C. B.; Timmerman, S.; Lorino, G.; Rogers, T.; Pyle, M.; Shrestha, T. B.; Basel, M. T.; Aparicio-Lopez, C. B.; Timmerman, S.; Lorino, G.; et al. Thermosensitive Liposomes for Gemcitabine Delivery to Pancreatic Ductal Adenocarcinoma. *Cancers 2024, Vol. 16, Page 3048* **2024-09-01**, *16* (17). DOI: 10.3390/cancers16173048.
(119) Matsumoto, T.; Komori, T.; Yoshino, Y.; Ioroi, T.; Kitahashi, T.; Kitahara, H.; Ono, K.; Higuchi, T.; Sakabe, M.; Kori, H.; et al. A Liposomal Gemcitabine, FF-10832, Improves Plasma Stability, Tumor Targeting, and Antitumor Efficacy of Gemcitabine in Pancreatic Cancer Xenograft Models. *Pharmaceutical Research* **2021**, *38* (6), 1093-1106. DOI: 10.1007/s11095-021-03045-5 (acccessed 2022-11-11 19:22:03).Springer Link.
(120) Haran, G.; Cohen, R.; Bar, L. K.; Barenholz, Y. Transmembrane ammonium sulfate gradients in liposomes produce efficient and stable entrapment of amphipathic weak bases. *Biochimica Et Biophysica Acta* **1993**, *1151* (2), 201-215. DOI: 10.1016/0005-2736(93)90105-9 PubMed.
(121) MT, F.; Z, I.; E, A.; GE, B.; G, M. A. Ionic gradient liposomes: Recent advances in the stable entrapment and prolonged released of local anesthetics and anticancer drugs - PubMed. *Biomedicine & pharmacotherapy = Biomedecine & pharmacotherapie* **2018 Nov**, *107*. DOI: 10.1016/j.biopha.2018.07.138.
(122) Suhail, N.; Alzahrani, A. K.; Basha, W. J.; Kizilbash, N.; Zaidi, A.; Ambreen, J.; Khachfe, H. M. Frontiers | Microemulsions: Unique Properties, Pharmacological Applications, and Targeted Drug Delivery. *Frontiers in Nanotechnology* **2021/11/12**, *3*. DOI: 10.3389/fnano.2021.754889.
(123) Arredondo-Ochoa, T.; Silva-Martínez, G. A. Frontiers | Microemulsion Based Nanostructures for Drug Delivery. *Frontiers in Nanotechnology* **2022/01/06**, *3*. DOI: 10.3389/fnano.2021.753947.
(124) Zhang, J.; Froelich, A.; Michniak-Kohn, B. Topical Delivery of Meloxicam using Liposome and Microemulsion Formulation Approaches. *Pharmaceutics* **2020/03**, *12* (3). DOI: 10.3390/pharmaceutics12030282.
(125) Goindi, S.; Arora, P.; Kumar, N.; Puri, A. Development of Novel Ionic Liquid-Based Microemulsion Formulation for Dermal Delivery of 5-Fluorouracil. *AAPS PharmSciTech* **2014/08**, *15* (4). DOI: 10.1208/s12249-014-0103-1.
(126) Schmidt, R. F.; Prévost, S.; Gradzielski, M.; Zemb, T.; Schmidt, R. F.; Prévost, S.; Gradzielski, M.; Zemb, T. Structure of microemulsions in the continuous phase channel. *The European Physical Journal E 2023 46:9* **2023-09-05**, *46* (9). DOI: 10.1140/epje/s10189-023-00337-z.
(127) G, S.; K, W.; CF, v. d. W.; N, S.; JR, P.; MN, R. K. Microemulsions for oral delivery of insulin: design, development and evaluation in streptozotocin induced diabetic rats - PubMed.

European journal of pharmaceutics and biopharmaceutics : official journal of Arbeitsgemeinschaft fur Pharmazeutische Verfahrenstechnik e.V **2010 Oct**, *76* (2). DOI: 10.1016/j.ejpb.2010.07.002.
(128) Liu, D.; Kobayashi, T.; Russo, S.; Li, F.; Plevy, S. E.; Gambling, T. M.; Carson, J. L.; Mumper, R. J. In Vitro and In Vivo Evaluation of a Water-in-Oil Microemulsion System for Enhanced Peptide Intestinal Delivery. *The AAPS Journal* **2012 Nov 30**, *15* (1). DOI: 10.1208/s12248-012-9441-7.
(129) Mushtaq, A.; Wani, S. M.; Malik, A. R.; Gull, A.; Ramniwas, S.; Nayik, G. A.; Ercisli, S.; Marc, R. A.; Ullah, R.; Bari, A. Recent insights into Nanoemulsions: Their preparation, properties and applications. *Food Chemistry: X* **2023/06/30**, *18*. DOI: 10.1016/j.fochx.2023.100684.
(130) Angstadt, S.; Zhu, Q.; Jaffee, E. M.; Robinson, D. N.; Anders, R. A. Pancreatic Ductal Adenocarcinoma Cortical Mechanics and Clinical Implications. *Frontiers in Oncology* **2022**, *12*. (acccessed 2022-12-07 19:18:58).Frontiers.
(131) Placido, D.; Yuan, B.; Hjaltelin, J. X.; Zheng, C.; Haue, A. D.; Chmura, P. J.; Yuan, C.; Kim, J.; Umeton, R.; Antell, G.; et al. A deep learning algorithm to predict risk of pancreatic cancer from disease trajectories. *Nature Medicine* **2023**, *29* (5), 1113-1122. DOI: 10.1038/s41591-023-02332-5 (acccessed 2023-09-11 15:21:23).www.nature.com.
(132) Bakasa, W.; Viriri, S. Pancreatic Cancer Survival Prediction: A Survey of the State-of-the-Art. *Computational and Mathematical Methods in Medicine* **2021**, *2021*, 1188414. DOI: 10.1155/2021/1188414 (acccessed 2023-09-11 15:22:10).PubMed Central.
(133) Freelove, R.; Walling, A. D. Pancreatic Cancer: Diagnosis and Management. *American Family Physician* **2006**, *73* (3), 485-492. (acccessed 2023-09-12 20:57:16).www.aafp.org.
(134) Zhang, L.; Sanagapalli, S.; Stoita, A. Challenges in diagnosis of pancreatic cancer. *World Journal of Gastroenterology* **2018**, *24* (19), 2047-2060. DOI: 10.3748/wjg.v24.i19.2047 (acccessed 2023-09-12 20:45:40).PubMed Central.
(135) Barreto, S. G.; Shukla, P. J.; Shrikhande, S. V. Tumors of the Pancreatic Body and Tail. *World Journal of Oncology* **2010**, *1* (2), 52-65. DOI: 10.4021/wjon2010.04.200w (acccessed 2023-09-28 15:52:28).PubMed Central.
(136) Wei, K.; Hackert, T. Surgical Treatment of Pancreatic Ductal Adenocarcinoma. *Cancers* **2021**, *13* (8), 1971. DOI: 10.3390/cancers13081971 (acccessed 2023-09-24 01:29:53).PubMed Central.
(137) Sarantis, P.; Koustas, E.; Papadimitropoulou, A.; Papavassiliou, A. G.; Karamouzis, M. V. Pancreatic ductal adenocarcinoma: Treatment hurdles, tumor microenvironment and immunotherapy. *World Journal of Gastrointestinal Oncology* **2020/02/02**, *12* (2). DOI: 10.4251/wjgo.v12.i2.173.
(138) Regine, W. F.; Winter, K. A.; Abrams, R. A.; Safran, H.; Hoffman, J. P.; Konski, A.; Benson, A. B.; Macdonald, J. S.; Kudrimoti, M. R.; Fromm, M. L.; et al. Fluorouracil vs gemcitabine chemotherapy before and after fluorouracil-based chemoradiation following resection of pancreatic adenocarcinoma: a randomized controlled trial. *JAMA* **2008**, *299* (9), 1019-1026. DOI: 10.1001/jama.299.9.1019 PubMed.
(139) Brunner, M.; Wu, Z.; Krautz, C.; Pilarsky, C.; Grützmann, R.; Weber, G. F. Current Clinical Strategies of Pancreatic Cancer Treatment and Open Molecular Questions. *International Journal of Molecular Sciences* **2019**, *20* (18), 4543. DOI: 10.3390/ijms20184543 (acccessed 2023-09-27 17:11:54).PubMed Central.

(140) Ciccolini, J.; Serdjebi, C.; Peters, G. J.; Giovannetti, E. Pharmacokinetics and pharmacogenetics of Gemcitabine as a mainstay in adult and pediatric oncology: an EORTC-PAMM perspective. *Cancer Chemotherapy and Pharmacology* **2016**, *78* (1). DOI: 10.1007/s00280-016-3003-0.
(141) Cai, H.; Wang, R.; Guo, X.; Song, M.; Yan, F.; Ji, B.; Liu, Y. Combining Gemcitabine-Loaded Macrophage-like Nanoparticles and Erlotinib for Pancreatic Cancer Therapy. *Molecular Pharmaceutics* **2021**, *18* (7), 2495-2506. DOI: 10.1021/acs.molpharmaceut.0c01225 (acccessed 2023-01-12 21:13:51).ACS Publications.
(142) Cells, D. o. a. N. I. L. B. M. S. f. G. H. a. i. V. E.-t. i. H. C. C. H. Development of a Novel Ionic Liquid Based Microemulsion System for Gemcitabine Hydrochloride and in Vitro Evaluation in Human Cervical Cancer HeLa Cells. *Indian J. Pharm. Educ. Res* **2021**, *55*, 685–691. DOI: 10.5530/ijper.55.3.140.
(143) Nurgali, K.; Jagoe, R. T.; Abalo, R. Editorial: Adverse Effects of Cancer Chemotherapy: Anything New to Improve Tolerance and Reduce Sequelae? *Frontiers in Pharmacology* **2018**, *9*. (acccessed 2023-09-27 17:15:14).Frontiers.
(144) Wei, X.; Shamrakov, D.; Nudelman, S.; Peretz-Damari, S.; Nativ-Roth, E.; Regev, O.; Barenholz, Y. Cardinal Role of Intraliposome Doxorubicin-Sulfate Nanorod Crystal in Doxil Properties and Performance. *ACS Omega* **2018**, *3* (3), 2508-2517. DOI: 10.1021/acsomega.7b01235 (acccessed 2023-09-11 15:45:14).ACS Publications.
(145) Sivadasan, D.; Sultan, M. H.; Madkhali, O. A.; Alsabei, S. H.; Alessa, A. A. Stealth Liposomes (PEGylated) Containing an Anticancer Drug Camptothecin: In Vitro Characterization and In Vivo Pharmacokinetic and Tissue Distribution Study. *Molecules* **2022**, *27* (3), 1086. DOI: 10.3390/molecules27031086 (acccessed 2023-09-27 17:39:26).PubMed Central.
(146) Storm, G.; Woodle, M. C. Long Circulating Liposome Therapeutics: From Concept to Clinical Reality. In *Long Circulating Liposomes: Old Drugs, New Therapeutics*, Woodle, M. C., Storm, G. Eds.; Biotechnology Intelligence Unit, Springer, 1998; pp 3-16.
(147) Lombardo, D.; Kiselev, M. A. Methods of Liposomes Preparation: Formation and Control Factors of Versatile Nanocarriers for Biomedical and Nanomedicine Application. *Pharmaceutics* **2022**, *14* (3), 543. DOI: 10.3390/pharmaceutics14030543 (acccessed 2023-03-09 23:43:05).PubMed Central.
(148) Li, M.; Jiang, S.; Simon, J.; Paßlick, D.; Frey, M.-L.; Wagner, M.; Mailänder, V.; Crespy, D.; Landfester, K. Brush Conformation of Polyethylene Glycol Determines the Stealth Effect of Nanocarriers in the Low Protein Adsorption Regime. *Nano Letters* **2021**, *21* (4), 1591-1598. DOI: 10.1021/acs.nanolett.0c03756 (acccessed 2024-04-29 11:38:53).ACS Publications.
(149) Amoozgar, Z.; Yeo, Y. Recent advances in stealth coating of nanoparticle drug delivery systems. *WIREs Nanomedicine and Nanobiotechnology* **2012**, *4* (2), 219-233. DOI: 10.1002/wnan.1157 (acccessed 2024-04-29 11:40:20).Wiley Online Library.
(150) Wu, J. The Enhanced Permeability and Retention (EPR) Effect: The Significance of the Concept and Methods to Enhance Its Application. *Journal of Personalized Medicine* **2021**, *11* (8), 771. DOI: 10.3390/jpm11080771 (acccessed 2024-04-29 11:41:18).PubMed Central.
(151) Maeda, H.; Nakamura, H.; Fang, J. The EPR effect for macromolecular drug delivery to solid tumors: Improvement of tumor uptake, lowering of systemic toxicity, and distinct tumor imaging in vivo. *Advanced Drug Delivery Reviews* **2013**, *65* (1), 71-79. DOI: 10.1016/j.addr.2012.10.002 PubMed.
(152) Miao, L.; Lin, C. M.; Huang, L. Stromal Barriers and Strategies for the Delivery of Nanomedicine to Desmoplastic Tumors. *Journal of controlled release : official journal of the*

Controlled Release Society **2015**, *219*, 192-204. DOI: 10.1016/j.jconrel.2015.08.017 (acccessed 2023-05-17 16:12:24).PubMed Central.
(153) Seynhaeve, A. L. B.; Amin, M.; Haemmerich, D.; van Rhoon, G. C.; ten Hagen, T. L. M. Hyperthermia and smart drug delivery systems for solid tumor therapy. *Advanced Drug Delivery Reviews* **2020**, *163-164*, 125-144. DOI: 10.1016/j.addr.2020.02.004 (acccessed 2024-04-29 11:50:53).ScienceDirect.
(154) Jin, Y.; Liang, X.; An, Y.; Dai, Z. Microwave-Triggered Smart Drug Release from Liposomes Co-encapsulating Doxorubicin and Salt for Local Combined Hyperthermia and Chemotherapy of Cancer. *Bioconjugate Chemistry* **2016**, *27* (12), 2931-2942. DOI: 10.1021/acs.bioconjchem.6b00603 (acccessed 2022-08-11 19:13:38).ACS Publications.
(155) Fleige, E.; Quadir, M. A.; Haag, R. Stimuli-responsive polymeric nanocarriers for the controlled transport of active compounds: Concepts and applications. *Advanced Drug Delivery Reviews* **2012**, *64* (9), 866-884. DOI: 10.1016/j.addr.2012.01.020 (acccessed 2024-04-29 11:54:09).ScienceDirect.
(156) Kong, G.; Braun, R. D.; Dewhirst, M. W. Characterization of the effect of hyperthermia on nanoparticle extravasation from tumor vasculature. *Cancer Research* **2001**, *61* (7), 3027-3032. PubMed.
(157) Shevtsov, M.; Multhoff, G. Heat Shock Protein–Peptide and HSP-Based Immunotherapies for the Treatment of Cancer. *Frontiers in Immunology* **2016**, *7*. (acccessed 2023-09-11 16:49:50).Frontiers.
(158) Deng, Z.-S.; Liu, J. Chemothermal Therapy for Localized Heating and Ablation of Tumor. *Journal of Healthcare Engineering* **2013**, *4* (3), 409-425. DOI: 10.1260/2040-2295.4.3.409 (acccessed 2022-08-13 02:38:10).www.hindawi.com.
(159) Gabizon, A. A.; Shmeeda, H.; Zalipsky, S. Pros and Cons of the Liposome Platform in Cancer Drug Targeting. *Journal of Liposome Research* **2006**, *16* (3), 175-183. DOI: 10.1080/08982100600848769 (acccessed 2023-10-05 16:00:20).Taylor and Francis+NEJM.
(160) Gupta, S.; De Mel, J. U.; Schneider, G. J. Dynamics of liposomes in the fluid phase. *Current Opinion in Colloid & Interface Science* **2019**, *42*, 121-136. DOI: 10.1016/j.cocis.2019.05.003 (acccessed 2023-03-09 23:46:02).ScienceDirect.
(161) Keller, D.; Larsen, N. B.; Møller, I. M.; Mouritsen, O. G. Decoupled Phase Transitions and Grain-Boundary Melting in Supported Phospholipid Bilayers. *Physical Review Letters* **2005**, *94* (2), 025701. DOI: 10.1103/PhysRevLett.94.025701 (acccessed 2023-03-28 18:27:22).DOI.org (Crossref).
(162) Lu, T.; ten Hagen, T. L. M. Inhomogeneous crystal grain formation in DPPC-DSPC based thermosensitive liposomes determines content release kinetics. *Journal of Controlled Release* **2017**, *247*, 64-72. DOI: 10.1016/j.jconrel.2016.12.030 (acccessed 2024-05-09 17:59:35).ScienceDirect.
(163) Motamarry, A.; Wolfe, A. M.; Ramajayam, K. K.; Pattanaik, S.; Benton, T.; Peterson, Y.; Faridi, P.; Prakash, P.; Twombley, K.; Haemmerich, D. Extracorporeal Removal of Thermosensitive Liposomal Doxorubicin from Systemic Circulation after Tumor Delivery to Reduce Toxicities. *Cancers* **2022**, *14* (5), 1322. DOI: 10.3390/cancers14051322 (acccessed 2024-08-20 04:42:16).PubMed Central.
(164) Chamani, F.; Pyle, M. M.; Shrestha, T. B.; Sebek, J.; Bossmann, S. H.; Basel, M. T.; Sheth, R. A.; Prakash, P. In Vitro Measurement and Mathematical Modeling of Thermally-Induced Injury in Pancreatic Cancer Cells. *Cancers* **2023**, *15* (3), 655. DOI: 10.3390/cancers15030655 (acccessed 2024-05-17 05:02:21).www.mdpi.com.

(165) Kaasgaard, T.; Leidy, C.; Crowe, J. H.; Mouritsen, O. G.; Jørgensen, K. Temperature-Controlled Structure and Kinetics of Ripple Phases in One- and Two-Component Supported Lipid Bilayers. *Biophysical Journal* **2003**, *85* (1), 350-360. DOI: 10.1016/S0006-3495(03)74479-8 (acccessed 2024-05-09 18:39:43).www.cell.com.
(166) Tataranni, T.; Agriesti, F.; Ruggieri, V.; Mazzoccoli, C.; Simeon, V.; Laurenzana, I.; Scrima, R.; Pazienza, V.; Capitanio, N.; Piccoli, C. Rewiring carbohydrate catabolism differentially affects survival of pancreatic cancer cell lines with diverse metabolic profiles. *Oncotarget* **2017**, *8* (25), 41265-41281. DOI: 10.18632/oncotarget.17172 (acccessed 2024-05-02 17:05:48).PubMed Central.
(167) Michalopoulou, E.; Auciello, F. R.; Bulusu, V.; Strachan, D.; Campbell, A. D.; Tait-Mulder, J.; Karim, S. A.; Morton, J. P.; Sansom, O. J.; Kamphorst, J. J. Macropinocytosis Renders a Subset of Pancreatic Tumor Cells Resistant to mTOR Inhibition. *Cell Reports* **2020/02/02**, *30* (8). DOI: 10.1016/j.celrep.2020.01.080.
(168) Chintamaneni, P. K.; Pindiprolu, S. K. S. S.; Swain, S. S.; Karri, V. V. S. R.; Nesamony, J.; Chelliah, S.; Bhaskaran, M. Conquering chemoresistance in pancreatic cancer: Exploring novel drug therapies and delivery approaches amidst desmoplasia and hypoxia. *Cancer Letters* **2024**, *588*, 216782. DOI: 10.1016/j.canlet.2024.216782 (acccessed 2024-04-29 11:49:08).ScienceDirect.
(169) Nakaoka, K.; Ohno, E.; Kawabe, N.; Kuzuya, T.; Funasaka, K.; Nakagawa, Y.; Nagasaka, M.; Ishikawa, T.; Watanabe, A.; Tochio, T.; et al. Current Status of the Diagnosis of Early-Stage Pancreatic Ductal Adenocarcinoma. *Diagnostics* **2023/01**, *13* (2). DOI: 10.3390/diagnostics13020215.
(170) Jiang, B.; Zhou, L.; Lu, J.; Wang, Y.; Liu, C.; You, L.; Guo, J. Stroma-Targeting Therapy in Pancreatic Cancer: One Coin With Two Sides? *Frontiers in Oncology* **2020**, *10*. DOI: 10.3389/fonc.2020.576399.
(171) Shah, V. M.; Sheppard, B. C.; Sears, R. C.; Alani, A. W. Hypoxia: Friend or Foe for drug delivery in Pancreatic Cancer. *Cancer letters* **2020/11/11**, *492*. DOI: 10.1016/j.canlet.2020.07.041.
(172) Hartupee, C.; Nagalo, B. M.; Chabu, C. Y.; Tesfay, M. Z.; Coleman-Barnett, J.; West, J. T.; Moaven, O. Frontiers | Pancreatic cancer tumor microenvironment is a major therapeutic barrier and target. *Frontiers in Immunology* **2024/02/01**, *15*. DOI: 10.3389/fimmu.2024.1287459.
(173) Beutel, A. K.; Halbrook, C. J. Barriers and opportunities for gemcitabine in pancreatic cancer therapy. *American Journal of Physiology - Cell Physiology* **2023/02/02**, *324* (2). DOI: 10.1152/ajpcell.00331.2022.
(174) Wang, Y.; Fan, W.; Dai, X.; Katragadda, U.; Mckinley, D.; Teng, Q.; Tan, C. Enhanced Tumor Delivery of Gemcitabine via PEG-DSPE/TPGS Mixed Micelles. *Molecular Pharmaceutics* **March 10, 2014**, *11* (4). DOI: 10.1021/mp4005904.
(175) Amrutkar, M.; Gladhaug, I. P.; Amrutkar, M.; Gladhaug, I. P. Pancreatic Cancer Chemoresistance to Gemcitabine. *Cancers 2017, Vol. 9, Page 157* **2017-11-16**, *9* (11). DOI: 10.3390/cancers9110157.
(176) PLGA nanoparticles containing various anticancer agents and tumour delivery by EPR effect. *Advanced Drug Delivery Reviews* **2011/03/18**, *63* (3). DOI: 10.1016/j.addr.2010.10.008.
(177) Employment of enhanced permeability and retention effect (EPR): Nanoparticle-based precision tools for targeting of therapeutic and diagnostic agent in cancer. *Materials Science and Engineering: C* **2019/05/01**, *98*. DOI: 10.1016/j.msec.2019.01.066.

(178) De Leo, V.; Milano, F.; Agostiano, A.; Catucci, L. Recent Advancements in Polymer/Liposome Assembly for Drug Delivery: From Surface Modifications to Hybrid Vesicles. *Polymers* **2021**, *13* (7), 1027. DOI: 10.3390/polym13071027 (acccessed 2023-01-11 22:00:02).www.mdpi.com.
(179) Yusuf, A.; Almotairy, A. R. Z.; Henidi, H.; Alshehri, O. Y.; Aldughaim, M. S. Nanoparticles as Drug Delivery Systems: A Review of the Implication of Nanoparticles' Physicochemical Properties on Responses in Biological Systems. *Polymers* **2023/04**, *15* (7). DOI: 10.3390/polym15071596.
(180) Review of the efficacy of nanoparticle-based drug delivery systems for cancer treatment. *Biomedical Technology* **2024/03/01**, *5*. DOI: 10.1016/j.bmt.2023.09.001.
(181) Sharma, H.; Kumar Sahu, G.; Kaur, C. D.; Sharma, H.; Kumar Sahu, G.; Kaur, C. D. Development of ionic liquid microemulsion for transdermal delivery of a chemotherapeutic agent. *SN Applied Sciences 2021 3:2* **2021-01-25**, *3* (2). DOI: 10.1007/s42452-021-04235-x.
(182) Shukla, M. K.; Tiwari, H.; Verma, R.; Dong, W.-L.; Azizov, S.; Kumar, B.; Pandey, S.; Kumar, D. Role and Recent Advancements of Ionic Liquids in Drug Delivery Systems. *Pharmaceutics* **2023/02**, *15* (2). DOI: 10.3390/pharmaceutics15020702.
(183) Liu, C.; Chen, B.; Shi, W.; Huang, W.; Qian, H. Ionic Liquids for Enhanced Drug Delivery: Recent Progress and Prevailing Challenges. *Molecular Pharmaceutics* **March 11, 2022**, *19* (4). DOI: 10.1021/acs.molpharmaceut.1c00960.
(184) Goindi, S.; Arora, P.; Kumar, N.; Puri, A. Development of Novel Ionic Liquid-Based Microemulsion Formulation for Dermal Delivery of 5-Fluorouracil. *AAPS PharmSciTech* **2014**, *15* (4), 810-821. DOI: 10.1208/s12249-014-0103-1 (acccessed 2024-06-22T20:04:25).
(185) Beaven, E.; Kumar, R.; An, J. M.; Mendoza, H.; Sutradhar, S. C.; Choi, W.; Narayan, M.; Lee, Y.-k.; Nurunnabi, M. Potentials of ionic liquids to overcome physical and biological barriers. *Advanced drug delivery reviews* **2024/01**, *204*. DOI: 10.1016/j.addr.2023.115157.
(186) Chen, X.; Li, Z.; Yang, C.; Yang, D. Ionic liquids as the effective technology for enhancing transdermal drug delivery: Design principles, roles, mechanisms, and future challenges. *Asian Journal of Pharmaceutical Sciences* **2024/04**, *19* (2). DOI: 10.1016/j.ajps.2024.100900.
(187) Dharman, M. M.; Ju, H.-Y.; Shim, H.-L.; Lee, M.-K.; Kim, K.-H.; Park, D.-W. Significant influence of microwave dielectric heating on ionic liquid catalyzed transesterification of ethylene carbonate with methanol. *Journal of Molecular Catalysis A: Chemical* **2009/04/15**, *303* (1-2). DOI: 10.1016/j.molcata.2009.01.004.
(188) Augmentation of the EPR effect by mild hyperthermia to improve nanoparticle delivery to the tumor. *Biochimica et Biophysica Acta (BBA) - Reviews on Cancer* **2024/07/01**, *1879* (4). DOI: 10.1016/j.bbcan.2024.189109.
(189) Foo, K. S.; Bavoh, C. B.; Lal, B.; Shariff, A. M. Rheology Impact of Various Hydrophilic-Hydrophobic Balance (HLB) Index Non-Ionic Surfactants on Cyclopentane Hydrates. *Molecules* **2020/08**, *25* (16). DOI: 10.3390/molecules25163725.
(190) BB, M.; V, S.; MS, K. Simultaneous localized 915 MHz external and interstitial microwave hyperthermia to heat tumors greater than 3 cm in depth - PubMed. *International journal of radiation oncology, biology, physics* **1990 Sep**, *19* (3). DOI: 10.1016/0360-3016(90)90495-6.

Appendix A - NMR Analysis

Appendix Figure A. ^{1}H of 1-Methyl-imidazole

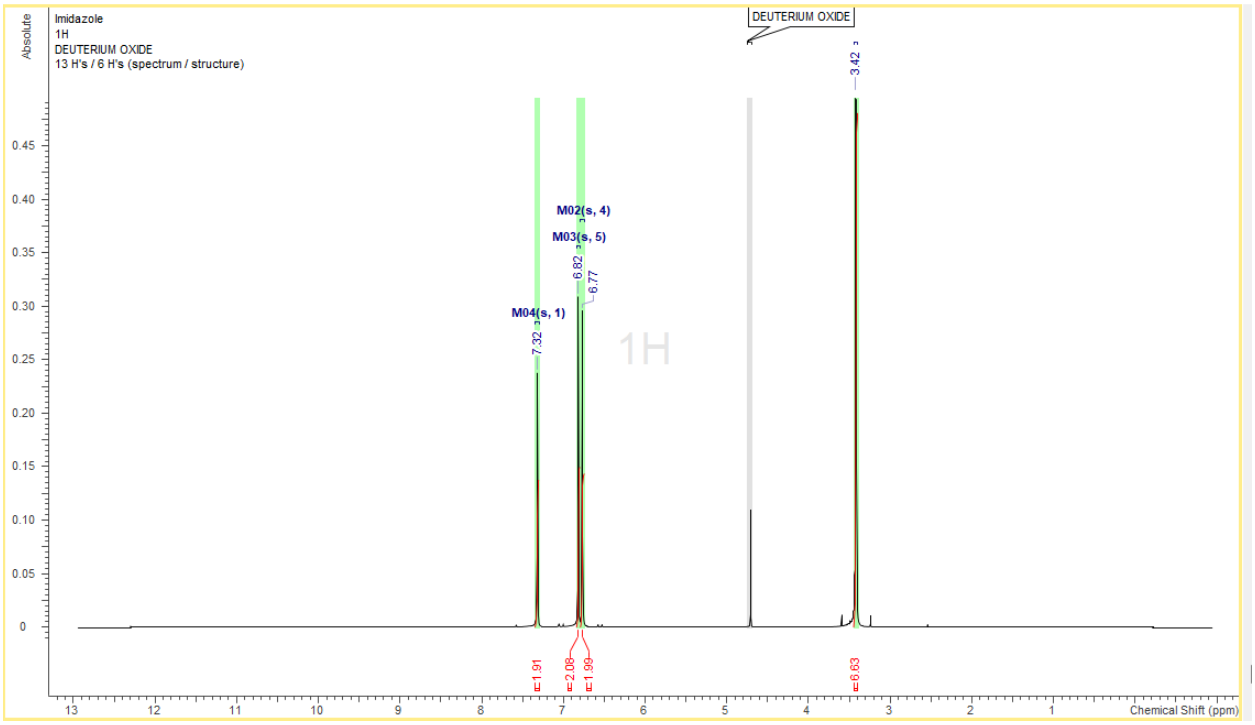

Appendix Figure A.2 ^{13}C of Bromobutane

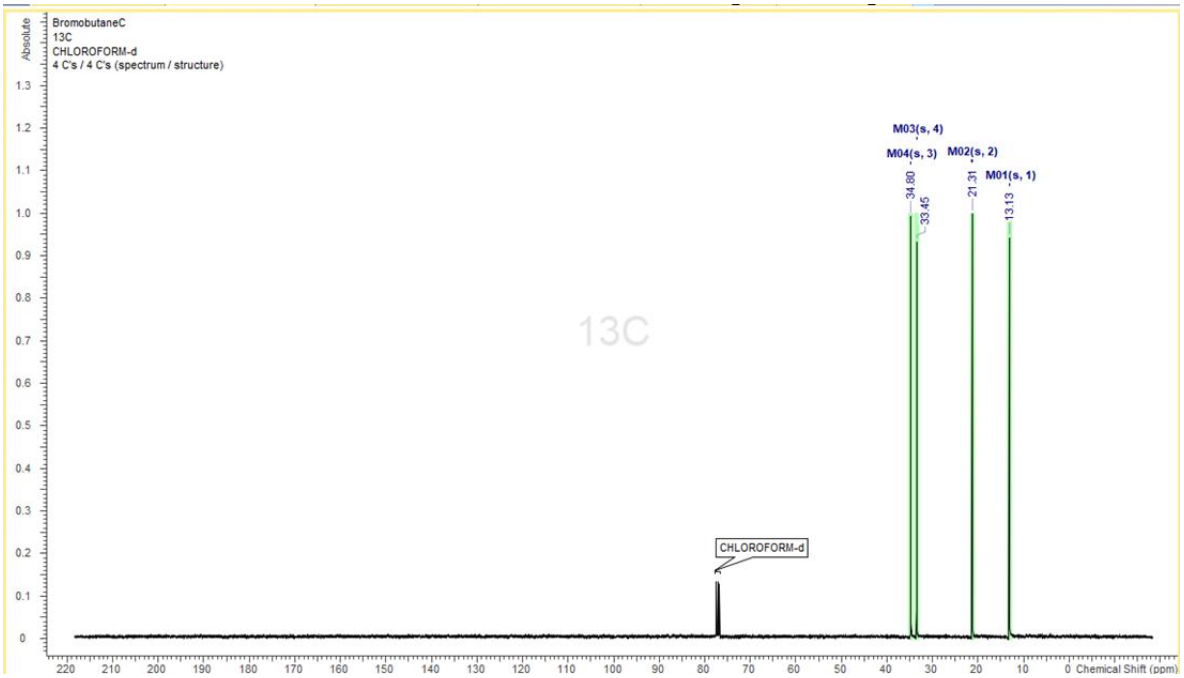

Appendix Figure A.3 ^{1}H of Bromobutane

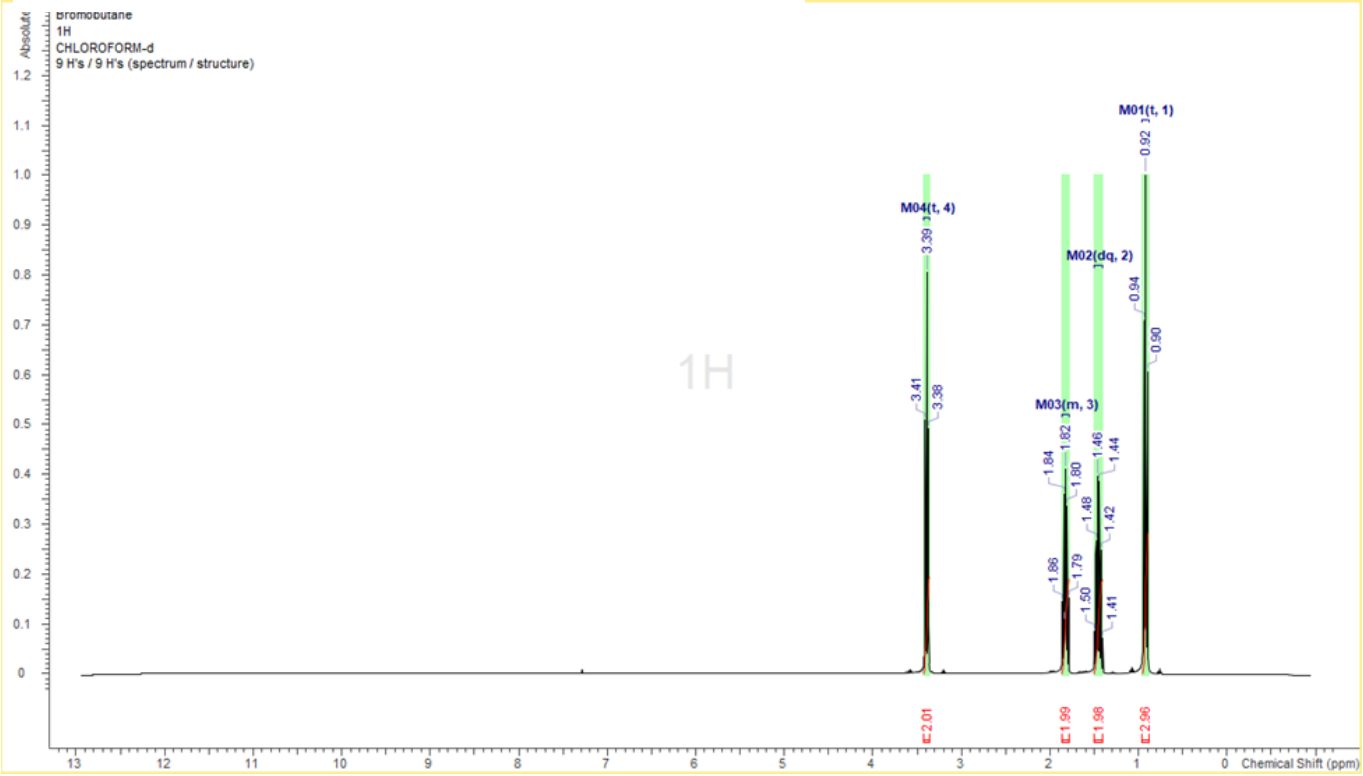

Appendix Figure A.4 ^{1}H of 1-Butyl-3-Methylimidazolium Bromide

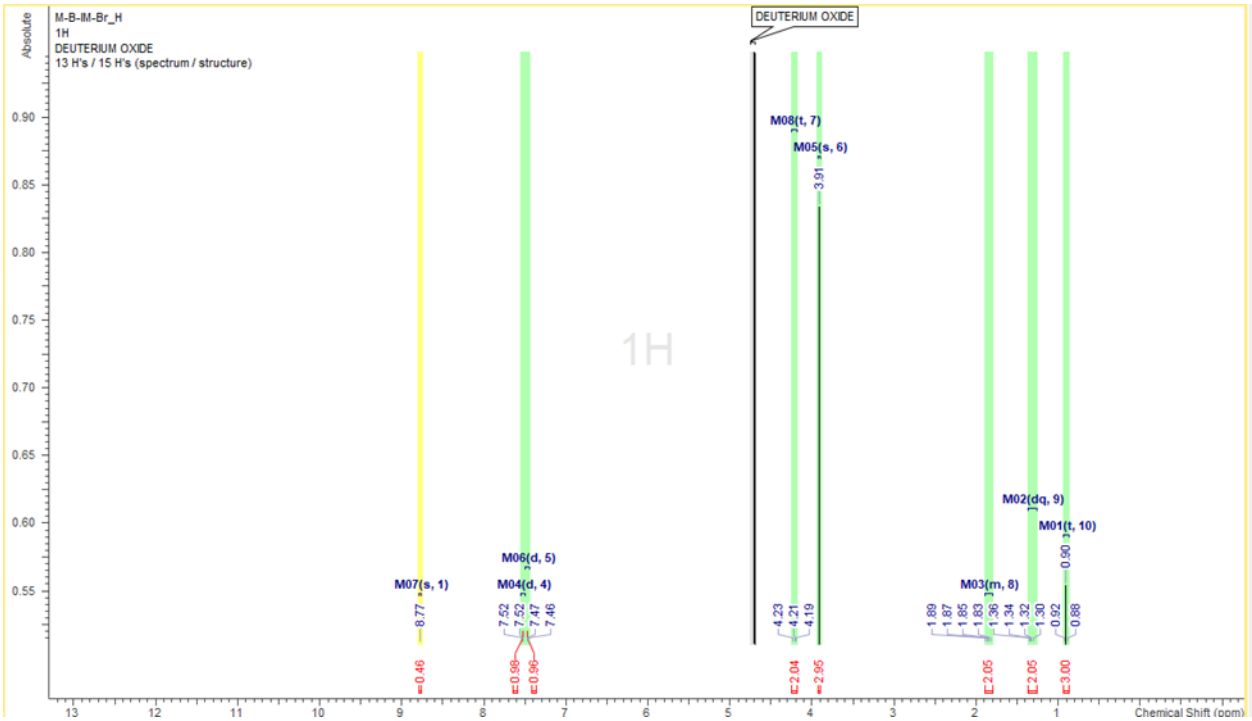

Appendix Figure A.6 ^{13}C of 1-Methyl-imidazole

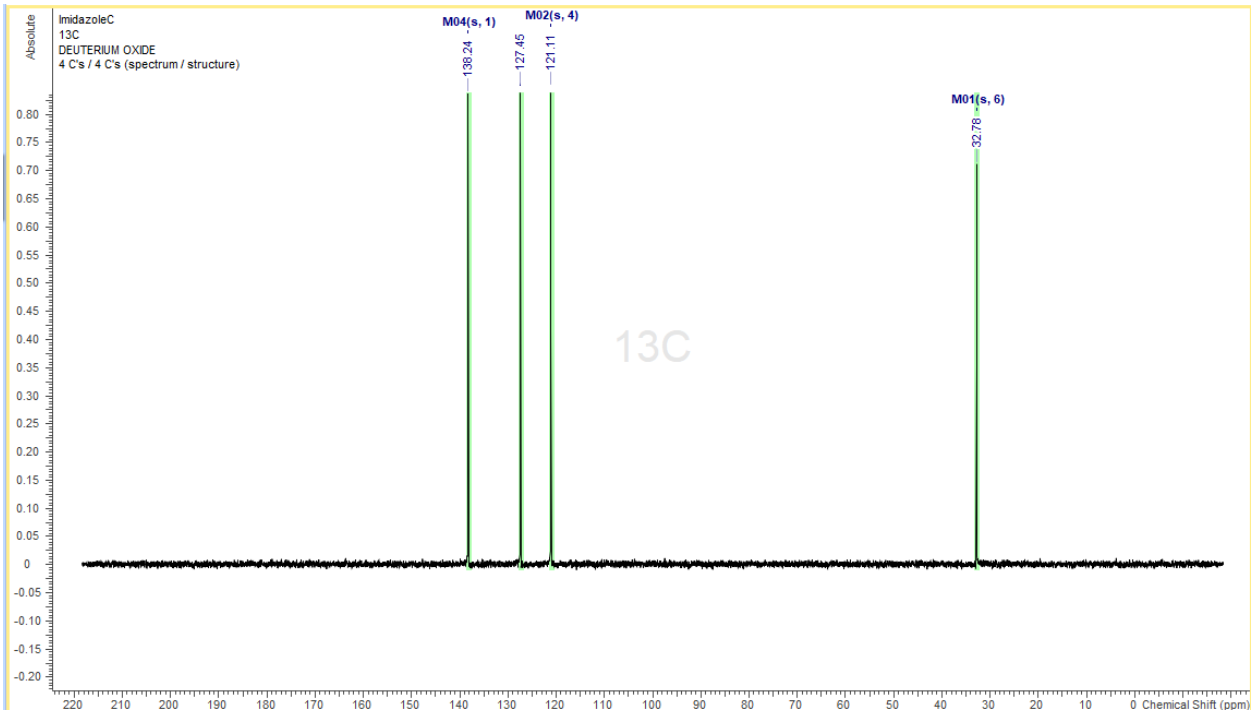

Appendix Figure A.5 ^{13}C of 1-Butyl-3-Methylimidazolium Bromide

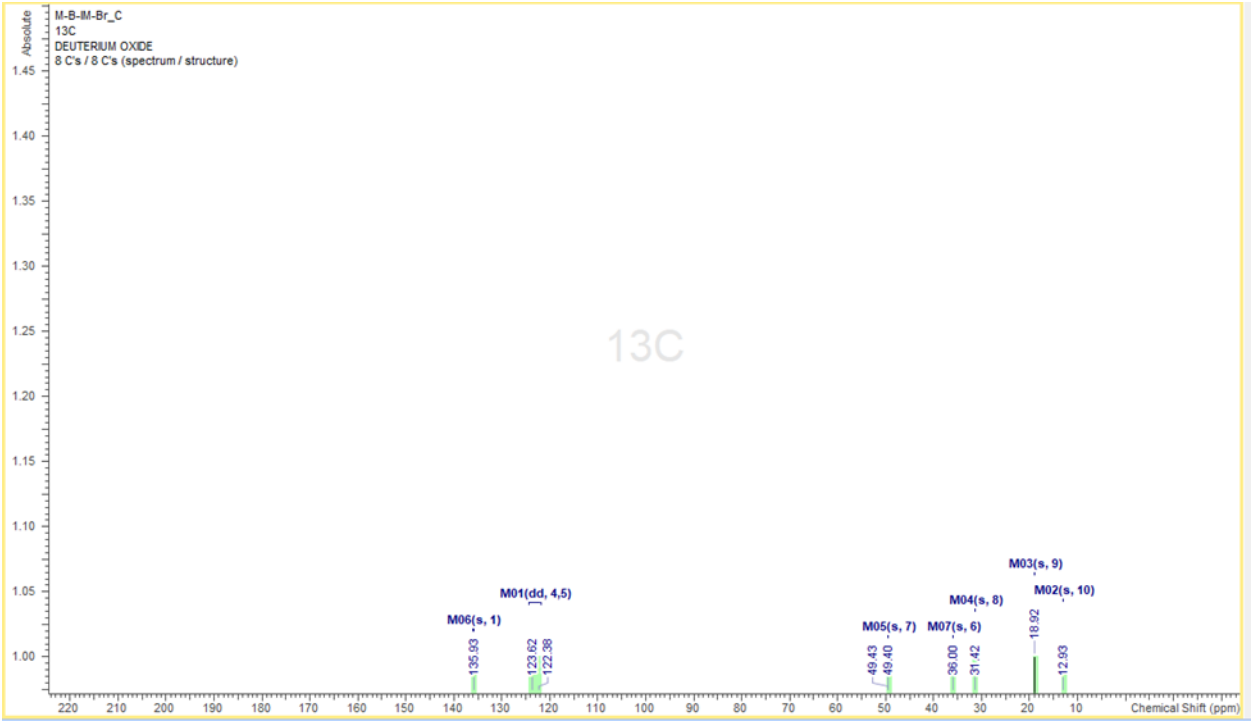

Appendix B - List of Abbreviations

Pancreatic Ductal Adenocarcinoma	**PDAC**
2′,2′-Difluorodeoxycytidine	**dFdC**
Difluoro-Uridine Derivative	**dFdU**
Polyethylene Glycol	**PEG**
Thermosensitive Liposomes	**TSL**
Fetal Bovine Serum	**FBS**
Dulbecco's Modified Eagle Medium	**DMEM**
Lipophilic Hydrophilic Balance	**HLB**
1,2-Dipalmitoyl-sn-Glycero-3-Phosphocholine	**DPPC**
1,2-Distearoyl-sn-Glycero-3-Phosphocholine	**DSPC**
1,2-Dipalmitoyl-sn-Glycero-3-Phosphoethanolamine-N-[Methoxy (Polyethylene Glycol)-2000]	**PEG2k**
Mild Hyperthermia	**MHT**
Intravenous	**IV**
Isopropyl Myristate	**IPM**
Water-in-Oil	**W/O**
Ionic Liquid	**IL**
Oil-in-Water	**O/W**
Deionized	**DI**
Microemulsion	**ME**
Nano Tracking Analysis	**NTA**
Transmission Electron Microscopy	**TEM**
Phospholipid	**PL**
1-Butyl-3-Methylimidazolium Bromide	**Br-IL**
1-Butyl-3-Methylimidazolium Hexafluorophosphate	**F6P-IL**
Nanotechnology Innovation Center of Kansas State	**NICKS**
Carboxyfluorescein	**CF**
Phosphate Buffered Saline	**PBS**
Roswell Park Memorial Institute Medium	**RPMI**
3-(4,5-dimethylthiazol-2-yl)-2,5-diphenyltetrazolium bromide	**MTT**
Thermosensitive Liposomes	**TSLs**
Hydrodynamic Size	**HS**
Polydispersity Index	**PDI**
Encapsulation Efficiency	**EE**
Dimethyl Sulfoxide	**DMSO**
Enhanced Permeation and Retention	**EPR**
Triton™ X-100	**TX-100**
Molecular Weight Cut-Off	**MWCO**
Thermocouple Data Logger	**TC08**